Systematic analysis of alt-EJ regulation in irradiated cells at the interface of G_0/G_1 cell cycle phases: focus on growth factor signaling and CtIP

Inaugural-Dissertation

zur

Erlangung des Doktorgrades

Dr. rer. nat.

der Fakultät für

Biologie

an der

Universität Duisburg-Essen

vorgelegt von

Anna Katharina Broich

aus Baden/Schweiz

Dezember 2019

Die der vorliegenden Arbeit zugrunde liegenden Experimente wurden am Institut für Medizinische Strahlenbiologie am Universitätsklinikum Essen durchgeführt.

1. Gutachter: Prof. Dr. George Iliakis
2. Gutachter: Prof. Dr. Hemmo Meyer
Vorsitzender des Prüfungsausschusses: Prof. Dr. Dominik Boos
Tag der mündlichen Prüfung: 03. März 2020

DOI: 10.17185/duepublico/71789
URN: urn:nbn:de:hbz:464-20200630-132807-3

Draco dormiens nunquam titillandus.

J. K. Rowling, Harry Potter and the Philosopher's Stone, 1997

Table of Contents

1. Abbreviations and symbols

Protein names	are expressed with a capital letter followed by at least one lowercase letter
GENE names	are expressed exclusively in capital letters
°C	degrees centigrade
Ø	diameter
>	greater than
≥	greater than or equal to
53Bp1	tumor suppressor p53-binding protein 1
82-6 hTERT	human hTERT transfected fibroblast cell line
α	alpha
γ	gamma
δ	delta
ε	epsilon
θ	theta
λ	lamda
µ	micro/mu
A	ampere
ad	adjust to final volume of
Akt	also known as: protein kinase B (Pkb)
alt-EJ	alternative non-homologous end joining
Ap-1	activator protein 1
APC	aphidicolin
Apc/c^{Cdh1}	anaphase-promoting complex/cadherin-1
Aqua dest.	double-distilled water
Atm	ataxia telangiectasia mutated protein
Atr	Atm-Rad3 related protein
Atrip	Atr interacting protein
Bcl-2	B cell lymphoma 2 protein
bFGF	basic fibroblast growth factor
BOR	bortezomib
Brca1/2	breast cancer protein 1 and 2
BSA	bovine serum albumin
Ca	calcium
Cdc25	cell division cycle protein 25
Cdh1	cadherin-1
Cdk	cyclin dependent kinase
cDNA	complementary DNA
Cds1	checking DNA synthesis kinase 1
Chk1/2	checkpoint kinase 1 and 2
CHO	Chinese hamster ovary
CHX	cycloheximide
c-NHEJ	classical non-homologous end joining

CO_2	carbon dioxide
C_P	crossing point
CSR	class switch recombination
Ctbp	C-terminal-binding protein
CtIP	Ctbp interacting protein
Ctrl	control
Cul3	Cullin 3 protein
$CuSO_4$	copper (II) sulfate pentahydrate
d	day
D-loop	displacement loop
DAG	diacylglycerol
DDR	DNA damage response
Deq	DNA DSB damage, expressed as dose equivalent
DF	dilution factor
Dmc1	disrupted meiotic cDNA recombinase 1
DMEM	Dulbecco's Modified Eagle Medium
DMSO	dimethyl sulfoxide
DNA	deoxyribonucleic acid
Dna2	DNA replication helicase/nuclease 2
Dna-Pk	DNA-dependent protein kinase
Dna-Pkcs	DNA-dependent protein kinase catalytic subunit
DNS	Desoxyribonukleinsäure
dNTP	nucleoside triphosphate containing deoxyribose instead of ribose
DSB	double strand break
DSBR	double strand break repair
DT40	avian leukosis virus induced chicken lymphoma cell line
DTT	dithiothreitol
E2F	E2 factor
EDTA	ethylenediaminetetraacetic acid
EdU	5-ethynyl-2'-deoxyuridine
EGF	epidermal growth factor
EGFR	epidermal growth factor receptor
ELISA	enzyme-linked immunosorbent assay
Eme1	essential meiotic structure-specific endonuclease 1
Erk	extracellular signal-regulated kinase
EtBr	ethidium bromide
EtOH	ethanol
Exo1	exonuclease 1
FBS	fetal bovine serum
FHA	forkhead-associated
FW	forward
g	gram
G_0	postmitotic quiescent cell cycle condition/gap

G_1	first gap
G_2	second gap
GapdH	glyceraldehyde 3-phosphate dehydrogenase
Gen1	Holliday junction 5’ flap endonuclease
GOI	gene of interest
Gy	gray
h	hour
H1	histone 1
H2AX	histone variant 2AX
H_2O	water
H_3PO_4	phosphoric acid
HEPES	4-(2-hydroxyethyl)-1-piperazineethanesulfonic acid
HJ	Holliday junction
HRR	homologous recombination repair
Hs	*Homo sapiens*
hTert	human telomerase reverse transcriptase
Hus1	checkpoint protein
IP_3	inositol 1,4,5-triphosphate
IR	ionizing radiation
IRDye	infrared dye
I-SceI	*Saccharomyces cerevisiae* intron-encoded endonuclease I
Jnk	c-Jun N-terminal kinase
KCl	potassium chloride
kDa	kilodalton
KH_2PO_4	potassium dihydrogenphosphate
Ki67	Kiel-67 protein
Klhl15	kelch-like protein 15
kV	kilovolt
l	liter
Lig	ligase
lim	limit
m	milli
M	mitosis
M (chemistry)	Molar
MAPK	mitogen activated protein kinase, also known as: Erk
MAP2K	MAP kinase kinase or Mek
MAP3K	MAP kinase kinase kinase
MAP4K	MAP kinase kinase kinase kinase
Mdc1	mediator of DNA damage checkpoint protein 1
MEF	mouse embryonic fibroblast
Mek	mitogen activated protein kinase kinase
MEM	Minimum Essential Medium
MeOH	methanol
MIM	L-mimosine

min	minute
MK	MK-2206
mm	millimeter
Mre11	meiotic recombination 11-like protein
MRN	Mre11-Rad50-Nbs1 complex
mRNA	messenger RNA
Mus81	crossover junction endonuclease
Myc	myelocytomatosis viral oncogene
N	Normal
na	not available
NaCl	sodium chloride
Na_2HPO_4	sodium hydrogen phosphate
$NaHCO_3$	sodium hydrogen carbonate
NaOH	sodium hydroxide
Nbs1	Nijmegen breakage syndrome 1 protein
NEA	non-essential amino acids
NF-κB	nuclear factor kappa-light-chain-enhancer of activated B cells
NHEJ	non-homologous end joining, including c-NHEJ and alt-EJ
NLS	N-lauroylsarcosine
OBB	Odyssey blocking buffer
OH^-	hydroxide
Oligo $(dT)_{18}$	18-mer oligonucleotide
p	phosphorylated
p21	cyclin-dependent kinase inhibitor 1
p27	cyclin-dependent kinase inhibitor 1b
p53	tumor suppressor protein 53
p57	cyclin-dependent kinase inhibitor 1c
Palb2	partner and localizer of Brca2
Parp-1	poly(ADP-ribose) polymerase 1
PARylation	poly(ADP-ribosyl)ation
PBS	phosphate buffered saline
PC-3	prostate cancer cell line 3
PCR	polymerase chain reaction
PD	PD-0332991
Pdk1/2	3’-phosphoinositide-dependent kinase 1 and 2
PFA	paraformaldehyde
PFGE	pulsed-field gel electrophoresis
PI	propidium iodide
Pi3k	phosphatidylinositol 3-kinase
PIKK	phosphatidylinositol 3-kinase-related kinase
PIP_2	phosphatidylinositol 4,5-bisphosphate
PIP_3	phosphatidylinositol 3,4,5-trisphosphate
Pkb	protein kinase B, also known as: Akt
Pkc	protein kinase c

Plcγ	phospholipase C gamma
Pol	polymerase
pre	before
Pten	phosphatase and tensin homolog
Rad	radiation sensitive mutant
Raf	rapidly accelerated fibrosarcoma protein
Ras	rat sarcoma viral oncogene homologue
Rb	retinoblastoma
RNA	ribonucleic acid
Rpa	replication protein A
RPE-1 hTERT	retinal pigment epithelial cell line 1
RT	room temperature
RTK	receptor tyrosine kinase
RT-qPCR	quantitative real-time PCR
RV	reverse
S	DNA synthesis
SD	serum deprivation
SDS	sodium dodecyl sulfate
SDSA	synthesis dependent strand annealing
Ser	serine
SR	serum replenishment
SSB	single strand break
ssDNA	single stranded DNA
Stat	signal transducers and activators of transcription
StDev	standard deviation
t_{10Gy}	temporal requirement to resolve 50 % of induced DNA DSB damage
Taq	*Thermus aquaticus*
TBS	tris-buffered saline
TdT	terminal deoxynucleotidyl transferase
TEMED	tetramethylethylenediamine
Thr	threonine
TRA	trametinib
Topbp1	DNA topoisomerase 2-binding protein 1
Tyr	tyrosine
Ube2S	ubiquitin-conjugating enzyme E2 S
V	Volt
V(D)J	variable (diversity) joining
Xlf	Xrcc4-like factor, also known as: Cernunnos
Xrcc	X-ray repair cross-complementing protein

2. Figures

3. Tables

4. Introduction

4.1 The onset of cancer and the delicacy of DNA as carrier of genetic information

Cancer is one of the major challenges of health care systems in the industrialized world and patients experience their disease to be a life threatening menace. In the United States of America cancer ascended to be now the second leading cause of death [1]. In Germany cancer incidence almost doubled since the 1970s and every second person will fall ill with cancer at least once in is his or her life time [2].

The onset of cancer is a multistep progression process in which normal healthy cells are transformed into carcinogenic cells. The origin of carcinogenesis is the instability of the genome leading to genetic alterations in the deoxyribonucleic acid (DNA). Alterations in the DNA, that is mutations, are acquired by cells over time and finally disrupt the regulation circuits of cellular differentiation, metabolic household and tissue homeostasis [3, 4].

DNA is made of a backbone structure and four organic bases. The backbone is made of deoxyribose and phosphate groups that are attached to each other in an alternating fashion. The bases, which protrude from this sugar-phosphate-backbone, are the two pyrimidines thymine and cytosine and the two purines adenine and guanine. Sugar molecule, phosphate group and organic base together form a nucleotide. Each DNA molecule consists of two DNA strands forming a double helix in which each base from one strand faces a specific base from the other strand. The whole structure is stabilized by hydrogen bonds that emanate between these base pairs. Each base can only pair with one specific other base: cytosine can only base-pair with guanine and thymidine can only base-pair with adenine. In this way, the two DNA strands forming the double helix are exactly complementary to each other. The sequence in which the bases are arranged at the DNA strand encodes genetic information, thus every genetic characteristic an individual possesses [5].

The smallest genetic alteration that can occur in DNA, and that could be termed a mutation, is a change in one single base. There are hereditary diseases and cancer conditions that require mutations involving more genetic alterations than the exchange of a sole base. But conceptually, the latter is already sufficient to alter the sense of the genetic code, thus leading to another composition of gene products. During cellular proliferation, a mother cell has to divide into two daughter cells. In order to faithfully pass on genetic information to the next generation of cells, the DNA

of the mother cell has to be exactly copied and distributed to both daughter cells to ensure genesis of two genetically identical cell clones. Damage in the genetic sequence in the mother cell would be copied and propagated into next cell generations. This error propagation highlights „the central role of DNA in heredity“ [6] and its fundamental significance in genomic integrity [3].

4.2 DNA damage induction by ionizing radiation

Damage to the DNA structure in cells, and thus potentially oncogenic events, can have multiple sources. It can occur intrinsically by free radical species arising from cellular metabolism, errors during DNA replication, endonuclease cleavage and more. But DNA damage can be caused by external factors, too. These can be genotoxic chemicals or ionizing radiation (IR). IR can have extraterrestrial or terrestrial sources. The source of extraterrestrial IR is cosmic rays. Terrestrial IR can occur naturally, like from radioactive elements in the Earth crust, and from manmade generation for industry and medical purposes [7].

Effects of IR are caused by absorption of the radiation’s kinetic or electromagnetic energy. The primary event by which X- and gamma-rays deposit their energy in matter is either the Compton process (for high photon energies) or the photoelectric process (for low photon energies). During the Compton process (Figure 1A), a photon interacts with an electron from the valence shell of an atom. During the photoelectric process (Figure 1B), a photon is absorbed by an electron from any atom shell below the absorbing atom’s valence shell. In both cases, energy of the photon is transferred to the electron which is ejected from its atomic shell thereupon. The free and now fast travelling electron interacts with other molecules of the absorbing matter and generates secondary ionizations [7].

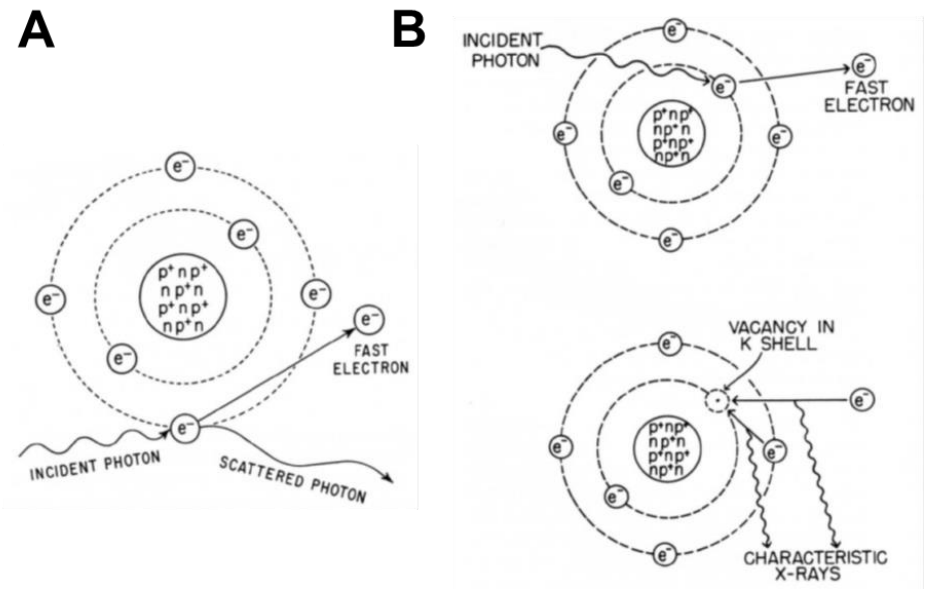

Figure 1: Effects of IR are caused by absorption of the radiation's energy.
A) For high photon energies, energy is deposited in matter by the Compton process. Photons interact with valence electrons, which are ejected from their shell. B) For low photon energies, energy is deposited in matter by the photoelectric process. Photons interact with electrons from any atom shell below the valence shell. Electrons are ejected and resulting vacant positions are backfilled with electrons from outer shells. p^+: proton, n: neutron, e^-: electron. See text for details. Adapted from [7].

If DNA itself gets ionized and thus damaged (Figure 2), either by these ejected electrons or by secondary ionizing events the ejected electrons can cause, this is termed direct action of radiation. However, DNA can also get damaged by indirect action of radiation. In this case, the generated electron interacts with another molecule, most likely water as it is the main component of cells. During the interaction of electrons and water molecules, water ion radicals are generated. Water ion radicals in turn react with further water molecules to form highly reactive hydroxyl radicals which interact with DNA and cause damage. X-rays, which are used in the experimental setups in this thesis, are of lower energy in comparison to other kinds of IR. For the most part, they are indirectly exerting their action on DNA [7].

There are various kinds of DNA damage (or lesions) that are caused by IR. Base damages include the chemical alteration or loss of bases without interrupting the physical integrity of the sugar-phosphate-backbone of the DNA molecule. Disruption of the sugar-phosphate-backbone of one strand of the DNA double helix is termed a single strand break (SSB). SSBs might involve base damage, as well. In both cases, base damages and SSBs, the second and complementary DNA strand of the double helix is used to faithfully restore information of the damaged strand. The third kind of DNA lesion that is caused by IR is the double strand break (DSB). In DNA DSBs, two SSBs happen to coincide directly opposed to each other in both strands of the DNA double helix or in close vicinity to each other (up to 10 base pairs). In these cases,

the cell lacks the possibility to simply employ one strand of the double helix as a template to restore sequence information of the other strand. As this DNA damage bears the threat of loss of genetic information and implies also more complicated mechanisms of repair, it is considered to be the most severe kind of DNA damage [7]. The quite sophisticated mechanisms of signaling and repairing DNA DSBs in eukaryotic cells will be presented further below.

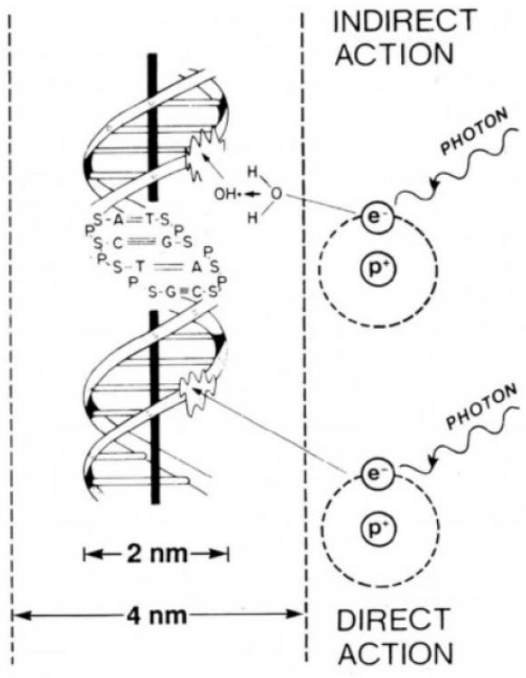

Figure 2: Ionization of DNA molecules by direct and indirect action of radiation.
DNA can get damaged by direct action of radiation. Here, electrons being ejected during the Compton or photoelectric process ionize DNA. During indirect action of radiation, ejected electrons first interact with other molecules and generate radicals. These radicals in turn interact with DNA and damage it. p^+: proton, e^-: electron, SP: sugar-phosphate-backbone, G/C/T/A: bases, H_2O: water, OH^-: hydroxide. See text for details [7].

4.3 DNA damage signaling

The number of DNA lesions occurring in human cells every day goes into the tens of thousands. The cellular answer towards these damages is termed DNA damage response (DDR). It is a functional surveillance network involving DNA damage signaling and repair and parries the forwarding of mutations that arise from DNA damages from mother to daughter cells [8, 9]. DDR has been monitored in pre-carcinogenic neoplasias, where it probably safeguards the organism from further oncogenesis. Vice versa, defective mutations in DDR contributors themselves allow downregulation of this sentinel process, resulting in genetic instability and oncogenic progression [10, 11].

Proteins involved in DNA damage signaling (Figure 3) can be divided into damage sensors, apical kinases or transducer kinases, mediators and effectors [12].

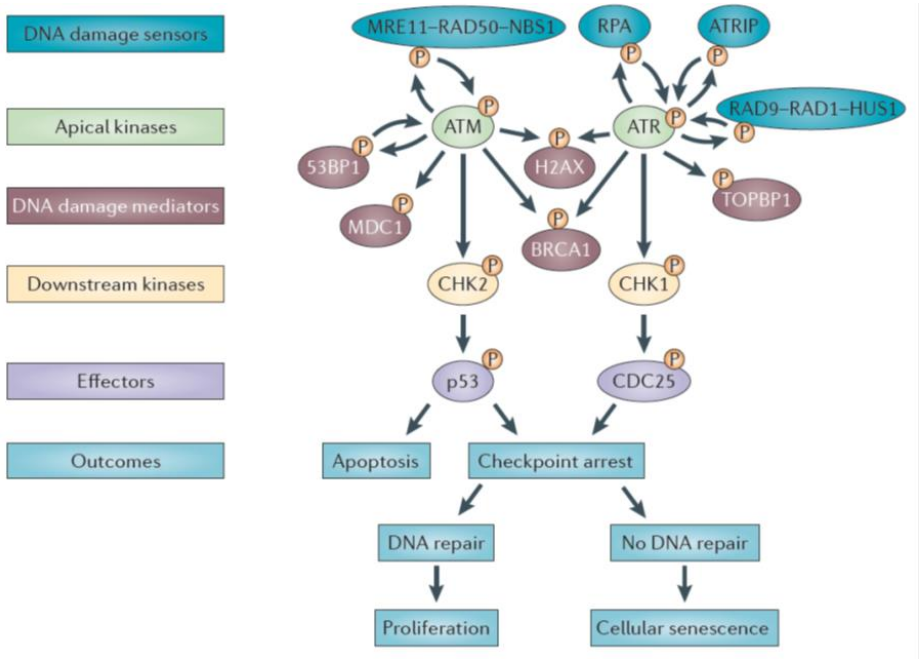

Figure 3: DNA damage signaling.
DNA damage signaling proteins can be divided into damage sensors, apical kinases, mediators and effectors. Final outcomes can be resumption of proliferation, apoptosis or senescence. Phosphorylations are depicted by the letter "P". See text for details [12].

Sensor proteins are responsible for recognition of DNA damage and for recruitment of apical kinases. Among the first proteins sensing DNA discontinuities and accumulating at damaged sites are meiotic recombination 11-like protein (Mre11), radiation sensitive mutant (Rad) 50 and Nijmegen breakage syndrome protein 1 (Nbs1), which together form MRN complex. Further very early proteins are replication protein A (Rpa), Ku, Dna-dependent protein kinase catalytic subunit (Dna-Pkcs) and poly(ADP—ribose) polymerase 1 (Parp-1). MRN complex senses DNA DSBs and recruits apical kinase Ataxia telangiectasia mutated protein (Atm) to the damaged site. Rpa senses single stranded DNA (ssDNA) together with its partner Atr interacting protein (Atrip) and Rad9-Rad1-Hus1 complex. SsDNA is generated during resection of DSB breaks and at stalled or collapsed replication forks during DNA synthesis (S) phase. Rpa recruits apical kinase Atm-Rad3 related protein (Atr) to the damaged site. Ku and Dna-Pkcs are repair factors of DNA DSB repair pathway classical non-homologous end joining (c-NHEJ) and recruit further downstream proteins of this repair mechanism. Parp-1 senses ssDNA and is a repair factor of DNA DSB repair pathway alternative non-homologous end joining (alt-EJ) [9, 11, 12]. DNA DSB repair pathways will be explained separately in this introduction.

Atm and Atr are termed apical kinases to emphasize their pronounced role in DNA damage signaling. In combination with their mediators, they activate effector kinases in order to initialize outcome responses to DNA damage. One of the first proteins being activated by apical kinases is histone variant 2AX (γH2AX). γH2AX is important for chromatin remodeling, a prerequisite for DNA repair. It also recruits Atm mediator of DNA damage checkpoint protein 1 (Mdc1) to damaged sites. This protein serves as a binding platform for DNA repair proteins and induces a positive feedback loop of Atm signaling via the recruitment of more MRN complexes to the breaks. Further mediators of Atm are p53-binding protein 1 (53Bp1) and breast cancer protein 1 (Brca1) [9, 11, 12]. 53Bp1 maintains DNA damage signaling and plays a role in DNA DSB repair pathway choice as it is promoting c-NHEJ [13]. Brca1 contributes to homologous recombination repair (HRR), another DNA DSB repair pathway. Mediators of Atr are DNA topoisomerase 2-binding protein 1 (Topbp1) and Claspin. [9, 11, 12] Topbp1 is important for Atr kinase activity. Claspin is regulating downstream checkpoint kinase 1 (Chk1) [8].

Atm and Atr also activate downstream kinases Chk1 and Chk2 and the effectors tumor suppressor protein 53 (p53) and cell division cycle protein 25 (Cdc25), which exert final responses to DNA damage. Possible outcomes involve proliferation arrest by imposing cell cycle checkpoints, DNA repair and subsequent continuation of proliferation. In case of unfaithful DNA repair, cellular senescence and apoptosis can be induced, as well [9, 11, 12]. Imposition of cell cycle checkpoints and contribution of the downstream kinases and effector proteins therein will be presented in the next paragraph.

4.4 Cell cycle and DNA damage checkpoints

In order to pass on genetic information of DNA from one cell generation to the next, cells have to progress through the cell cycle (Figure 4). The cell cycle can be divided into the interphase, in which DNA gets replicated and cells are given time to prepare for cell division, and mitosis (M) phase in which the two copies of the genome get equally separated and two developing daughter cells finally divide [5].

Interphase consists of three phases occurring in a rigorously sequential order: a first gap (G_1) phase that takes place right after M phase has finished, S phase and a second gap (G_2) phase. Once G_2 phase has finished, cells undergo the next round of mitosis and the cell cycle starts anew. Strict execution of cell cycle phases in the

outlined sequence is controlled by a machinery of cyclins and cyclin dependent kinases (Cdks). Cyclins themselves do not possess any enzymatic activity. They bind to their respective Cdks causing an activation of enzymatic Cdk activity. The active complex is called cyclin-Cdk-complex. There are both, cyclins and Cdks assigned for each cell cycle phase. While different cyclins get periodically synthesized and degraded, protein expression of Cdks remains stable during the course of the cell cycle. Active cyclin-Cdk-complexes induce initiation of and transition through cell cycle phases. Degradation of cyclins induces termination of cell cycle phases [5]. Specific cyclins and Cdks will be presented during the further presentation of individual cell cycle phases.

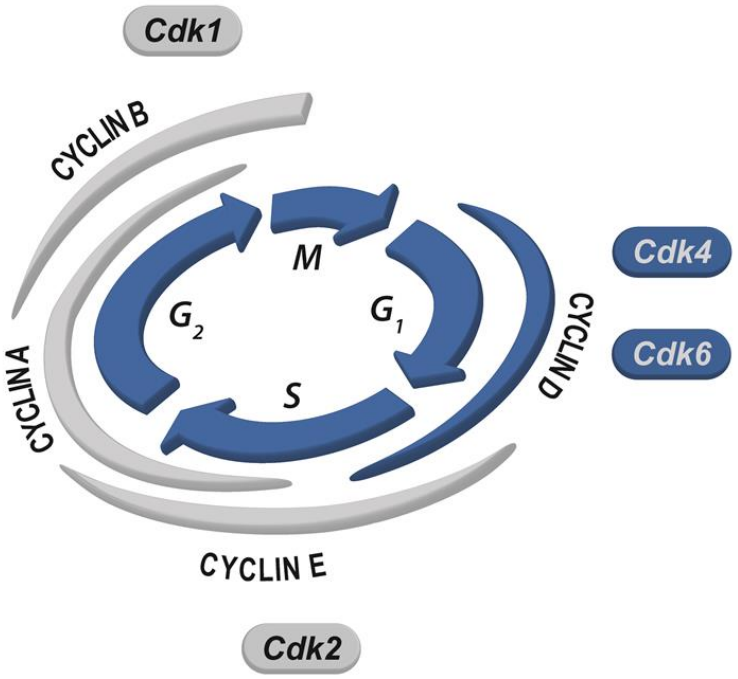

Figure 4: Cell cycle engine.
The cell cycle consists of G_1, S, G_2 and M phase, which are executed in a strictly sequential order. Complexes of cyclins and Cdks constitute the engine of the cell cycle and drive cells through different phases. See text for details.

4.4.1 G_1 phase

During M phase it is not only DNA content getting distributed onto daughter cells. All other cellular organelles and the cytoplasm get apportioned, too. In consequence, the two daughter cells enter G_1 phase with only half of the cellular content the mother cell had before it underwent M phase. Thus, missing cytoplasm and organelles get

replaced in G_1 phase. Additionally, DNA replication proteins are generated in preparation of subsequent S phase [5].

Initiation of G_1 phase specific cyclin production is controlled externally, by cell cycle inducing signaling, for example by growth factors or mitogens. Growth factors are present in the cellular microenvironment and described in paragraph 4.5. Their signaling induces synthesis of cyclin D, which binds to Cdk4 and 6 during mid G_1 phase and initiates further transition through this phase by inactivating retinoblastoma (Rb) proteins through phosphorylation and induction of late G_1/early S phase cyclin E. Phosphorylated Rb proteins trigger the activity of E2 transcription factors (E2F) which are necessary for S phase initiation. Cyclin D is degraded in late G_1 phase until early S phase. Cyclin E binds to Cdk2 and cyclin E-Cdk2-complex promotes transition from G_1 to S phase [14-16].

Before cells enter S phase and start DNA replication, it is controlled whether DNA is intact. In case of DNA damage, a cell cycle phase checkpoint is imposed. In general, several DNA damage checkpoints are strategically distributed over cell cycle phases (Figure 5) and prevent cells from further transition, fatal replication of damaged DNA (G_1/S phase checkpoint, S phase checkpoint) or distribution of damaged DNA onto daughter cells (G_2/M phase checkpoint). They also facilitate DNA repair. Once DNA damage is resolved, checkpoint pathways are stopped and the cell is allowed to resume transition through the cell cycle.

G_1/S phase checkpoint is imposed upon recognition of DNA DSBs by Atm and MRN complex. Atm induces activation of Chk2, which initiates proteolysis of cyclin-Cdk activating phosphatase Cdc25. This prevents activation of cyclin E-Cdk2-complex. Atm and Chk2 can also activate p53, which in turn induces production of Cdk2 inhibitor p21. Repair of DNA DSBs in late G_1 phase allows stable activation of cyclin E-Cdk2-complex and cells enter S phase [17, 18].

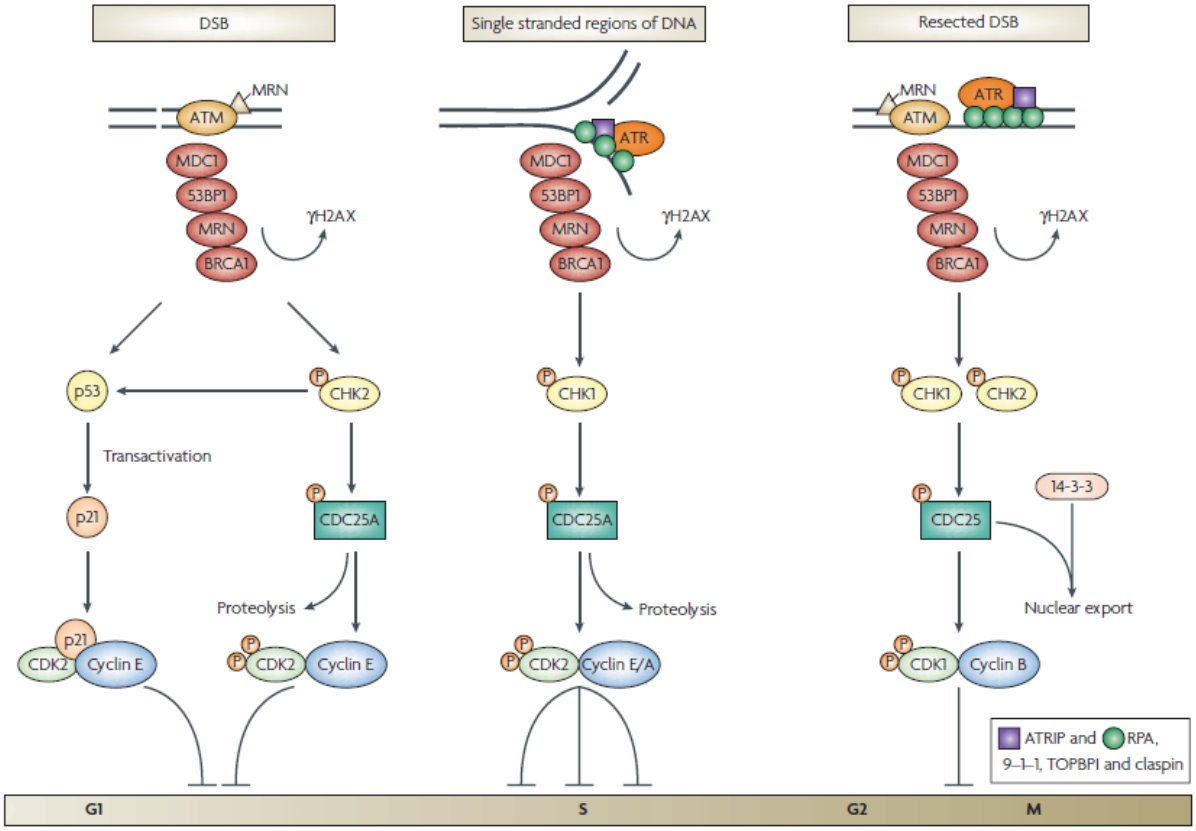

Figure 5: DNA damage induced cell cycle checkpoints.
Several DNA damage checkpoints are strategically distributed over cell cycle phases and prevent cells from further transition, fatal replication of damaged DNA or distribution of damaged DNA onto daughter cells. See text for details [17].

4.4.2 S phase

In S phase, the whole genome is copied exactly once in order to distribute one chromosome set, each, onto both daughter cells [5]. Cyclin E-Cdk2-complex induces the start of chromosomal DNA replication and cyclin E is subsequently degraded. S phase is further characterized by synthesis of cyclin A. Similar to cyclin E in G_1 phase, cyclin A forms an active complex with Cdk2. Cyclin A-Cdk2-complex controls DNA replication [14, 15, 19].

DNA damage in S phase imposes an S phase checkpoint. SsDNA but also stalled or collapsed replication forks activate Atr. Atr in turn activates Chk1 by phosphorylation and Chk1 initiates the proteolysis of Cdc25, leaving cyclin A-Cdk2-complex inactive. This suppresses DNA replication origins and slows down replication in consequence. Repair of DNA damage in S phase permits cyclin A-Cdk2-complex driven transition into G_2 phase [17, 18].

4.4.3 G_2 phase

G_2 phase serves for M phase preparation. Mitosis specific proteins are synthesized, cells lose contact to each other and increase in size [5]. G_2 phase progression is driven by constant increase of cyclin A synthesis, reaching its peak in late G_2 phase. It is degraded in late G_2 up to early M phase. In G_2 phase, active cyclin A-Cdk2-complex regulates replication origin relicensing [14]. It activates breakdown of the nuclear envelope and cyclin B relocation into the nucleus. Cyclin B is also termed M-cyclin to emphasize its critical role in M phase preparation and transition. Cyclin A-Cdk2-complex is further involved in regulation of cyclin B-Cdk1-complex inactivating Wee1. Finally, it is regulating Chk1 and the G_2/M phase checkpoint via cadherin-1 (Cdh1) and Claspin [19].
DNA damage in G_2 phase initializes G_2/M phase checkpoint via activation of Atm and/or Atr. Via their effector kinases Chk2 and Chk1, respectively, Atm and Atr can prevent members of the Cdc25 family from activating cyclin B-Cdk1-complex and thereby stop entry into M phase [17, 18].

4.4.4 M phase

Steady increase in cyclin B synthesis and complexing with Cdk1 drives cells into M phase [14, 19]. In M phase, DNA is first condensed into chromosomes and then equally distributed onto the emerging daughter cells. Afterwards, daughter cells divide during cytokinesis [5]. M phase is terminated by degradation of cyclin B, which releases the daughter cells into G_1 phase [14].

4.4.5 G_0 phase

In the beginning of G_1 phase, cells express no or only very limited amounts of any cyclins. The next cell cycle only starts, as mentioned above, upon cell cycle inducing stimulus [20]. If this stimulus fails to appear in G_1 phase, due to unfavorable environmental cell conditions, cyclin synthesis does not start and cells withdraw from active cycling. In this case, cells exit the cell cycle towards a postmitotic condition, which is termed G_0 phase (Figure 6) [21].
The discovery of G_0 phase emerged from the observation that not all cells of a population actively progress through the cell cycle, but that there is a subpopulation which is most likely non-proliferative. The term “growth fraction” was designated to

quantitatively express this phenomenon. Unfavorable conditions that drive cells into G_0 phase can be deprivation of nutrients [21, 22] or contact inhibition. It can also be induced, and this is mostly the case in stem cells, to maintain their key function of genomic integrity and to protect them from metabolic stress. As a tissue's stem cells give rise to all differentiated descendent cells, it is of paramount importance that their genome is protected from being damaged and that errors in the DNA are prevented from being passed on to the next cell generation. A stem cell's withdrawal from the cell cycle can also decrease the proliferation rate of a tissue and appears therefore crucial for tissue homeostasis [22].

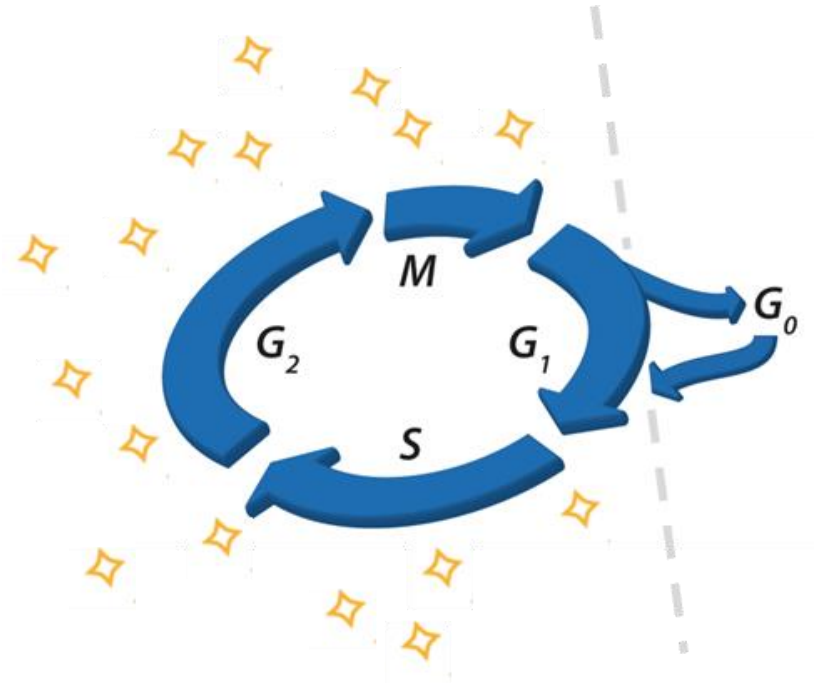

Figure 6: Cell cycle exit towards G_0 phase.
If cell cycle inducing stimulus fails to appear after M phase, cells withdraw from active cycling into a postmitotic condition named G_0 phase. This can happen upon unfavorable environmental conditions like nutrient/growth factor deprivation (exemplified by yellow rhombs) or contact inhibition. Cell cycle withdrawal can be reversible: if environmental conditions improve, cells re-enter G_1 phase and commence cycling. See text for details.

Withdrawal from the cell cycle and persistence in G_0 phase can be irreversible or reversible, depending on cell type. Terminally differentiated cells like neurons or cardiomyocytes but also senescent cells remain rather irreversibly in G_0 phase. Stem cells can switch reversibly between cycling and G_0 phase upon physiological stimulus. Similar behavior can be monitored in many experimental cell lines exiting the cell cycle upon cell culture serum deprivation (SD) and re-entering it upon serum replenishment (SR). SR is providing cell cycle inducing stimuli via growth factors or other mitogens that are contained therein. Once in G_0 phase, those cells have been also termed to be quiescent. Other cell types can persist in G_0 phase for very long

times or even for the rest of their lives, but would re-enter the cell cycle upon extraordinary stimuli if they must. Examples are differentiated hepatocytes that are able to rebuild big parts of the liver after partial hepatectomy or fibroblasts upon wound healing. Interestingly, there are also stem cell subsets described that proliferate only upon extraordinary events. In 2005, a subset of epidermal stem cells that does not contribute in tissue homeostasis but proliferates only upon tissue damage and in order to heal wounds was presented [23].

Biochemically, G_0 phase is characterized by low transcription patterns of proteins that are involved in cell cycle progression and checkpoint control. Cyclins E, A and B, for example, are expressed on low levels or not at all. Interestingly, G_0 phase cells display high levels of p53 and Rb proteins, which are also involved in perpetuating cell cycle checkpoints. Expression of Cdk inhibitors p21, p27 and p57 has been shown to be increased in G_0 phase stem cells. p27 and p57 are involved in transport of cyclin D into the nucleus [22, 24]. Finally, one peculiarity of G_0 phase cells is the absence of protein Ki67, a circumstance which will be described further below.

4.5 Growth factor signaling – the cell cycle kick-start

In paragraph 4.4.1 of this introduction it is mentioned that an active progression through the cell cycle is initiated in G_1 phase upon external stimulus. Most important in this regard is signaling that cells receive from soluble growth factors that are present in the cells' microenvironment. The following paragraph is concerned with intracellular growth factor downstream signaling and it starts with the presentation of receptor tyrosine kinases (RTKs), which are the major type of receptors transferring extracellular growth factor signals into the intracellular compartment.

4.5.1 Receptor tyrosine kinases

RTKs are transmembrane receptors integrated in the cell membrane and are the major type of receptors transferring extracellular growth factor signals into the cell. RTKs comprise three domains: an extracellular domain, a transmembrane helix and a cytoplasmic domain consisting of tyrosine kinases, juxtamembrane regulatory and carboxy-terminal sites. In general, mediation of growth factor signals by RTKs requires four sequential steps. A ligand binds to the extracellular domain of an inactive monomeric receptor molecule or an inactive receptor that already preexists as a dimer. Upon growth factor binding, monomeric receptor molecules dimerize.

Irrespective whether dimerization occurs before or after ligand binding, contact between ligand and receptor causes conformational changes of the receptor molecule, thereby activating it. At the intracellular part of the receptor, the tyrosine residue of each monomer autophosphorylates the tyrosine residue of the adjacent monomer. Therefore, one could also speak of a transphosphorylation. Finally, mediators of different downstream signaling pathways are recruited to the site of phosphorylated tyrosine domains [25, 26]. Major contributors of downstream signaling pathways (Figure 7) are serine/threonine kinases.

4.5.2 Pi3k pathway

The first major signal transduction cascade which is triggered upon growth factor activation, is the phosphatidylinositol 3-kinase (Pi3k) pathway (Figure 7, light blue pathway). Although Pi3k contributes to several biological processes, its main function is the upregulation of cell cycle progression as well as inhibition of apoptosis. Thus, Pi3k is a cell survival signal [27, 28]. Upon RTK activation, Pi3k is recruited to the receptor site and becomes phosphorylated. The catalytic subunit p110 of activated Pi3k induces conversion of phosphatidylinositol 4,5-bisphosphate (PIP_2) into phosphatidylinositol 3,4,5-trisphosphate (PIP_3). Several proteins are activated by PIP_3 and further downstream signaling is primarily fostered by 3'-phosphoinositide-dependent kinase 1 and 2 (Pdk1/2). Phosphorylation of both is required for subsequent activation of protein kinase B (Akt). Phosphorylated Akt is translocated into the cell nucleus, where it interacts with regulators of cell cycle progression and apoptosis [28, 29].

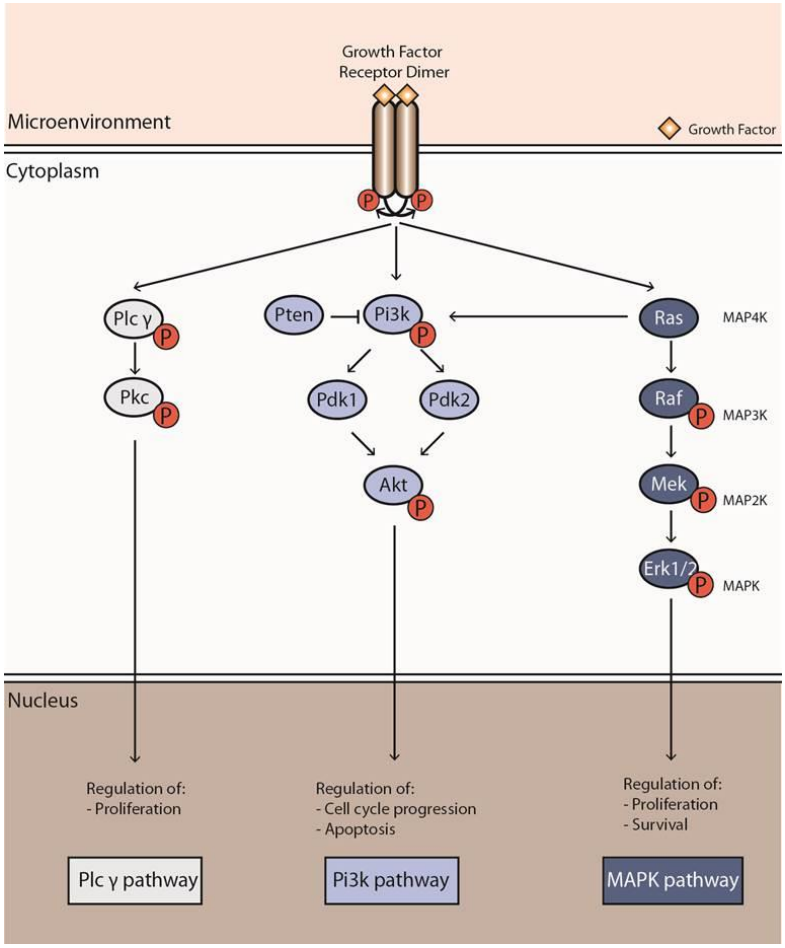

Figure 7: Major growth factor downstream signaling pathways.
Extracellular growth factors (yellow rhombs) bind to their receptors and induce downstream signaling via several pathways. Here, the major pathways Plc (white), Pi3k (light blue) and MAPK (dark blue) are presented in a simplified way. Arrows symbolize activating signals, normally executed through phosphorylations, which are depicted as the letter "P". Inhibitory signal is symbolized by an arrow with vertical arrow head. See text for details.

Akt regulates cell cycle progression at different levels: It is known to promote G_0/G_1, G_1/S and G_2/M phase transition. Of particular interest for this thesis is its function in the transition from G_0 via G_1 to S phase. It promotes progression of resting G_0 phase cells into G_1 phase of the cell cycle by enhancing transcription of myelocytomatosis viral oncogene (Myc), which positively regulates expression of D-type cyclins. Transition from G_1 into S phase is regulated by inactivation of Cdk inhibitors, p21 and p27. p21 and p27 prevent complexing of Cdks with cyclins and inhibit in this way the normal cell cycle progression. Akt, by phosphorylating p21 and p27 mediates their translocation from the nucleus into the cytoplasm allowing free interaction between Cdks and cyclins and, thus, progression through the cell cycle [29].

Akt itself underlies several regulative mechanisms. For instance, it can be activated by second messenger cyclic adenosine monophosphate, as well. On the other hand, Akt is negatively regulated by phosphatase and tensin homolog (Pten). Pten

dephosphorylates PIP_3, turns it into PIP_2 consequently rendering Akt into its inactive state [29].

4.5.3 MAPK pathways

The second group of major pathways, which are activated in response to growth factor signaling are mitogen activated protein kinase (MAPK) pathways (Figure 7, dark blue pathway). These signaling cascades influence gene expression by phosphorylating several transcription factors. In this way, they contribute to proliferation, but also to cellular morphology, metabolism and survival [28, 30].
Each MAPK signaling pathway can be subdivided into a four-stage cascade, starting with a MAP kinase kinase kinase kinase (MAP4K, for example Ras). Interestingly, mutated Ras proteins can activate the Pi3k pathway in an indirect fashion by increasing the production of RTK ligands [28]. Activation of a MAP4K is followed by a MAP kinase kinase kinase (MAP3K, for example Raf), a MAP kinase kinase (MAP2K or Mek) and, finally, a MAP kinase (MAPK, for example extracellular signal-regulated kinase Erk). The different MAPK pathways are not easy to contour as their participating proteins exhibit many pleiotropic and also redundant interactions. However, they can be characterized on the basis of the final MAPK that is activated and the distinct biological processes that are triggered thereupon. To date, four families of MAPKs have been described: The Jnk family is activated by growth factor signaling or by physiological and radiation-induced stresses and contributes to the development of the adaptive immune system and to hormonal responses. The p38 MAPKs are primarily activated upon chemical stresses and cytokines and play a role in inflammatory and autoimmune processes. A less studied family of MAPKs includes Erk3 and Erk5. Erk3 is atypical as it regulates itself via autophosphorylation. Erk5 is stimulated by growth factors and participates in cardiovascular development [30]. The best described family of MAPKs comprises Erk1 and Erk2, which are primarily activated by growth factors and are involved in proliferation and differentiation and are, thus, of interest for this thesis [28]. Active Erk proteins are transported into the nucleus were they bind to transcription factors in order to exert the above stated biological functions. Known interaction partners among transcription factors are NF-κB, Myc, Stat, Ap-1 and apoptotic machinery regulators of the Bcl-2 family [30].

4.5.4 Plcγ pathway

A third pathway being induced by growth factor signaling is the phospholipase C gamma (Plcγ) pathway (Figure 7, white pathway). Signal transduction via this pathway is mainly associated with malignant transformation, cell cycle regulation and apoptosis [31]. Upon RTK activation, Plcγ binds to the autophosphorylated receptor. This leads to the phosphorylation of Plcγ itself and an increase of its lipase activity. Thereby, Plcγ hydrolyses PIP_2. Hydrolysis products are inositol 1,4,5-triphosphate (IP_3) and the second messenger diacylglycerol (DAG). IP_3 induces release of calcium ions (Ca^{2+}) from the endoplasmic reticulum into the cytosol. Both, DAG and Ca^{2+} bind protein kinase c (Pkc) for activation. Further downstream signaling seems to be mediated by Pkc and also by Plcγ itself. There is less information available about substrate identity and substrate binding mechanisms of Pkc. This can be explained by an ample amount of distinct Pkc isozymes and a huge cell type dependency of Pkc function. Here, three Pkc isozymes will be mentioned, which display regulative functions in cell cycle promotion: Pkcα and Pkcδ exhibit a rather anti-proliferative function, as both increase expression of p21 and p27, and, in case of Pkcδ, downregulate cyclin A, D and E. In contrast to that, Pkcε displays an opposing role by increasing proliferation. This is exerted by an upregulation of cyclin D and E and sometimes also by trans-activation of Pi3k and MAPK pathways [31, 32].

4.6 Ki67 – a tool for cell cycle investigation

Nuclear protein Ki67 was discovered in the early 1980s at university hospital in Kiel, Germany (“Ki” stands for Kiel). In first reports about this protein it was shown to be present in actively cycling cells from various healthy tissues and in proliferating tumor tissues. In detail, it was demonstrated that Ki67 is constitutively present in all phases of the interphase, G_1, S, G_2, as well as in M phase. Only in non-cycling cells in G_0 phase and cells that were about to transit from G_0 to G_1 phase it could not be detected. The authors of these studies concluded that Ki67 might become a suitable indicator for cycling cells and proliferation in experimental procedures and in tumor diagnostics [33-35].

In later years, more information could be gathered. The gene encoding for Ki67 protein is located on chromosome 10 [36]. It is encoding for 30’000 base pairs which results in a large gene product between approximately 320 and 395 kilodaltons (kDa) exhibiting two different splice variants. Ki67 contains two different groups of potential

nuclear targeting sites (ten sites in total) and about 200 putative phosphorylation sites that might be targeted, amongst others, by Pkc, tyrosine kinases and Cdk1 [37, 38]. At least some of these sites were proven to be phosphorylated by Cdk1 in preparation of and during M phase [38, 39]. Ki67 further contains a forkhead-associated (FHA) domain. Ki67 shares the FHA domain with several other proteins that have been shown to regulate the cell cycle, like for example Rad53 in *Saccharomyces cerevisiae* and checking DNA synthesis kinase 1 (Cds1) in *Schizosaccharomyces pombe* [35, 38, 40, 41]. The human orthologue of both, Rad53 and Cds1, is Chk2.

Although a lot is known about Ki67, this protein lacks homologies to other proteins and, thus, its function cannot be inferred easily and still needs to be identified [35, 38, 41]. In general, the aforementioned FHA domains interact with Rad9, when phosphorylated, and might be involved in DNA damage signaling [42]. Ki67 seems to be obligatory for active cell cycling as treatment with antisense nucleotides results in abrogated cell proliferation [35, 37, 38, 41]. More recently, some nuclear functions of Ki67 have been detected: it is involved in ribosomal ribonucleic acid (RNA) transcription [43, 44] and helps to successfully distribute mitotic chromosomes onto daughter cells during M phase [45].

4.7 DNA double strand break repair pathways

It is estimated that there are 10-100 DNA DSBs occurring per nucleus and per day [46] and there are several pathways cells can employ to repair this kind of damage. These pathways operate with differences in fidelity and speed and also make use of different mechanisms to rejoin broken DNA molecules.

4.7.1 Homologous recombination repair

Homologous recombination is a process that occurs during meiosis I, where it is responsible for successful separation of chromosomes and recombination of paternal genes increasing diversity among offspring. It can also function in DNA DSB repair. Here, it is termed HRR and constitutes a high fidelity repair pathway, in which not only DNA DSBs are rejoined, but which also restores genetic integrity of DNA (Figure 8). For restoration of genetic information, involved pathway proteins are seeking for DNA sequences being homologous to the damaged DNA part and use this as a template to copy the sequence into the broken site. Typically, homologous

sequences are found in sister chromatids. As search for homology is time-consuming, it is a rather slow repair pathway.

HRR is extensively reviewed in [6, 47-49] and summarized here. The pathway can be divided into several different phases. DNA DSBs are first sensed by MRN complex. The complex also initiates 5'-3' DNA end resection, which constitutes the initial phase of HRR (Figure 8A). Mre11 is a nuclease, which has both, endonuclease and exonuclease activity on ssDNA. Rad50 is an ATPase that, together with Mre11, binds to DNA in close proximity to the DNA DSB. Nbs1 induces DDR through activation of Atm and recruits Ctbp interacting protein (CtIP), another nuclease and essential resection factor. Additionally, also Brca1 was shown to be contributive to DNA end resection. Although being quite important for initiation of HRR, resection by MRN complex and CtIP occurs on rather short ranges. Extensive resection is taken over by exonuclease 1 (Exo1) and DNA replication helicase/nuclease 2 (Dna2). End processing by all these nucleases generates 3'-OH DNA tails [6, 48]. Those bare ssDNA overhangs are quickly covered by Rpa, which has a high affinity for binding DNA, protects it from being cleaved nucleolytically and also eliminates secondary structures from it [47, 49].

The next phase of HRR is called presynaptic stage (Figure 8A), in which recombinase Rad51 gets recruited to the DNA DSB and covers the ssDNA in form of the so-called presynaptic filament (in meiosis I it is disrupted meiotic cDNA recombinase 1 (Dmc1)) [47]. Formation of the presynaptic filament is facilitated via Brca2 and its partner and localizer (Palb2), which remove Rpa and, instead, load Rad51 onto ssDNA tails [47, 50]. Brca2 is recruited by Brca1. X-ray repair cross-complementing proteins 2 and 3 (Xrcc2/3) support the buildup of the presynaptic filament and are paralogous to Rad51 [49]. Rad51 executes the next step of HRR: invasion of the ssDNA strand into other DNA stretches (Figure 8B). Here, Rad51 catalyzes DNA pairing and search for homologous sequences. Therefore, dsDNA stretches form so-called displacement loops (D-loops) in order to enable proper strand invasion and DNA annealing. DNA annealing is facilitated by HRR mediator Rad52. Once homology is found, the 3'-end of the invading strand will get extended [47].

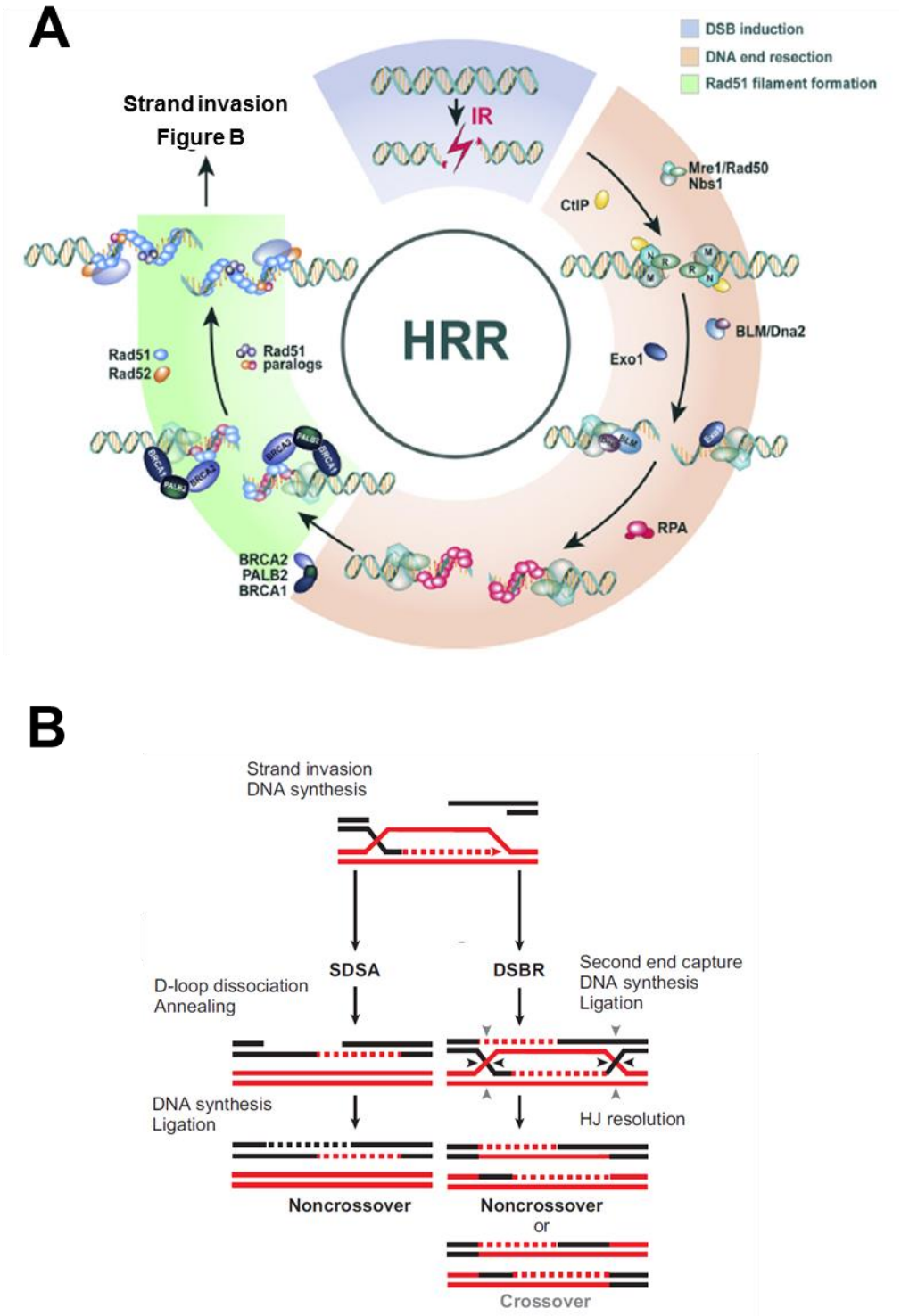

Figure 8: Slow, but high fidelity - DNA DSB repair by homologous recombination repair.
A) DNA DSB induction, end resection and presynaptic filament formation by Rad51 during HRR. Figure adapted from [6]. B) DNA strand invasion, D-loop formation, DNA synthesis and ligation in the two HRR repair models synthesis dependent strand annealing (SDSA) and double strand break repair (DSBR). In DSBR, HJs can be resolved in non-crossover products (cleavage occurs at black triangles) or in crossover products (cleavage occurs at grey triangles). Figure adapted from [47]. See text for details.

Homology-based repair of DNA DSBs can occur now by two different mechanisms – the synthesis dependent strand annealing (SDSA) model or the double strand break repair (DSBR, Figure 8B) model. During SDSA, the D-loop is migrating alongside DNA synthesis. Upon faithful restoration of the lost genetic sequence, the invading

strand detaches from the homologous site and ligates with the DNA end it originally broke from. Gap-filling of the second break occurs thereupon. During DSBR, not only the invading strand forms a joint with the homologous sequence in the D-loop, the second end of the DNA DSB is caught, as well, and anneals to the other strand of the D-loop. DNA synthesis occurs on both resected DNA strands and two X-shaped Holliday junctions (HJs) are formed. Their resolution can be realized in two ways: they either result in non-crossover products or crossover products, depending on how the intermediate DNA strands get cleaved by special enzymes (Figure 8B, refer to black and grey triangles). Here, HRR mediator Rad54 should be mentioned, too. It is involved in several of the lately mentioned steps. It functions during search for homology and D-loop construction, but also removes Rad51 from DNA after repair [6, 47, 49]. Enzymes resolving HJs are resolvases, for example Holliday junction 5’ flap endonuclease (Gen1), crossover junction endonuclease (Mus81), essential meiotic structure-specific endonuclease 1 (Eme1) and more [6, 49].

4.7.2 Classical non-homologous end joining

C-NHEJ operates with lower fidelity than HRR. Broken ends of DNA DSBs are simply rejoined without reconstructing integrity of the DNA sequence information [6] (Figure 9). Furthermore, c-NHEJ does not necessarily rejoin correct DNA ends. DNA ends of different origin, which happen to occur close to each other, can be rejoined, too. Thereby, c-NHEJ bears a higher risk of generating sequence and chromosomal aberrations than HRR [6, 51]. C-NHEJ is also operating fast: in experimental setups it has been shown that DNA repair by c-NHEJ resolves DSBs in less than half an hour [52].

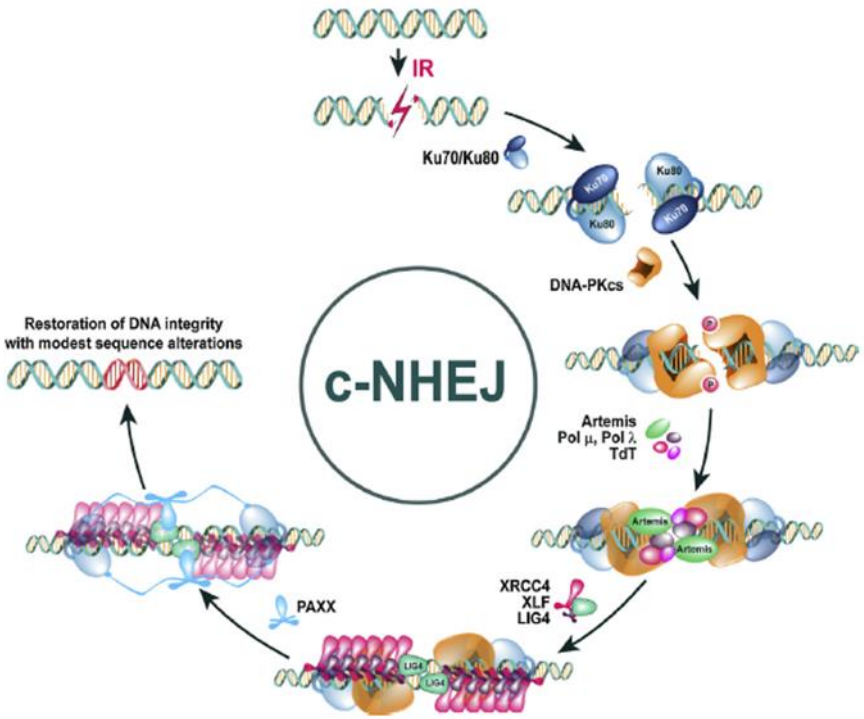

Figure 9: Fast, but error-prone - DNA DSB repair by classical non-homologous end joining.
DNA DSBs are first sensed by Ku which recruits Dna-Pkcs. DNA-Pkcs is a kinase orchestrating many protein actions during c-NHEJ. Breaks are processed by Artemis and several polymerases. Ligation is executed by Xrcc4/Xlf/Lig4 complex. See text for details. Figure adapted from [6].

Upon DNA DSB induction, discontinuities in DNA are first sensed by the two Ku proteins Ku70 and Ku80, which dimerize and bind DNA ends at each side of the break [6, 53, 54]. Ku recruits Dna-Pkcs to the damaged site [6, 55, 56] and Ku and Dna-Pkcs form together the Dna-Pk holoenzyme [55]. Dna-Pkcs is a member of the phosphatidylinositol 3-kinase-related kinase (PIKK) family (other members are Atm and Atr) and with its kinase activity it is able to recruit downstream participants of c-NHEJ pathway to the DNA DSB site and to phosphorylate them [6, 55]. Artemis is one of the first proteins that is recruited to the break by Dna-Pkcs [55, 57]. Artemis has a 5'-3' exonuclease and also a 5'-3' endonuclease activity and trims broken DNA ends to prepare them for further processing [6, 55, 57]. Afterwards, polymerases (Pol) are recruited and add nucleotides to the breaks. These polymerases are Polμ, Polλ and terminal deoxynucleotidyl transferase (TdT) [6, 58, 59]. In a final step, broken DNA ends are ligated by Xrcc4/ Xrcc4-like factor (Xlf)/Ligase (Lig) 4 complex. Xrcc4 and Xlf stabilize DNA ends [6, 60, 61] while final ligation is executed by Lig4 [6, 62].

C-NHEJ also occurs during variable (diversity) joining (V(D)J) recombination in lymphocytes and class switch recombination (CSR) in B cells. In these physiological processes, DNA DSBs are generated on purpose and resolved by c-NHEJ [63].

4.7.3 Alternative non-homologous end joining

In the past, it was discovered, that DNA DSBs can be resolved even if HRR and c-NHEJ fail to repair the damage. A third repair process was unveiled backing up deficiencies or abrogations in the first two pathways and, back then, it was therefore termed backup end joining to emphasize its substituting role in DNA DSB repair [52, 64]. Today, this Dna-Pkcs independent pathway is mainly called alt-EJ. Although knowledge about its participants and functions are still under development, many details are already discovered [6] and it has been validated that it is, indeed, a “robust pathway” functioning in the absence of Ku and Lig4 [48]. During alt-EJ, DNA DSB ends are rejoined while sequence information remains uncorrected. In contrast to c-NHEJ, broken ends are further resected prior to ligation, thereby turning alt-EJ into a slow and highly error-prone pathway [6] (Figure 10). This can result in tumorigenic rearrangements like chromosome translocations, eventually leading to malignancies of the hematological system but also to solid tumors [48].

Upon DNA DSB induction, Parp-1 senses breaks and binds to the damaged ends. The Parp family consists of polymerases catalyzing poly(ADP-ribosyl)ation (PARylation) events in proteins. This posttranslational modification was found to occur during DNA DSB repair. Inhibition of Parp-1 causes radiosensitization and is employed in cancer therapy. In comparison to Ku, Parp-1 has only inferior abilities to bind DNA ends, but once bound, it can shunt DNA DSBs into being processed by alt-EJ instead of c-NHEJ [6, 65-67]. Broken ends are further stabilized by histone 1 (H1), which also has a role in Parp-1 activation [6, 49, 68]. Subsequent end resection is executed by MRN complex and CtIP [6, 69]. Alt-EJ might involve DNA end alignment based on microhomologies and, thus, the involvement of Polθ, which can extend overhanging ssDNA at DSB ends. Polθ can also suppress Rad51 and could thereby be involved in DNA DSB repair pathway choice, channeling repair further into alt-EJ once it has been shunted into resection dependent repair pathways by MRN complex and CtIP [6, 70, 71]. Finally, ligation of DNA DSB ends is executed by Lig1 and Lig3 [6, 72, 73].

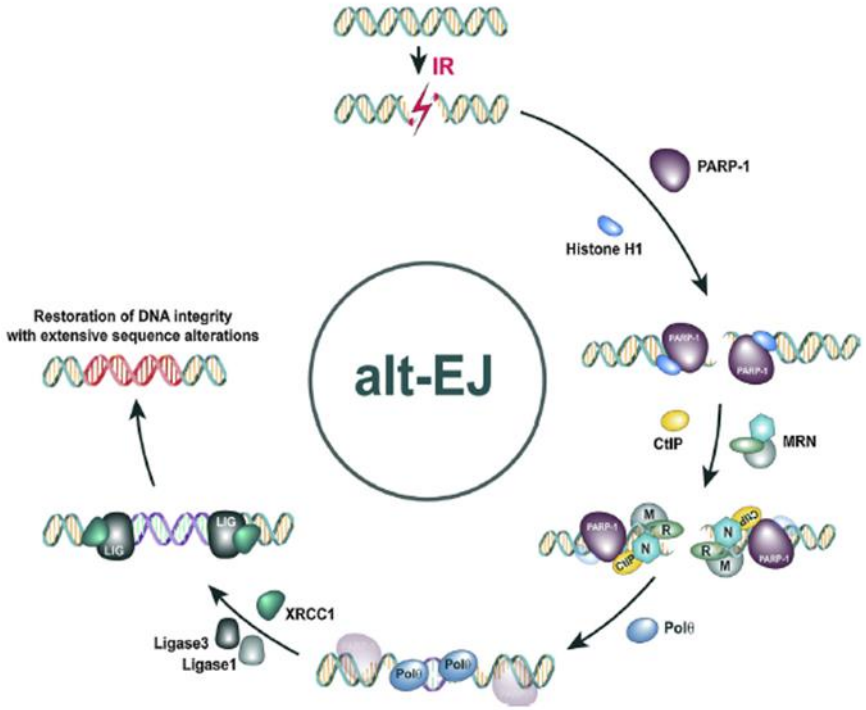

Figure 10: Slow and highly error-prone - DNA DSB repair by alternative non-homologous end joining. DNA DSBs are first sensed by Parp-1, followed by DNA end resection executed by MRN complex and CtIP. Ends are further processed by Polθ before ligation through Lig1 and Lig3. See text for details [6].

4.8 DNA double strand break repair pathway regulation

The focus on different cell cycle phases and molecular mechanisms driving cells through the cell cycle are of particular interest in radiobiology as the cell cycle is one of the major determinants on how cells can process DNA damage and especially how they can repair DNA DSBs. This, but also the mutual regulation of repair pathways by each other via resection are outlined below and ought to contour the interface of different cellular processes at which DNA DSB repair regulation, especially regulation of alt-EJ, occurs.

4.8.1 By the cell cycle machinery

The three repair pathways that are described above do not contribute equally to the removal of DNA DSBs (Figure 11). Repair efficiencies, but also the presence of pathways themselves vary throughout the cell cycle. Only c-NHEJ has been shown to operate independently from DNA damage imposed cell cycle checkpoints and is rather omnipresent in all cell cycle phases and in G_0 phase [6, 74-79].

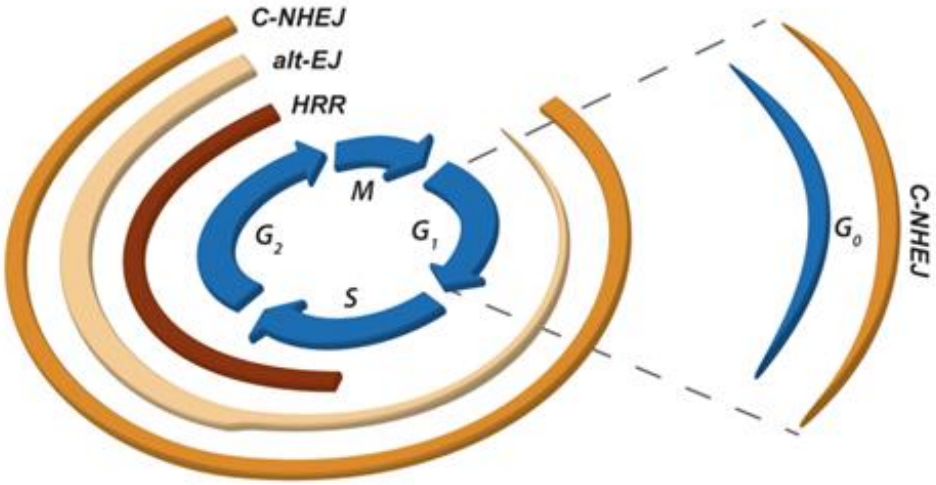

Figure 11: DNA DSB repair efficiencies of HRR, c-NHEJ and alt-EJ.
The three repair pathways do not contribute equally to the removal of DNA DSBs.

In comparison to c-NHEJ, utilization of HRR and alt-EJ are regulated extensively during cell cycle transition. An integral part of HRR is search for homology, which would be ideally found in sister chromatids. Based on this idea, it was assumed that HRR in higher eukaryotes should be present in S and G_2 phase when sister chromatids become available. Indeed, Takata and colleagues have shown that HRR is engaged in S and G_2 phase DT40 cells and that it is not present before DNA replication is initiated (in opposition to HRR in yeast, where it is present throughout the cell cycle) [80]. The dependency of HRR on S and G_2 phase and also its dependency on G_2 phase checkpoint have been shown later by others, as well [47, 48, 81].

Alt-EJ has been shown to be present throughout the cell cycle, but with varying efficiencies in certain cell cycle phases [77, 82]. In early experimental setups, wild type and Lig4 deficient mouse embryonic fibroblast (MEF) cells were used to differentiate between activity of c-NHEJ and alt-EJ and DNA DSB repair efficiency of proliferating cells and elutriated G_1 phase cells were analyzed. Alt-EJ, albeit performing with slower kinetics than c-NHEJ, could be documented in both cell subsets [76]. In further publications, an additional look was taken on the contribution of alt-EJ on the DNA DSB repair seen in G_2 phase. DNA DSB repair efficiency of proliferating, elutriated G_1 and G_2 phase cells was investigated and an increase of alt-EJ activity could be detected in G_2 phase. As HRR is active during G_2 phase, it might have had contributed to the observed increase in repair efficiency. To rule out this possibility, Rad54 deficient and Lig4 / Rad54 double deficient MEF cells were included in the study. In these cells, DNA DSB repair in G_2 phase could be detected,

too, and was therefore attributed to alt-EJ activity [83]. In Chinese hamster ovary (CHO) cells, an increased efficiency of alt-EJ in G_2 phase could be shown, as well [84].

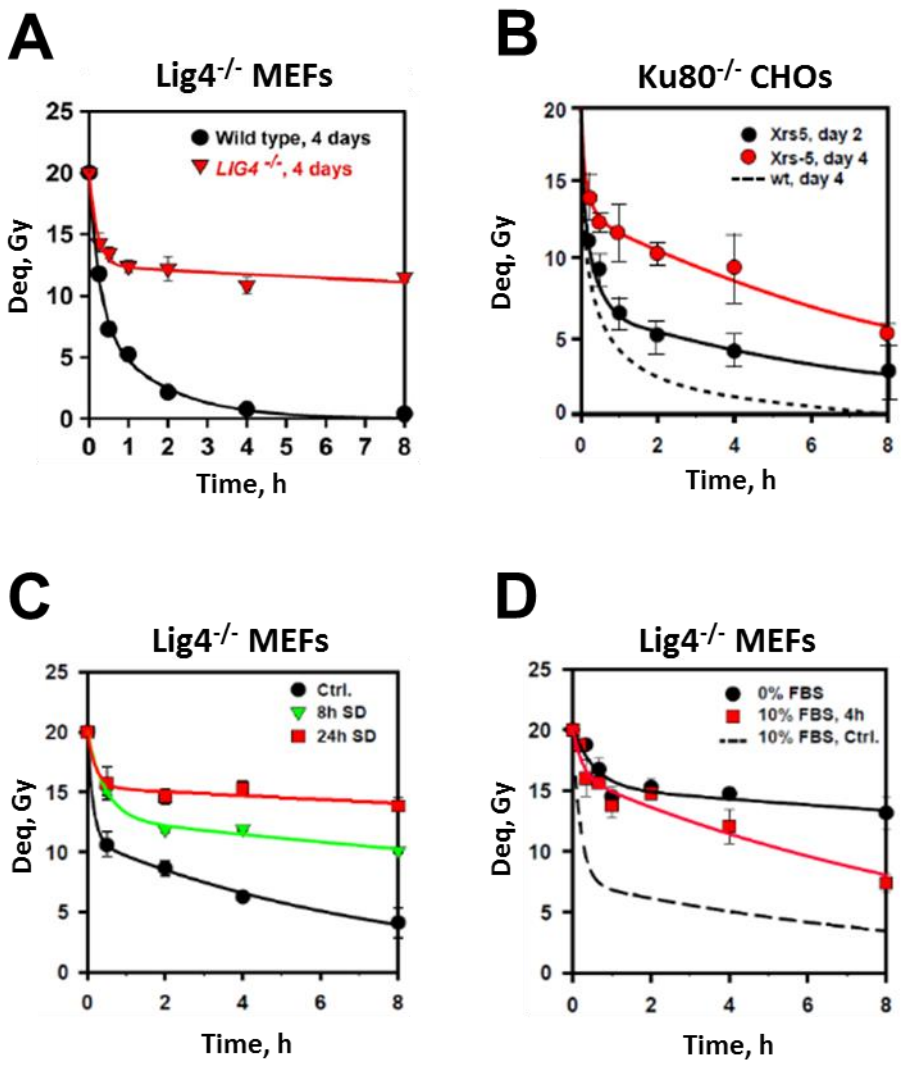

Figure 12: DNA DSB repair by alt-EJ is dependent on cell cycle status in rodent cell lines.
A) DNA DSB repair by alt-EJ is abrogated in Lig4 deficient MEF cells in plateau phase. 4 days: plateau phase. Figure adapted from [76]. B) DSB repair by alt-EJ is abrogated in Ku80 deficient CHO cells in plateau phase. Day 2: proliferating cells, day 4: plateau phase cells. Xrs-5: Ku80 deficient CHO cells, wt: wild type CHO cells in plateau phase. Figure adapted from [85]. C) DSB repair by alt-EJ is abrogated in serum deprived Lig4 deficient MEF cells. SD: serum deprivation, Ctrl.: non-serum deprived proliferating Lig4 deficient MEF cells. D) Abrogated DNA DSB repair by alt-EJ in serum deprived Lig4 deficient MEF cells recovers upon serum replenishment. 0 % FBS: serum deprivation from fetal bovine serum. 10 % FBS, 4h: serum replenishment with 10% serum for 4 hours. 10 % FBS, Ctrl.: non-serum deprived proliferating Lig4 deficient MEF cells. C-D) Figures adapted from [86]. h: hour, Deq: DNA damage, expressed as dose equivalent.

Even more important for this thesis is, that alt-EJ was shown to be strongly compromised as soon as cells withdrew from proliferation and exited the cell cycle towards G_0 phase. Windhofer and colleagues, whose contribution to the demonstration of alt-EJ presence in proliferating cells is presented above, also generated plateau phase cells from their wild type and Lig4 deficient MEF cells and measured alt-EJ activity in these non-cycling cells. In plateau phase of growth, alt-EJ

was clearly decreased (Figure 12A) [76]. As it was of question whether the observed decrease is specific only to the used cell lines, experiments were repeated in other c-NHEJ deficient mutants later on: Singh and colleagues [85] generated plateau phase cells from Ku70 and Ku80 deficient MEF cells, but also from Xrcc4 and Ku80 deficient CHO cells and found similar abrogation of alt-EJ in non-cycling cells (Figure 12B). However, generation of plateau phase cells bears one difficulty: cells enter their natural plateau of growth when the culture reaches a high cell density [22]. Factors that contribute to plateau phase induction can be contact inhibition due to the increasing lack of space and deprivation of nutrients due to high cell numbers. Spatial and/or nutritional conditions do not permit further proliferation, which allows experimentation in non-cycling cells but prevents investigation whether DNA DSB repair would recover when cells resumed cycling. Therefore, non-cycling cells were generated from Lig4 deficient MEF cells by SD in further experiments. SD was conducted at 50 % confluence, so before plateau phase was reached. Similar to results found in plateau phase cells, alt-EJ efficiency in serum deprived non-cycling cells was compromised, as well (Figure 12C).

Subsequently, cells were serum replenished in order to re-initiate cycling and evidence was provided that the seen effect of compromised alt-EJ was reversible thereupon (Figure 12D) [86].

4.8.2 By growth factor signaling

How do SD and SR manipulate transition through the cell cycle and, subsequently, DNA repair? The decision whether cells actively cycle or withdraw from it is directly dependent on the presence of growth factors. Growth factors are contained in serum. If growth factors are present, the cell cycle engine is engaged and cells transit through the cell cycle. If growth factors are absent, cells withdraw into G_0 phase. Here, the question arises whether absence of growth factors in G_0 phase is involved in the downregulation of alt-EJ and whether alt-EJ is engaged in proliferating cells as they receive growth factor signaling.

In general, it has been shown that growth factor signaling is of importance for regulation of DNA DSB repair. Especially the influence of epidermal growth factor/epidermal growth factor receptor (EGF/EGFR) induced signaling, as well as Akt mediated downstream signaling in c-NHEJ have been investigated. In this regard, it has long been known that EGFR and Dna-Pkcs are able to form complexes and it

was assumed that EGFR is contributing to the function of Dna-Pkcs in c-NHEJ. Chemical inhibition of EGFR or its targeting by antibodies (for example Cetuximab as it is used in cancer therapy) are delaying c-NHEJ and are causing radiosensitization [87, 88]. Akt, which is often overexpressed in cancer, was shown to be involved in accumulation of mutations and to be able to restrain IR induced G_2/M checkpoint, yet by unknown mechanism [89]. Later on, it was discovered that Akt has indeed a role in c-NHEJ. It complexes with Dna-Pkcs, guides it to sites of DNA DSBs, improves Dna-Pkcs kinase activity and, finally, is beneficial for the dissociation of Dna-Pkcs from DNA once damage is repaired [90, 91].

First efforts to analyze involvement of growth factor signaling in alt-EJ regulation have been made, too. Interestingly, treatment of serum deprived Lig4 deficient cells with EGF did not improve repair efficiency by alt-EJ and inhibition of EGFR did not decrease alt-EJ in proliferating cells, either. Nonetheless, the fact that SR improved alt-EJ in this experimental setup [86] might be indicative for an involvement of growth factors in this context. Elucidation of the contribution of growth factor signaling to alt-EJ downregulation in G_0 phase is of interest as human tissues are not only composed of proliferating, but also of differentiated G_0 phase cells. In fact, the latter largely dominate in number and their quiescent nature and their inability to employ two pathways of DNA DSB repair, HRR and alt-EJ, constitutes a major difference in comparison to tenaciously proliferating tumor cells. Understanding of the differential responses of proliferating and G_0 phase cells towards DNA DSBs is required for an improvement of radiation therapy as, to date, it is not possible to completely exclude healthy tissue that comprises non-proliferating cells in great abundance from irradiation treatment plans.

4.8.3 By CtIP

CtIP was first discovered to be an interacting protein of C-terminal-binding protein (Ctbp). It is a 125 kDa protein which can directly bind to Ctbp and was found to be involved in inhibition of tumorigenic processes caused by adenovirus E1A proteins [92]. Later on, it was shown that CtIP takes part in cell cycle regulation, too. It interacts with Rb proteins in G_1 phase and is crucial for G_1/S phase transition [93].

As knowledge about the protein increased, it was recognized that CtIP has manifold further functions in DNA metabolism, especially in DNA repair. It is recruited to sites of DNA DSBs during S and G_2 phase. Here, it is interacting with Nbs1 of MRN

complex and with Brca1. The complex of CtIP, MRN and Brca1 is activated by phosphorylation through Cdk2 and is involved in resection of DNA DSBs prior to repair [94-97]. Resection is a prerequisite for HRR and alt-EJ. It is also a process which is decisive for DNA DSB repair pathway choice as it shunts DSB repair towards HRR and alt-EJ and is excluding c-NHEJ ("point of no-return" [98]). If resection is taking place, c-NHEJ will not resolve damage occurring at the respective site [48, 96, 99, 100]. Thereby, CtIP is directly regulating DNA DSB repair pathway choice.

CtIP itself gets modified by several posttranslational processes, which cause further indirect involvement of the protein in the regulation DNA DSB repair pathways. As described above, CtIP is activated upon phosphorylation by Cdk2 [101]. Additionally, it receives further activating phosphorylation by Atm [102, 103]. Deacetylation and sumoylation of CtIP support DNA end resection and constitute further layers of control over the protein aside from Cdk activation [104, 105]. Additionally, CtIP can be ubiquitylated which leads to its degradation via the ubiquitin-proteasome pathway [106, 107]. Further studies in this respect were identifying anaphase-promoting complex/cadherin-1 (Apc/c^{Cdh1} complex) and Cullin 3 protein- kelch-like protein 15 (Cul3-Klhl15) ubiquitin ligase to playing major roles in targeting CtIP for proteasomal degradation and stated them to regulate CtIP's expression and thereby resection, predominantly in S/G_2 phase [108, 109], but also in G_0/G_1 phase of the cell cycle [108]. Proteasomal degradation is provoking a fluctuating expression of CtIP throughout the cell cycle, being absent in G_0 phase, low in G_1 phase and high in S and G_2 phase [108, 110-112].

In summary, CtIP seems to be a core factor for DNA DSB repair pathway choice as it directly regulates employment of repair pathways via its function as resection factor and indirectly as a protein which is involved in cell cycle progression and is controlled by the cell cycle machinery itself. This makes CtIP a very interesting candidate to study DNA DSB repair pathway choice in general and the regulation of alt-EJ in particular.

5. Objective

This thesis aims to investigate the regulation of DNA repair pathway alt-EJ. Its efficiency varies in cycling cells of different cell cycle phases and furthermore it is absent in non-cycling cells. As it constitutes one of the three major pathways resolving IR induced DNA DSBs from the genome, it is of interest to explore why not all cells are able to employ it and how it is regulated on a molecular level.

It is anticipated that regulation of alt-EJ can be studied best at the transition of G_0 phase, when it is absent, to G_1 phase, when it is present. Potential determinants controlling this process can be the cell cycle machinery itself, growth factor signaling and presence of resection factor CtIP. These determinants are mutually dependent to each other to some extent. Therefore, the project targets the elucidation of alt-EJ regulation at the interface of these determinants.

In the presented thesis it is first examined whether an abrogation of alt-EJ can be detected in human G_0 phase cells. Used cell lines are mainly generated from non-tumorigenic human fibroblast and epithelial cells, thus constituting good candidates to study DNA DSB repair in healthy tissue. G_0 phase cells are generated via SD. For this purpose it is important to employ advanced biochemical characterizations of distinct cell cycle phases and to detect necessary requirements for cell cycle exit and the generation of G_0 phase cells. DNA DSB repair kinetics of G_0 phase cells are analyzed and compared to the repair of cycling cells. In order to specifically assess DNA DSB repair that is conducted by alt-EJ and to exclude any repair events by c-NHEJ, an inhibitor of c-NHEJ engaging Dna-Pkcs is used throughout the thesis.

In a next step, G_0 phase cells are serum replenished to induce re-entrance into the cell cycle. By application of several inhibitors blocking cells in certain cell cycle phases and thereby excluding them from the experimental setup, it is attempted to determine the exact onset of alt-EJ and to narrow it down to a specific cell cycle phase. G_0 phase cells are further treated with single growth factors and effects are compared to those seen upon SR. Growth factor downstream signaling is examined in detail, inhibited and alt-EJ efficiency is measured thereupon.

Finally, CtIP contribution to alt-EJ regulation is investigated. CtIP expression in G_1 phase cells is downregulated and it is analyzed whether this treatment leads to an abrogation of alt-EJ. Vice versa, CtIP in G_0 phase is prevented from degradation and it is tested whether alt-EJ efficiency would converge to levels seen in G_1 phase.

6. Material and Methods

6.1 Material

Table 1: Cell lines.

Cell line	Cell type	Species	Characteristics
82-6 hTERT	fibroblastic	human	immortalized wild type
RPE-1 hTERT	epithelial	human	immortalized wild type
PC-3	epithelial	human	carcinogenic

Table 2: Cell culture media and supplements.

Cell culture medium	Supplier
Minimum Essential Medium (MEM)	Sigma-Aldrich, USA
Dulbecco's Modified Eagle Medium (DMEM)	Sigma-Aldrich, USA

Supplements	Supplier
Cell culture serum 82-6 hTERT	Gibco Cell Culture Media, Germany; Capricorn Scientific, Germany
Cell culture serum RPE-1 hTERT	Gibco Cell Culture Media, Germany
Cell culture serum PC-3	Gibco Cell Culture Media, Germany
Non-essential amino acids (NEA)	Merck Millipore, USA

Table 3: Composition of final cell culture media.

Cell line	Cell culture medium	Cell culture serum	NEA
82-6 hTERT	MEM	10 %	1 %
RPE-1 hTERT	DMEM	10 %	-
PC-3	MEM	10 %	-

Table 4: Inhibitors.

Inhibitor	Mode of action	Working concentration	Incubation time	Supplier
APC	Inhibition of polymerases α/δ/ε	3.0 µM	16 h pre IR	Santa Cruz Biotechnology, USA
BOR	Inhibition of proteasome	2.0 µM	2 h pre IR	SelleckChem, USA
CHX	Inhibition of eukaryotic protein synthesis	100 µg/ml	2 h pre IR	AppliChem, Germany
MIM	Late G_1 arrest*	400 µM	16 h pre IR	Sigma-Aldrich, USA

MK	Inhibition of Akt	various	1h pre IR	SelleckChem, USA
Nu7441	Inhibition of Dna-Pkcs	2.5 µM	1 h pre IR	Haoyuan ChemExpress, China
PD	Arrest between early and late G_1	0.5 µM	24 h pre IR** / 16 h pre IR***	SelleckChem, USA
TRA	Inhibition of Mek	various	1 h pre IR	

*dependent on cell line and treatment conditions
**for experimentation during SD
*** for experimentation during SR

Table 5: Primary antibodies.

Antigen (Clone)	Species / Type	$DF_{Western\ blotting}$	$DF_{Flow\ Cytometry}$	Supplier
Akt 1/2/3 (H-136)	rabbit / polyclonal	1:500 in 5 % milk/TBS-T	-	Santa Cruz Biotechnology, USA
pAkt Ser473 (D9E)	rabbit / monoclonal	1:2000 in 5 % BSA/TBS-T	-	Cell Signaling, USA
Cyclin A (C-19)	rabbit / polyclonal	1:1'000 in 5 % milk/TBS-T	-	Santa Cruz Biotechnology, USA
Cyclin D1 (na)	rabbit / polyclonal	1:1'000 in 5 % BSA/TBS-T	-	Cell Signaling, USA
Cyclin E1 (HE12)	mouse / monoclonal	1:1'000 in 5 % milk/TBS-T	-	Cell Signaling, USA
CtIP (D76F7)	rabbit / monoclonal	1:500 in 2.5 % milk/TBS-T	-	Cell Signaling, USA
Erk (3A7)	mouse / monoclonal	1:1'000 in 5 % milk/TBS-T	-	Cell Signaling, USA
pErk Thr202/Tyr204 (na)	rabbit / polyclonal	1:1'000 in 5 % BSA/TBS-T	-	Cell Signaling, USA
GapdH (6C5)	mouse / monoclonal	1:10'000 in 5 % milk/TBS-T	-	Merck Millipore, USA
Ki67 (na)	rabbit / polyclonal	-	1:500 in PBG	Abcam, UK
Ku70 (N3H10)	mouse / monoclonal	1:5'000 in 5 % BSA/TBS-T	-	GeneTex, USA
Ku86 (H-300)	rabbit / polyclonal	1:5'000 in 5 % milk/TBS-T	-	Santa Cruz Biotechnology, USA

Plc γ (D0H10)	rabbit / monoclonal	1:1'000 in BSA/TBS-T	-	Cell Signaling, USA
pPlc γ Tyr783 (D6M9S)	rabbit / monoclonal	1:1'000 in 5 % milk/TBS-T	-	Cell Signaling, USA
Pten (138G6)	rabbit / monoclonal	1:1000 in 5 % BSA/TBS-T	-	Cell Signaling, USA

Table 6: Secondary antibodies.

Specificity	Conjugate	Species / Type	$DF_{Western\ blotting}$	$DF_{Flow\ Cytometry}$	Supplier
anti-mouse	IRDye 680LT	goat / polyclonal	1:10'000 in TBS-T	-	Licor Biosciences, USA
anti-rabbit	IRDye 800CW	goat / polyclonal	1:10'000 in TBS-T	-	Licor Biosciences, USA
anti-rabbit	Alexa Fluor 488	goat / polyclonal	-	1:300 in PBG	Invitrogen, USA

Table 7: Chemicals and reagents.

Substance	Supplier
4-(2-hydroxyethyl)-1-piperazineethanesulfonic acid (HEPES)	Carl Roth, Germany
5-Ethynyl-2'-deoxyuridine (EdU)	Serva, Germany
Agarose LE Standard	Blirt, Poland
Ammonium persulfate (APS)	Sigma-Aldrich, USA
Ascorbic acid	Carl Roth, Germany
Basic FGF (bFGF)	Gibco Cell Culture Media, Germany
Boric acid	Carl Roth, Germany
Bovine serum albumin (BSA) fraction V	Carl Roth, Germany
Bromophenol blue	Sigma-Aldrich, USA
Coomassie brilliant blue G-250	Serva, Germany
Copper (II) sulfate pentahydrate ($CuSO_4$)	Sigma-Aldrich, USA
Cy5 azide dye	Lumiprobe, Germany
Dimethyl sulfoxide (DMSO)	Sigma-Aldrich, USA
Dithiothreitol (DTT)	Carl Roth, Germany
Ethanol (EtOH)	Sigma-Aldrich, USA
Ethidium bromide (EtBr)	Serva, Germany
Ethylenediaminetetraacetic acid (EDTA)	Carl Roth, Germany
Gelatin	Sigma-Aldrich, USA
Glycerol	Sigma-Aldrich, USA
Glycine	Carl Roth, Germany
Halt protease inhibitor cocktail (100X)	ThermoFisher Scientific, USA

LightCycler FastStart DNA Master Plus Sybr Green I	Roche Life Science, Switzerland
Low melting agarose	Carl Roth, Germany
Methanol (MeOH)	J.T. Baker, USA
N-Lauroylsarcosine (NLS)	Merck Millipore, USA
Non-fat dry milk	Carl Roth, Germany
Odyssey blocking buffer in TBS (OBB)	Licor Biosciences, USA
PageRuler plus prestained protein ladder	ThermoFisher Scientific, USA
Paraformaldehyde (PFA)	Carl Roth, Germany
Phosphatase inhibitor cocktail IV	Calbiochem, USA
Phosphoric acid (H_3PO_4)	Carl Roth, Germany
Potassium chloride (KCl)	Carl Roth, Germany
Potassium dihydrogenphosphate (KH_2PO_4)	Carl Roth, Germany
Propidium iodide (PI)	Sigma-Aldrich, USA
Proteinase K	Applichem, Germany
Ripa buffer	ThermoFisher Scientific, USA
RNase A	Applichem, Germany
Rotiphorese Gel 30	Carl Roth, Germany
Sodium chloride (NaCl)	Carl Roth, Germany
Sodium dodecyl sulfate (SDS)	Carl Roth, Germany
Sodium hydrogen carbonate ($NaHCO_3$)	Carl Roth, Germany
Sodium hydrogen phosphate (Na_2HPO_4)	Carl Roth, Germany
Sodium hydroxide (NaOH)	Carl Roth, Germany
Sucrose	Carl Roth, Germany
Tetramethylethylenediamine (TEMED)	Carl Roth, Germany
Tris base	Carl Roth, Germany
Triton X-100	Carl Roth, Germany
Trypsin	Biochrom, Germany
Tween-20	Carl Roth, Germany

Table 8: Formulations.

Solution	Formulation
Blocking buffer	TBS-T 2.5 % milk
Bradford solution	Aqua dest 0.05 % Coomassie brilliant blue G-250 25 % MeOH 45 % H_3PO_4
EdU Click-it reaction cocktail	1X PBS 100 mM Tris pH7.4 1.25 mM $CuSO_4$ 1.25 µM Cy5 azide dye, conjugate: Alexa Fluor 647 12.5 mM ascorbic acid

Electrode buffer (4X)	12.1 g Tris base 57.65 g glycine adjust to final volume of (ad) 1000 ml Aqua dest. pH 8.3
Fixation solution	50 ml 1X PBS 1.5 g PFA 20 µl 4N NaOH 1g sucrose pH 7.4
Lysis buffer	Aqua dest. 10 mM Tris base 100 mM EDTA 50 mM NaCl 2 % NLS pH 7.6 add 0.2 mg/ml proteinase K prior to use
PBG	50 ml 1X PBS 0.1 g gelatine 0.25 g BSA
PBS (10X)	1000 ml Aqua dest. 2.0 g KCl 2.0 g KH_2PO_4 80.0 g NaCl 10.5 g Na_2HPO_4
PI solution	100 ml 1X PBS 400 µg PI 620 µg RNase A
Resolving gel (10 %)	3.4 ml Rotiphorese Gel 30 2.5 ml 4X resolving gel buffer 3.8 ml Aqua dest. 0.1 ml 10% SDS 0.1 ml 10% APS 0.01 ml TEMED
Resolving gel buffer (4X)	18.2 g Tris base 0.4 g SDS ad 100 ml Aqua dest. pH 8.8
RNase buffer	Aqua dest. 10 mM Tris base 100 mM EDTA 50 mM NaCl pH 7.6 add 0.1 mg/ml RNase prior to use

Running buffer (10X)	30.2 g Tris base 144 g glycine 10 g SDS ad 1000 ml Aqua dest.
Sample loading buffer (2X)	0.65 ml 1M Tris-HCl pH 6.8 0.2 ml 0.5M EDTA 2 ml 100 % glycerol 3 ml 10% SDS 0.4 ml 0.5 % bromophenol blue ad 10 ml Aqua dest. add 200 µl 100 % DTT prior to use
Serum-free HEPES buffered medium	200 ml medium 0.084 g $NaHCO_3$ 0.953 g HEPES
Stacking gel (5 %)	0.84 ml Rotiphorese Gel 30 1.25 ml 4X stacking gel buffer 2.8 ml Aqua dest. 0.05 ml 10 % SDS 0.05 ml 10% APS 0.01 ml TEMED
Stacking gel buffer (4X)	6.5 g Tris base 0.4 g SDS ad 100 ml Aqua dest. pH 6.8
TBE (10X)	1000 ml Aqua dest. 107.81 g Tris base 55.02 g boric acid 40 ml 0.5 M EDTA pH 8.0
TBS	3 g Tris base 8 g NaCl ad 1000 ml Aqua dest. pH 7.6
TBS-T	TBS 0.05 % Tween-20
Washing buffer	Aqua dest. 10 mM Tris base 100 mM EDTA 50 mM NaCl pH 7.6
Transfer buffer	250 ml 4X Electrode buffer 200 ml 100% methanol ad 1000 ml Aqua dest.

Table 9: Primers for RT-qPCR.

GOI	Primer	Supplier
HsCTIP	FW: AGA AGA TCG GTT AAG AGC AGG C RV: TGC TGG AGT TGT TCA GAA AGC	personal design; generated by Eurogentec, Belgium
HsGAPDH	FW: TCC ATG ACA ACT TTG GTA TCG TGG RV: GAC GCC TGC TTC ACC ACC TTC T	sequence as offered from Biometra, Germany; generated by Eurogentec, Belgium

Table 10: Kits.

Kit	Supplier
High Pure RNA Isolation Kit	Roche Life Science, Switzerland
RevertAid H Minus First Strand cDNA Synthesis Kit	ThermoFisher Scientific, USA

Table 11: Consumables.

Consumable	Supplier
1.5 ml reaction tubes	Eppendorf, Germany
5 ml / 10 ml / 25 ml serological pipettes	Sarstedt, Germany
5 ml glass serological pipettes	Brand, Germany
10 µl / 20 µl / 200 µl / 1000 µl pipette tips	Starlab International, Germany
12 ml round bottom tubes	Greiner Bio-One, Austria
15 ml / 50 ml pointed bottom tubes	Greiner Bio-One, Austria
20 µl LightCycler capillaries	Roche Life Science, Switzerland
60 mm / 100 mm cell culture dishes	Greiner Bio-One, Austria
Blotting paper MN 827 B	Macherey-Nagel, Germany
Coulter Counter measurement vessels	Beckman Coulter, USA
Cuvettes, semimicro-cell	LLG Labware, Germany
Glass Pasteur pipettes	Brand, Germany
Odyssey nitrocellulose membrane	Licor Biosciences, USA

Table 12: Centrifuges.

Centrifuge	Supplier
Biofuge fresco	Heraeus, Germany
LC Carousel Centrifuge 2.0	Roche Life Science, Switzerland
Rotanta 460 R	Hettich Zentrifugen, Germany

Table 13: Incubating equipment.

Incubator	Supplier
C20 waterbath	Lauda, Germany
HeraCell 240 cell culture incubator	Heraeus, Germany
IncuSafe cell culture incubator	Sanyo, Japan
Medax heating plate	Oehmen Labortechnik, Germany
Thermomixer Comfort heating block	Eppendorf, Germany
WB-12 waterbath	PhoenixInstrument, Germany

Table 14: Laminar flow benches.

Laminar flow bench	Supplier
HeraSafe	Heraeus, Germany
MSC-Advantage	ThermoFisher Scientific, USA

Table 15: Measurement equipment.

Measurement device	Supplier
Gallios Flow Cytometer	Beckman Coulter, USA
LightCycler 2.0	Roche Life Science, Switzerland
Multisizer 3 Coulter Counter	Beckman Coulter, USA
Multisizer 4e Coulter Counter	Beckman Coulter, USA
ND-1000 spectrophotometer	NanoDrop Technologies, USA
Odyssey Infrared Imager	Licor Biosciences, USA
Typhoon 9410 Variable Mode Imager	Amersham, UK
UV-2401 PC spectrophotometer	Shimadzu, Japan

Table 16: Microscopes.

Microscope	Supplier
Olympus	HiTech Instruments, USA
Wilovert S	Hund Wetzlar, Germany

Table 17: Pipettes.

Pipette	Supplier
2 µl / 10 µl / 20 µl / 100 µl / 200 µl / 1000 µl pipettes	Rainin, Mettler Toledo, USA
Falcon Express Pipetboy	Becton Dickinson, USA

Table 18: Refrigeration units.

Refrigeration unit	Supplier
+ 4 °C / - 20 °C refrigeration unit	LG Electronics, South Korea
-20 °C Liebherr Profiline freezer	Liebherr, Switzerland
-80 °C MDF-U700VX freezer	Panasonic, Japan
-150 °C Ultralow freezer	Sanyo, Japan

Table 19: Further equipment.

Device	Supplier
Isovolt 320HS X-ray tube	General Electric, USA
Kern 572 scale	Kern, Germany
LightCycler centrifuge adapters	Roche Life Science, Switzerland
MilliQ Reference A+ ultrapure water system	Merck Millipore, USA
Mini-Protean Tetra Vertical Electrophoresis Cell	BioRad, USA
Mini Trans-Blot Cell	BioRad, USA
MR Hei-Mix L magnetic stirrer	Heidolph, Germany
Orbital rocking shaker 3012	GFL, Germany
PFGE electrophoresis chambers	Bespoke product, Universitätsklinikum Essen fine mechanics workshop, Germany
PFGE gel casting units	Bespoke product, Universitätsklinikum Essen fine mechanics workshop, Germany
PowerPac Basic power supply	BioRad, USA
VWR-124 special accuracy scale	Sartorius, Germany
FE20 pH-meter	Mettler Toledo, USA

Table 20: Software.

Software	Supplier
Adobe Illustrator 15.0	Adobe, USA
EndNote X8	Thomson Reuters, USA
ImageQuant 5.2	GE Healthcare, Germany
Kaluza 1.2	Beckman Coulter, USA
Microsoft Office 2010	Microsoft, USA
MultiCycle AV DNA Analysis	Phoenix Flow Systems, USA
Odyssey Infrared Imaging System	Licor Biosciences, USA
SigmaPlot 12.5	Systat Software, USA

6.2 Methods

6.2.1 Cell culture

Frozen cells were gently thawed and suspended in pre-warmed cell culture medium. Cell suspension was spun down to separate cells from DMSO-containing freezing medium and supernatant was aspirated. Pelleted cells were re-suspended in pre-warmed cell culture medium, seeded in 100 mm-dishes and passaged at least three times before seeding for experiments (Table 21).

Table 21: Cell culture conditions.

Cell cultivation				
Cell line	**Cell culture medium**	**Dish [Ø mm]**	**Passage [days]**	**Cells seeded [x10^6]**
82-6 hTERT	15 ml + 10 % serum + 1 % NEA	100	2	0.4
RPE-1 hTERT	15 ml + 10 % serum	100	2	0.5
PC-3	15 ml + 10 % serum	100	3 / 4	0.4 / 0.3
Seeding for experiments				
82-6 hTERT	5 ml + 10 % serum + 1 % NEA	60	2	0.2
RPE-1 hTERT	5 ml + 10 % serum	60	2	0.1
PC-3	5 ml + 10 % serum	60	2	0.2

For passaging, cells were controlled microscopically, cell culture medium was aspirated and cells were washed with 1 X phosphate buffered saline (PBS). Cells were detached by adding 1 ml trypsin. Trypsin was directly aspirated and cells were incubated on a heating plate for 3 minutes (min). Trypsinization was stopped by adding cell culture medium containing serum. Cells were gently re-suspended and counted with a Coulter Counter. Cells were seeded in new cell culture dishes according to Table 21 and incubated at 37 degrees centigrade (°C), 5 % carbon dioxide (CO_2) in a cell culture incubator.

6.2.2 Cell seeding for experimentation, serum deprivation and serum replenishment

For experimentation, cells harvested from cell culture were seeded in 60 mm-dishes in 5 ml of their respective medium (Table 21, if not stated otherwise) and incubated at 37 °C, 5 % CO_2. For SD, cell culture medium was aspirated and cells were washed twice with pre-warmed cell culture medium without supplements. Subsequently, 5 ml cell culture medium without supplements were pipetted onto the cells. Cells were incubated at 37 °C, 5 % CO_2. For SR, cell culture medium of serum deprived cells was aspirated and 5 ml of cell culture medium containing respective supplements were pipetted to the cells. Cells were incubated at 37 °C, 5 % CO_2.

6.2.3 Generation of growth curves and one-parametric flow cytometry analysis of cell cycle distribution

Cellular growth curves were generated in order to assess doubling time of cells and to identify the time point at which cells enter their natural plateau phase of growth. 0.1 x 10^6 cells were seeded and incubated for 1 – 10 days at 37 °C, 5 % CO_2. Each day, cells of one dish were controlled microscopically. Cell culture medium was aspirated and cells were washed with 1 X PBS. Cells were detached by adding 1 ml of trypsin. Trypsin was directly aspirated and cells were incubated for 3 min on a heating plate. Cells were collected in cell culture medium and counted. Remaining cell suspension was spun down, cell culture medium was aspirated and cells were fixed in ice-cold 70 % EtOH. Cells were stored at 4 °C until further cell cycle analysis by flow cytometry.

For cell cycle analysis by flow cytometry, cells being fixed in EtOH were spun down. EtOH was thoroughly aspirated and pelleted cells were re-suspended in propidium iodide (PI) solution. Cells were incubated for 30 min at 37 °C in a water bath and subjected to flow cytometry analysis, which was conducted with a Gallios flow cytometer. Cell cycle distribution was quantified with MultiCycle AV DNA Analysis application.

6.2.4 Two-parametric flow cytometry analysis of cell cycle distribution and Ki67 immunostaining

Cells were collected in ice-cold cell culture medium and placed on ice. If not stated otherwise, further processing took place on ice. Cells were counted. Remaining cell suspension was spun down, cell culture medium was aspirated and cells were

permeabilized for 5 min in 0.2 % Triton X-100 / 1 X PBS. Cells were spun down and supernatant was aspirated. Cells were fixed for 15 min at room temperature (RT) in fixation solution, spun down, blocked in PBG and stored at 4 °C until further processing.

Cells were spun down, supernatant was aspirated and cells were incubated with rabbit anti-human Ki67 antibody for 1.5 hours (h) at RT. Cells were spun down, supernatant was aspirated and cells were washed with 1 X PBS. Cells were spun down, supernatant was aspirated and cells were incubated with Alexa Fluor 488-coupled goat anti-rabbit antibody in the dark for 1.5 h at RT. Cells were spun down, supernatant was aspirated and cells were re-suspended in PI solution. Cells were incubated for 30 min at 37 °C in a water bath and subjected to flow cytometry analysis. Cell cycle distribution and Ki67 immunostaining was quantified with the applications Kaluza 1.2 and MultiCycle AV DNA Analysis application.

6.2.5 Three-parametric flow cytometry analysis of cell cycle distribution, Ki67 immunostaining and S phase cells

Seeded cells were controlled microscopically and pulsed-labelled with EdU for 30 min at 37 °C, 5 % CO_2. Cells were further processed as described in paragraph 6.2.4 until incubation with Alexa Fluor 488-coupled goat anti-rabbit antibody was accomplished. Cells were spun down and incubated with EdU Click-it reaction in the dark for 30 min while gently shaking on a rocking shaker. Cells were spun down, supernatant was aspirated and cells were washed with 1 X PBS. Cells were incubated with PI solution and subjected to flow cytometry analysis. Quantifications of all three parameters were conducted with the applications Kaluza 1.2 and MultiCycle AV DNA Analysis application.

6.2.6 Pulsed-field gel electrophoresis

During pulsed-field gel electrophoresis (PFGE) analysis, DNA DSB breaks are induced by IR and cells are given different time periods to rejoin broken DNA ends by non-homologous end joining (NHEJ, including c-NHEJ and alt-EJ). DNA of each sample is subjected to gel electrophoresis during which DNA migrates through an agarose gel. The electrophoretic mobility of DNA is according to the molecule’s size and charge. The shorter (thus more damaged) DNA is, the further it migrates through

the agarose gel. The longer (thus more intact or more repaired) DNA molecules are, the less they migrate through the gel.

6.2.6.1 Repair kinetics

For repair kinetics, cells seeded in 60 mm-dishes were controlled microscopically, irradiated with 20 gray (Gy) and directly replaced into the cell culture incubator at 37 °C, 5 % CO_2. Irradiation was conducted with an X-ray tube (320 kV, 12.5 mA, 1.65 mm aluminum filter). At each indicated time point, medium of two dishes was aspirated, cells were washed with 1 X PBS and 1 ml of trypsin was added to the cells. Trypsin was directly aspirated and cells were incubated on a heating plate for 3 min. Cells were re-suspended with glass serological pipettes in order to generate single-cell suspensions, pooled in ice-cold medium and placed on ice. If not stated otherwise, further processing took place on ice. Cells were counted and remaining cell suspension was spun down. Pelleted cells were thoroughly re-suspended in HEPES-buffered medium without supplements. HEPES-buffered cell suspension was mixed 1:1 with 1 % low melting agarose/HEPES-buffered medium and poured into glass tubes. Solidified cell-agarose mixture was cut in 5 mm long plugs, placed in protein degrading lysis buffer in 12 ml round-bottom tubes and stored at 4 °C until further processing. At two time points, plugs of unirradiated control cells were generated as controls, as well.

6.2.6.2 Dose response

For the “dose response” termed standard curve, cells seeded in 60 mm-dishes were not irradiated, but collected and processed into plugs as described above. Cell plugs were placed in 60 mm-dishes containing HEPES-buffered medium and irradiated with increasing dosages on ice. Afterwards, plugs were placed in protein degrading lysis buffer in 12 ml round-bottom tubes and stored at 4 °C.

6.2.6.3 Pulsed-field gel electrophoresis

Cell plugs were incubated in lysis buffer for 18 h at 50 °C, then washed in washing buffer for 1 h at 37 °C and finally incubated in RNA degrading RNase buffer for 1 h at

37 °C. All incubations took place in water bathes. RNase buffer was discarded and cell plugs were stored in washing buffer at 4 °C until further processing.
For pulsed-field gel electrophoresis, 0.5 % agarose/0.5 X TBE gels were poured and cell plugs were inserted into the gel pockets. Gels were subjected to a pulsed electrical field for 40 h at 4 – 6 °C in 0.5 X TBE. An electrophoresis run consisted of alternating forward and reverse pulses (forward: 900 seconds at 50 V, reverse 75 seconds at 200 V). The PFGE system consisted of bespoke systems for gel casting and PFGE electrical field switching units, as well as commercially available standard power supply units. Afterwards, gels were stained with 5mg/ml EtBr in the dark for 4 h, gently shaking on a rocking shaker. Gels were washed four times (3 x 1h, 1 x overnight) and finally scanned with a variable mode imager to visualize DNA release. DNA release of cells subjected to DNA DSB repair kinetic analysis and cells subjected to dose response analysis was analyzed with ImageQuant 5.2 application.

6.2.7 Western blotting

6.2.7.1 Generation of protein lysates

In order to make cellular proteins accessible to analysis, protein lysates were generated. Harvested cells were collected in ice-cold cell culture medium and placed on ice. If not stated otherwise, further processing took place on ice. Cells were counted. Remaining cell suspension was spun down and cell culture medium was aspirated. Pelleted cells were re-suspended in 1 X PBS and were spun down again. Pelleted cells were re-suspended very thoroughly in RIPA-buffer containing phosphatase inhibitor (diluted 1:100) and protease inhibitor (diluted 1:50) cocktails. Cells were incubated for 20 min and then sonicated for 3 x 1 seconds. Cells were incubated for further 20 min and then spun down. Protein containing supernatant was stored at – 20 °C and DNA containing pellet was discarded.

6.2.7.2 Determination of protein concentrations

For protein analysis by Western blotting, equal amounts of protein samples need to be loaded on SDS polyacrylamide gels. Therefore, protein concentrations were determined quantitatively by Bradford assay. 1 ml of Bradford solution was pipetted into cuvettes and thoroughly mixed with 1 µl of protein sample. Additionally, samples

for a BSA-standard curve were prepared as well. Protein concentrations were determined with a UV-2401 PC spectrophotometer.

6.2.7.3 SDS polyacrylamide gel electrophoresis

In order to detect proteins of interest, proteins in collected samples first had to be separated in a gel matrix. Separation occurrs according to the proteins' mass-to-charge ratio. Therefore, SDS containing polyacrylamide gels consisting of a 5 % stacking and a 10 % resolving component were poured. Concentration of protein lysates was adjusted to a final protein concentration between 30 – 80 µg / gel pocket and mixed 1:1 with 2 X sample loading buffer to a total volume of < 40 µl. Proteins were denatured for 5 min at 95 °C in a heating block, spun down, chilled on ice and loaded into the gels. Electrophoresis was performed in 1 X running buffer in electrophoresis cells at 100 V.

6.2.7.4 Protein transfer

Proteins were needed to be transferred from polyacrylamide gels to membranes in order to detect proteins of interest by immunochemistry. Transfer was conducted by wet electroblotting. Gels were placed on nitrocellulose membranes within a stack of blotting papers and foam pads. Membrane, blotting paper and foam pads were equilibrated in transfer buffer before stack assembly. Stacks were incorporated in trans-blot cells filled with ice-cold transfer buffer on ice. Electroblotting was executed at 120 V for 1 h. In this time, proteins migrated from gel to membrane.

6.2.7.5 Protein detection

Final detection of proteins was conducted by immunochemistry. After protein transfer, the membrane was incubated in blocking buffer for 1 h at RT to prepare it for protein detection and to exclude non-specific binding of antibodies to the membrane.
Incubation took place on a rocking shaker. For substrate reaction, membranes were then incubated with primary antibody solutions being specific for their target proteins at 4 °C overnight on a rocking shaker. Antibody solutions were prepared according to

Table 5 and Table 6. Membranes were washed 3 x 10 min in TBS-T and were incubated with secondary antibody solutions in the dark for 1 h at RT on a rocking shaker. Subsequently, membranes were washed 3 x 10 min in TBS-T and dried in the dark. Secondary antibodies were labelled with infrared dyes (IRDyes) which were detected using the Odyssey Infrared Imager.

6.2.8 Quantitative real-time polymerase chain reaction

6.2.8.1 Generation of RNA lysates

In order to be able to analyze expression of messenger RNA (mRNA), total cell lysates were to be generated in a first step. Cells seeded in 60 mm-dishes were controlled microscopically. Cell culture medium was aspirated and cells were washed with 1 X PBS. Cells were detached by adding 1 ml of trypsin. Trypsin was directly aspirated and cells were incubated for 3 min on a heating plate. Cells were collected in ice-cold cell culture medium and placed on ice. If not stated otherwise, further processing took place on ice. Cells were counted. The remaining cell suspension was spun down, cell culture medium was aspirated and pelleted cells were re-suspended thoroughly in 1 X PBS. Cell suspension was mixed with lysis buffer of the Pure RNA Isolation Kit at stored at – 80 °C until further processing.

6.2.8.2 Total RNA isolation

Isolation of total RNA was conducted with the High Pure RNA Isolation Kit according to manufacturer's instruction. The kit contains a DNase digestion step, several washing steps and a final RNA elution step. Concentration of total RNA was measured with the NanoDrop spectrophotometer.

6.2.8.3 cDNA synthesis

In order to make gene transcripts accessible for quantitative real-time polymerase chain reaction (RT-qPCR) analysis, total RNA templates had to be written into complementary DNA (cDNA). For this reverse transcription, RevertAid H Minus First Strand cDNA Synthesis Kit was used according to manufacturer's instructions. After preparation of master mixes containing RNA template, oligo $(dT)_{18}$ primers and

RNase-free water, the process contains an annealing, a cDNA synthesis and a termination step. cDNA was stored at – 80 °C.

6.2.8.4 Quantitative real-time PCR

RT-qPCR is a polymerase chain reaction in which cDNA is amplified. Therefore, cDNA was diluted 1:1'000 in nuclease-free water and pipetted into PCR-reaction capillaries. For preparation of reactions, capillaries were placed in ice-cold capillary-adapters. Diluted cDNA was carefully mixed with LightCycler FastStart DNA Master Plus Sybr Green I mix and primers for target gene and housekeeper gene, respectively. Forward and reverse primers for CTIP (target gene) were designed and tested by the author. Design of forward and reverse primers for glyceraldehyde 3-phosphate dehydrogenase gene (GAPDH, housekeeper gene) were taken from purchasable primers and tested for the current application by the author. Primers were designed / chosen to amplify cDNA written from mRNA only. LightCycler FastStart DNA Master Plus Sybr Green I mix contains a FastStart Taq DNA polymerase, DNA double-strand-specific Sybr Green I dye and a dNTP mix. Capillaries were spun down in LC Carousel Centrifuge 2.0 and placed into a LightCycler. Tag polymerase amplifies DNA and incorporates Sybr Green I dye molecules into the newly built DNA strands during the process of PCR. Sybr Green I dye offers a light signal which is proportional to the amplified amount of DNA. During DNA amplification, the light signal increases until it becomes detectable and exceeds background noise. This time point is termed crossing point (C_P), which can be analyzed later on. Here, DNA was amplified in up to 40 cycles. Melting curve analyses were conducted.
Afterwards, amplification of cDNA was relatively quantified according to [113]: C_P values of CTIP were normalized to those of GAPDH in order to detect fold-differences in expression of the target gene.

6.2.9 Quantification

In order to derive mean values for quantitative analysis, values obtained from several single determinations were averaged. Data variation was determined based on the amount of determinations that were used. For more than three single determinations,

variation was depicted as standard deviation (StDev, Equation 1). Calculation of means and StDev was conducted by Microsoft Excel 2010 application.

$$StDev = \sqrt{\frac{\sum(x_i - \bar{x})^2}{n}}$$

Equation 1: Calculation of standard deviation (StDev). x = mean value, n = amount of determinations.

If only two determinations were available, variation was depicted by plotting obtained minimal and maximal values.

For analysis of PFGE data, means and variation were plotted by SigmaPlot 12.5 application as indicated in tables 22-32. For the comparison of DNA DSB decay functions, residual DNA DSB damage, expressed as dose equivalent (Deq), was documented at the last time point of each experiment. Furthermore, t_{10Gy} value was established. It depicts the temporal requirement to resolve 50 % of induced DNA DSB damage, thus half-life values of decay functions. For this purpose, coefficients as indicated from SigmaPlot 12.5 were inserted in the equation for four-parametric exponential decay (Equation 2), which was solved for y = 10 Gy.

$$y = ae^{-bx} + ce^{-dx}$$

Equation 2: Calculation of half-life values of exponential decay functions (t_{10Gy}). a, b, c, d = variable coefficients, e = Euler's number.

7. Results

7.1 Alt-EJ is hampered in plateau phase of growth

In the present thesis, regulation of DNA DSB repair pathway choice and efficiency of alt-EJ in non-cycling cells are addressed. To investigate this objective, human 82-6 hTERT cell line was used. This non-tumorigenic cell line was generated by retroviral transfection with human telomerase catalytic subunit component (hTERT) in order to overcome replicative senescence [114, 115] and was considered to be a good candidate to examine DNA double strand break repair in healthy human tissue.

Presence and efficiency of potential DNA DSB repair pathways in non-cycling cells should be compared to DNA DSB repair in cycling cells. Therefore, actively cycling cells were ran into their natural plateau phase of growth in which cells cease cycling due to the high cell density in cell culture [22]. To generate plateau phase cells, actively cycling cells were incubated for several days without medium change. Each day, cells were counted, which revealed an exponential growth until day 5 (Figure 13A). Afterwards, cell numbers neither decreased nor increased, indicating that a plateau phase of growth was reached. Cells were analyzed by one-parametric flow cytometry for PI intensity to deduce their distribution throughout the cell cycle (Figure 13B). PI is a fluorescent molecule that intercalates into the bases of DNA, thereby offering valuable clues about the DNA content of a cell. DNA content fluctuates during the course of the cell cycle. Thus, intensity of the PI signal in a flow cytometry assay is an indication of a cell's position in the cell cycle. PI intensity analysis showed that cells being incubated for 2 days contained G_1, S and G_2 phase cells, while cells being incubated for 8 days were highly enriched in G_1 phase.

To compare efficiency of DNA DSB repair in cycling and plateau phase cells, both cell populations were further subjected to PFGE analysis (Figure 13C-D). In order to assess the influence of different factors to the speed of DNA DSB repair and to compare data of each condition to their corresponding control, several parameters were chosen as indicative. First, the type of DNA DSB decay function (exponential or linear) was identified (Table 22A). Second, t_{10Gy} value was established. It depicts the temporal requirement to resolve 50 % of induced DNA DSB damage, thus half-life values of decay functions. For this purpose, coefficients as indicated from SigmaPlot 12.5 were inserted in the equation for four-parametric exponential decay (see Equation 2 in paragraph 6.2.9). Finally, residual DNA DSB damage, expressed as

dose equivalent (Deq), was documented at the last time point of each experiment. Residual Deq and t_{10Gy} values are presented in Table 22B.

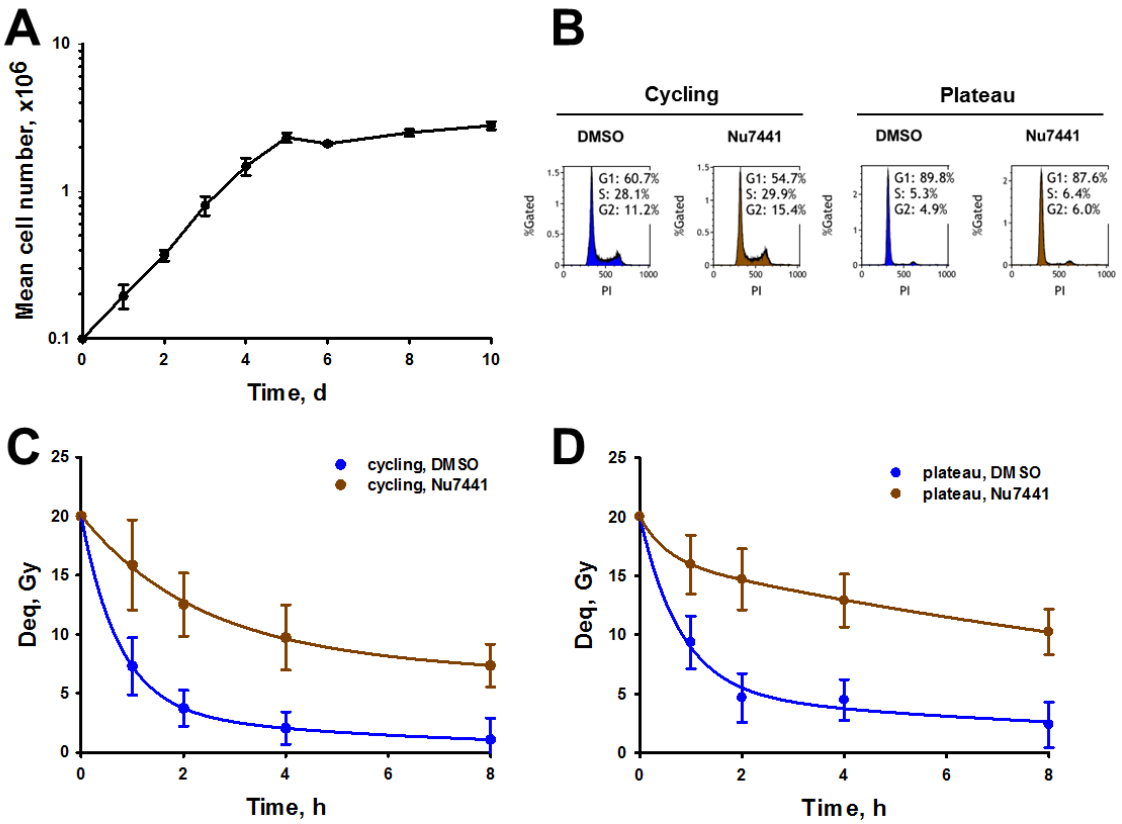

Figure 13: Alt-EJ is hampered in plateau phase of growth.
A) Cells were seeded and incubated for the indicated amount of days (d). Shown data points represent means, vertical lines represent minimal and maximal values obtained from two independent experiments. B) Flow cytometric validation of cell cycle status of cells being incubated for 2 d (cycling) or 8 d (plateau). Representative histograms of two independent experiments. C-D) PFGE analysis of DNA DSB repair in cycling (C) and plateau phase cells (D). Shown data points represent means and StDev from 8-12 determinations in three independent experiments.

In the present experiment, cells were treated with Dna-Pkcs inhibitor to inhibit DNA DSB repair by c-NHEJ [116]. Treatment was conducted 1 h before IR and remained during the given repair time. As Dna-Pkcs-inhibited cells cannot engage c-NHEJ, any repair that might be observed can only be attributed to the activity of alt-EJ. Inhibition of Dna-Pkcs did not affect cell cycle distribution (Figure 13B). All repair kinetics results could be fitted using four-parametric exponential decay functions. DMSO treated controls, either cycling or in plateau phase, displayed efficient repair by NHEJ. More than half of the generated DNA DSBs (t_{10Gy}) were resolved within the first hour and nearly all DSBs were resolved within the course of the experiment (residual Deq).

In comparison to that, Dna-Pkcs inhibited cycling cells showed slightly hampered DNA DSB repair by alt-EJ, which was expressed in an elevated t_{10Gy} of more than 3 h

and a residual Deq of 7.3 Gy. In Dna-Pkcs-inhibited plateau phase cells, efficiency of alt-EJ further declined. With a residual Deq of 10.7 Gy, nearly 54 % of DNA DSBs remained unresolved and this is indicating an effect of the cell cycle status on the DNA DSB repair by alt-EJ. In plateau phase cells, alt-EJ was less efficiently engaged than in cycling cells.

Table 22: Alt-EJ is hampered in plateau phase of growth: kinetics of DNA DSB decay.
A) Equations for DNA DSB repair kinetics. B) Half-life value (t_{10Gy}) and residual Deqs of repair kinetics. All data refer to DNA DSB repair kinetics shown in Figure 13C-D.

A

	DNA DSB repair kinetics
Cycling, DMSO	Four-parametric exponential decay function
Cycling, Nu7441	Four-parametric exponential decay function
Plateau, DMSO	Four-parametric exponential decay function
Plateau, Nu7441	Four-parametric exponential decay function

B

	t_{10Gy}	**Residual Deq**
Cycling, DMSO	39 min	1.1 Gy
Cycling, Nu7441	3 h 39 min	7.3 Gy
Plateau, DMSO	50 min	2.4 Gy
Plateau, Nu7441	8 h 21 min	10.7 Gy

7.2 Generation and standardization of cell growth conditions

In the results presented above and also in previous experiments (see paragraph 4.8.1 and [76, 85]) plateau phase cells are used to investigate DNA DSB repair in non-cycling cells. In these cells, quiescence is induced by a lack of nutrients and very high cell densities. Due to the lack of space, overcrowded cell populations cannot re-enter the cell cycle anymore [22, 86]. However, it was preferred to investigate whether hampered DNA DSB repair by alt-EJ in non-cycling cells would recover if cells resume cycling. Non-cycling cells can resume cycling if the spatial culture conditions allow further cell proliferation. Therefore, it was necessary to establish experimentation protocols that enable quiescence induction before cell populations become overcrowded. Cellular quiescence can be also induced by SD [22]. Therefore, it was decided to generate non-cycling cells by SD, which is carried out by transferring cells from full cell culture medium including serum into fresh serum-free medium. Cycling cells were serum deprived after 48 h of exponential growth, at a

time before they would have reached maximal confluence and would have entered a natural plateau phase of growth (refer also to Figure 13A).

Cells that have exited the cell cycle enter G_0 phase. It was recognized that analysis of DNA content by one-parametric flow cytometry for PI intensity is not sufficient to identify G_0 phase cells, as they have the same DNA content as G_1 phase cells. Therefore, it was important to include another parameter into the used flow cytometry protocol that would allow discrimination of G_1 and G_0 phase cells. Furthermore, in order to be able to investigate DNA DSB repair in G_0 phase cells and cells that re-entered the cell cycle from G_0 phase, it was necessary to detect the temporal requirements for cell cycle exit and subsequent cell cycle re-entry. Cell cycle status, the shift into G_0 phase and cell cycle re-entry can be monitored by two-parametric flow cytometry analysis combining PI staining and Ki67 immunostaining. Ki67 is a proliferation marker, a protein that is strictly present in M phase and interphase and absent in G_0 phase (see paragraph 4.6). A positive signal consists of all proliferating cells in G_1, S and G_2 phase, thus defining actively cycling cells. A negative signal defines G_0 phase cells.

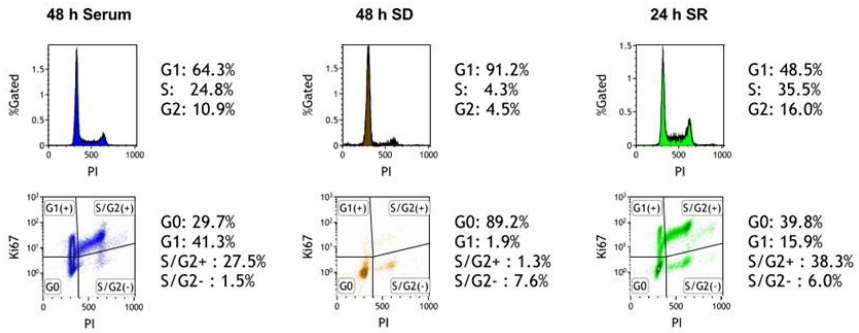

Figure 14: Flow cytometric analysis of growth state.
Cells were incubated for 48 h in cell culture medium containing serum (left panel). Cell cycle exit was generated by serum deprivation (SD, middle panel) for additional 48 h. Cell cycle re-entry was generated by serum replenishment (SR, right panel) for further 24 h. DNA content was evaluated by PI staining. Actively cycling and G_0 phase cells were discriminated by Ki67 immunostaining.

82-6 hTERT cells were cultured for 48 h in full cell culture medium containing serum (Figure 14). Analysis of the aforementioned parameters revealed a cell population composed of G_1, S and G_2 phase cells (PI intensity), that was actively proliferating (Ki67 intensity). After 48 h of SD, more than 91 % of cells showed a DNA content of G_1 phase cells and a closer look on the Ki67 signal revealed nearly no proliferative activity. Therefore, cells were considered to be successfully shifted into G_0 phase.

To answer the question whether G_0 phase arrested cells would be able to re-enter the cell cycle, SR was conducted. SR is the transfer of cells from serum deprived

medium into fresh cell culture medium containing serum. After 24 h of such treatment, a cell population was detected that contained G_1, S and G_2 phase cells and 54 % of the cells were proliferating. Consequently, it was concluded that 24 h of SR were sufficient to release cells from G_0 phase back into the cell cycle.

The biochemical characterization of distinct cell cycle phases by flow cytometry, as well as the detection of the temporal requirements for cell cycle exit and subsequent cell cycle re-entry allowed further investigation of DNA DSB repair in G_0 phase cells and in cells that re-entered the cell cycle after G_0 phase.

7.3 Alt-EJ is severely abrogated in G_0 phase

Generation of non-cycling G_0 phase cells by SD and the possibility to identify them by Ki67 immunostaining enabled the investigation of DNA DSB repair by alt-EJ in these cells: actively cycling 82-6 hTERT cells were serum deprived to yield G_0 phase cells. This was confirmed by two-parametric flow cytometry analysis for PI staining and Ki67 immunostaining (Figure 15A).

Decrease of proliferating cells during SD accounted for over 90 %. Treatment with Dna-Pkcs inhibitor Nu7441 did not affect the proportion of proliferating cells compared to DMSO treatment.

In order to compare efficiency of DNA DSB repair in cycling and G_0 phase cells, both cell populations were analyzed by PFGE (Figure 15B-C and Table 23). Cycling and G_0 phase cells efficiently resolved almost all DNA DSBs by NHEJ if treated with DMSO. To inhibit repair by c-NHEJ and to identify repair events of alt-EJ, cells were further treated with Dna-Pkcs inhibitor. DNA DSB repair by alt-EJ appeared to be dramatically altered in G_0 phase. Repair kinetics changed completely from four-parametric exponential decay function to linear decay function and t_{10Gy} was approximated to be more than 24 h. Residual Deq of 17.8 Gy and the mere repair of 2.2 Gy Deq damage showed the striking abrogation of alt-EJ in G_0 phase cells. It indicated that IR-induced DNA damage in G_0 phase remained unresolved in case of chemically inhibited Dna-Pkcs function and documented a very strong dependence of alt-EJ on the cell cycle status in human fibroblasts.

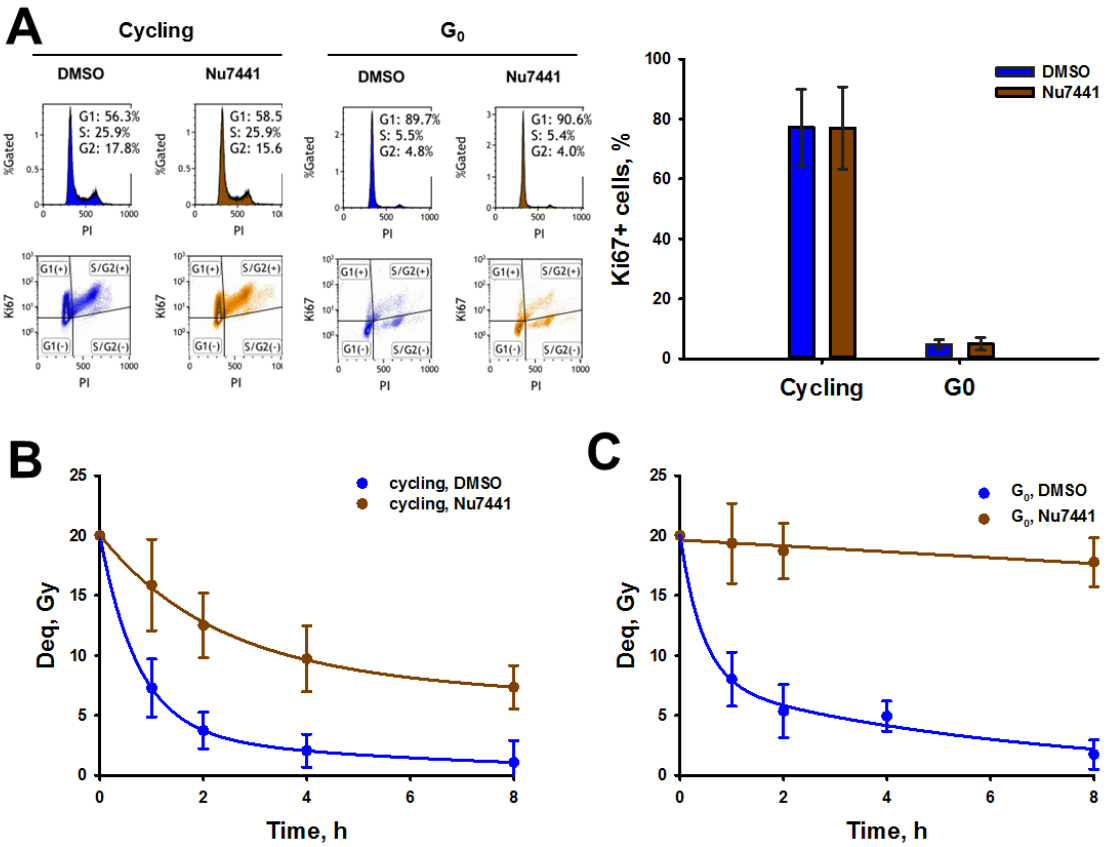

Figure 15: Alt-EJ is severely abrogated in G_0 phase.
A) Flow cytometric validation of cell cycle status in cycling and G_0 phase cells. Representative histograms of three independent experiments. Shown bars represent means and StDev of Ki67 positive cells in three independent experiments. B-C) PFGE analysis of DNA DSB repair in cycling (B) and G_0 phase cells (C). Shown data points represent means and StDev from 8-12 determinations in three independent experiments.

Table 23: Alt-EJ is severely abrogated in G_0 phase: kinetics of DNA DSB decay.
A) Equations for DNA DSB repair kinetics. B) Half-life value (t_{10Gy}) and residual Deqs of repair kinetics. All data refer to DNA DSB repair kinetics shown in Figure 15B-C.

A

	DNA DSB repair kinetics
Cycling, DMSO	Four-parametric exponential decay function
Cycling, Nu7441	Four-parametric exponential decay function
G_0 phase, DMSO	Four-parametric exponential decay function
G_0 phase, Nu7441	Linear decay function

B

	t_{10Gy}	**Residual Deq**
Cycling, DMSO	39 min	1.1 Gy
Cycling, Nu7441	3 h 39 min	7.3 Gy
G_0 phase, DMSO	37 min	1.7 Gy
G_0 phase, Nu7441	> 24 h	17.8 Gy

7.4 Abrogated alt-EJ in G_0 phase is rescued upon re-entry into the cell cycle

Abrogation of alt-EJ was pronounced in G_0 phase cells. In a next step, the question should be answered whether this abrogation was permanent or could be reversed. It is known that cycling cells can efficiently engage alt-EJ to repair DNA DSBs. Therefore, it was hypothesized that cells would be able to recover alt-EJ upon exiting G_0 phase and re-entering the cell cycle. To study the potential recovery of alt-EJ efficiency, G_0 phase 82-6 hTERT cells were serum replenished: they were transferred to fresh cell culture medium containing either 10 or 20 % serum and were incubated for 12 or 24 h, respectively.

Cell cycle status of serum replenished cells was monitored by two-parametric flow cytometry for PI and Ki67 staining. In comparison to G_0 phase cells, analysis revealed almost no impact of 12 h SR on cell cycle distribution or proliferative activity (Figure 16A). However, SR for 24 h showed an effect: proliferative activity rose from 3 to more than 50 % and cells were considered to be actively cycling again. Besides the impact of duration of SR, it was detected that serum concentration in cell culture medium, either 10 or 20 % serum, had only very minor impact on cell cycle distribution and proliferative activity.

PFGE analysis of alt-EJ efficiency in serum replenished cells displayed further differences between replenishment for 12 and 24 h (Figure 16B-C and Table 24). Although repair of DNA DSB damage changed back to four-parametric exponential decay function in all conditions of SR, incubation of 12 h was not sufficient to greatly improve abrogation of alt-EJ, neither with 10 % nor 20 % serum. In contrast to that, SR for 24 h showed a pronounced improvement of alt-EJ in Dna-Pkcs inhibited cells. In both conditions, 10 % and 20 % serum, remaining DNA damage decreased clearly. SR by 10 % for 24 h with t_{10Gy} = 1 h 43 min led to a residual Deq of 8.3 Gy. SR by 20 % for 24 h with t_{10Gy} = 1 h 13 min led to a residual Deq of 5.2 Gy. Similar to the results seen in flow cytometric analysis, differences between SR by 10 % and 20 % were only minor.

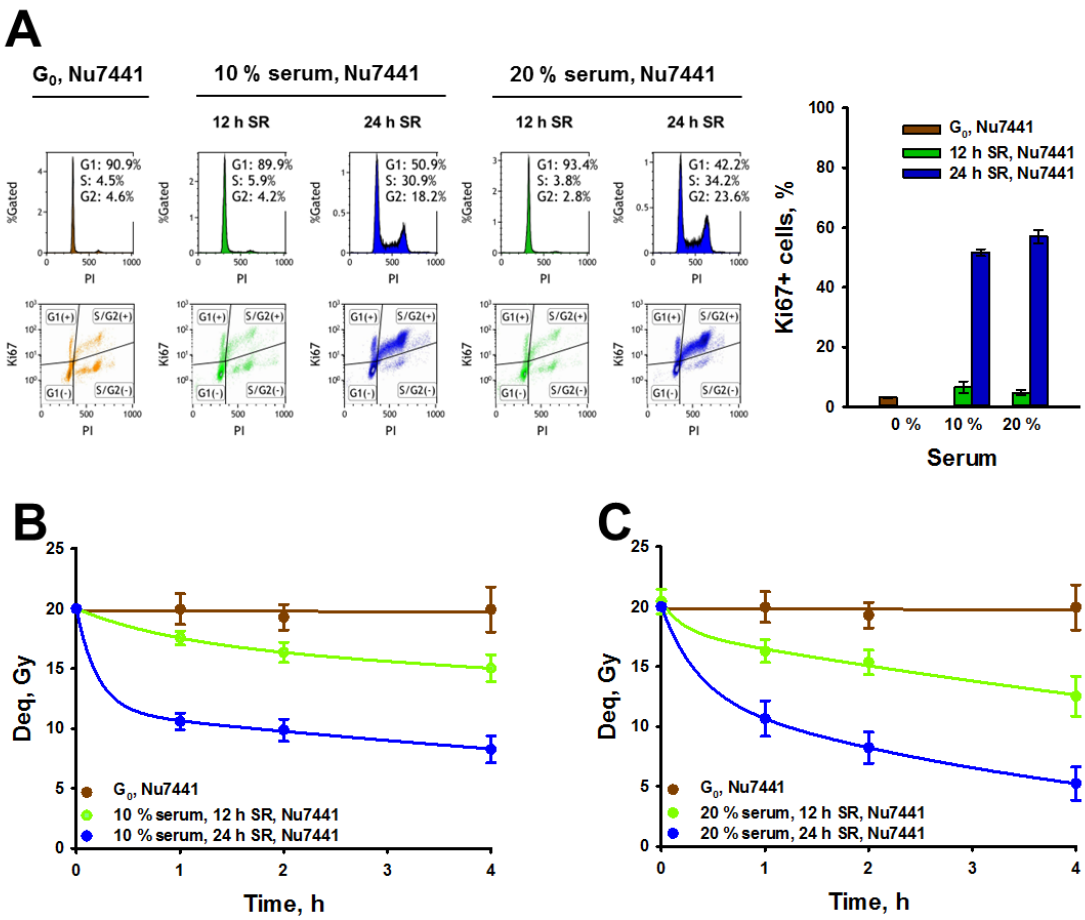

Figure 16: Abrogated alt-EJ in G_0 phase is rescued upon re-entry into the cell cycle.
A) Flow cytometric validation of G_0 phase and serum replenished (SR) cells. Representative histograms of two independent experiments. Shown bars represent means, vertical lines represent minimal and maximal values obtained from two independent experiments. B-C) PFGE analysis of alt-EJ during serum replenishment with 10 % serum (B) and 20 % serum (C). Shown data points represent means and StDev from 8 determinations in two independent experiments.

In summary, 12 h of SR were not sufficient to improve abrogated DNA DSB repair by alt-EJ in G_0 phase cells. This could be explained by the lack of impact of treatment time on cell cycle distribution. After 12 h of SR, G_0 phase cells did not re-enter the cell cycle again. Strikingly, abrogated DNA DSB repair by alt-EJ in G_0 phase cells could be rescued when cells were serum replenished for 24 h. This treatment time had an impact on cell cycle distribution. When cells re-entered the cell cycle and, moreover, were actively proliferating, alt-EJ improved. Furthermore, it was detected that 10 % of serum were sufficient to cause these effects. Additional 10 % of serum had no exceeding outcome.

Table 24: Abrogated alt-EJ in G_0 phase is rescued upon re-entry into the cell cycle: kinetics of DNA DSB decay.
A) Equations for DNA DSB repair kinetics. B) Half-life value (t_{10Gy}) and residual Deqs of repair kinetics. All data refer to DNA DSB repair kinetics shown in Figure 16B-C.

A

	DNA DSB repair kinetics
G_0 phase, Nu7441	Linear decay function
12 h SR, 10 % serum, Nu7441	Four-parametric exponential decay function
12 h SR, 20 % serum, Nu7441	Four-parametric exponential decay function
24 h SR, 10 % serum, Nu7441	Four-parametric exponential decay function
24 h SR, 20 % serum, Nu7441	Four-parametric exponential decay function

B

	t_{10Gy}	**Residual Deq**
G_0 phase, Nu7441	> 24 h	19.9 Gy
12 h SR, 10 % serum, Nu7441	16 h 41 min	15.0 Gy
12 h SR, 20 % serum, Nu7441	6 h 40 min	12.5 Gy
24 h SR, 10 % serum, Nu7441	1 h 43 min	8.3 Gy
24 h SR, 20 % serum, Nu7441	1 h 13 min	5.2 Gy

7.5 Cell cycle dependent dynamics of alt-EJ impairment and rescue show the same trend in cells of a different germinal layer origin

Presented experiments in this thesis were conducted in fibroblastic 82-6 hTERT cells so far. Now it was inquired whether detected alterations of alt-EJ efficiency were specific only to fibroblasts or whether similar alterations could be found in cells of a different germinal layer origin, as well. Fibroblasts derive from the mesoderm. For the experiments in this paragraph, it was decided to use cells of ectodermal origin and retinal pigment epithelial cell line 1 (RPE-1 hTERT) was chosen. RPE-1 cells were immortalized by hTERT, too, and are another good candidate to study DNA DSB repair in healthy tissue [117].

Effects of SD on the efficiency of alt-EJ in RPE-1 hTERT cells should be explored first. This required a preparatory effort on defining the optimal temporal requirements of SD in this cell line. Cycling RPE-1 hTERT cells were serum deprived for different amounts of time and cell cycle distribution and proliferative activity was monitored by two-parametric flow cytometry for PI and Ki67 staining (Figure 17).

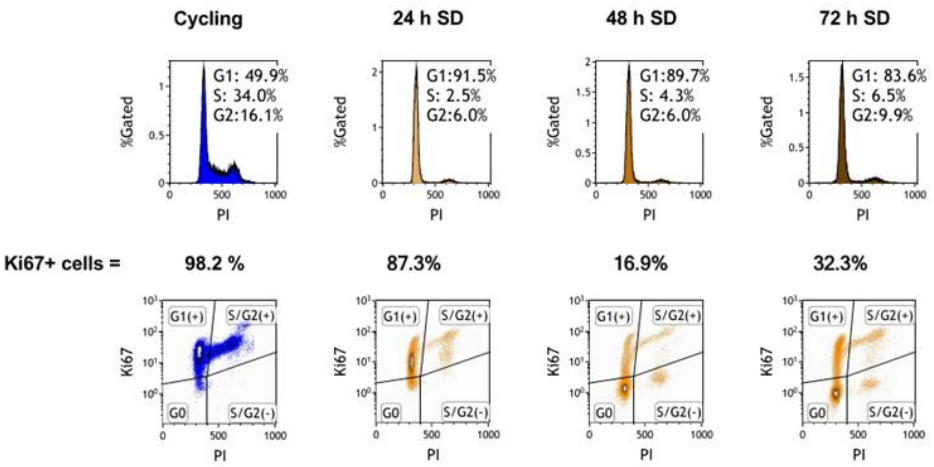

Figure 17: Temporal optimization of serum deprivation in RPE-1 hTERT cells.
Cycling cells were serum deprived (SD) for the indicated amounts of time. DNA content was evaluated by PI staining. Actively cycling cells were identified by Ki67 immunostaining.

SD for 24 h showed an accumulation of cells with the DNA content of G_1 phase cells. But still, after 24 h of SD, almost 90 % of the cells showed strong proliferative activity. After 48 h of SD, proliferative activity dropped extensively to about 17 %. This was a time point which was considered much more suitable to conduct experiments with. Nevertheless, experimentation was prolonged for another 24 h to find out whether proliferative activity could be decreased even further. Very interestingly though, after 72 h of SD, amounts of S and G_2 phase cells increased and proliferative activity resumed. This result was not expected and will be discussed further below.

It was recognized that results were best after 48 h of SD and it was decided to analyze alt-EJ efficiency at this time point. Actively cycling and serum deprived cells were again analyzed for their cell cycle status by flow cytometry to repeat results shown in Figure 17 and to investigate the impact of Dna-Pkcs inhibition on cell cycle distribution in epithelial cells. Flow cytometry analysis confirmed an effect on cell cycle distribution and proportion of proliferative activity (Figure 18A). Upon SD, amount of proliferating cells dropped from 96 % to 16 % in DMSO treated cells and 22 % in Dna-Pkcs inhibited cells, respectively. Thus, inhibition of Dna-Pkcs did rather not affect cell cycle distribution. SD did not lead to such a pronounced decrease of proliferative activity as it was seen in human fibroblasts (Figure 14). Although duration of SD was optimized, it did not lead to a sufficient cell cycle withdrawal into G_0 phase and cells could not be reliably classified to be G_0 phase cells. Thus, it was decided to continuing terming them serum deprived cells.

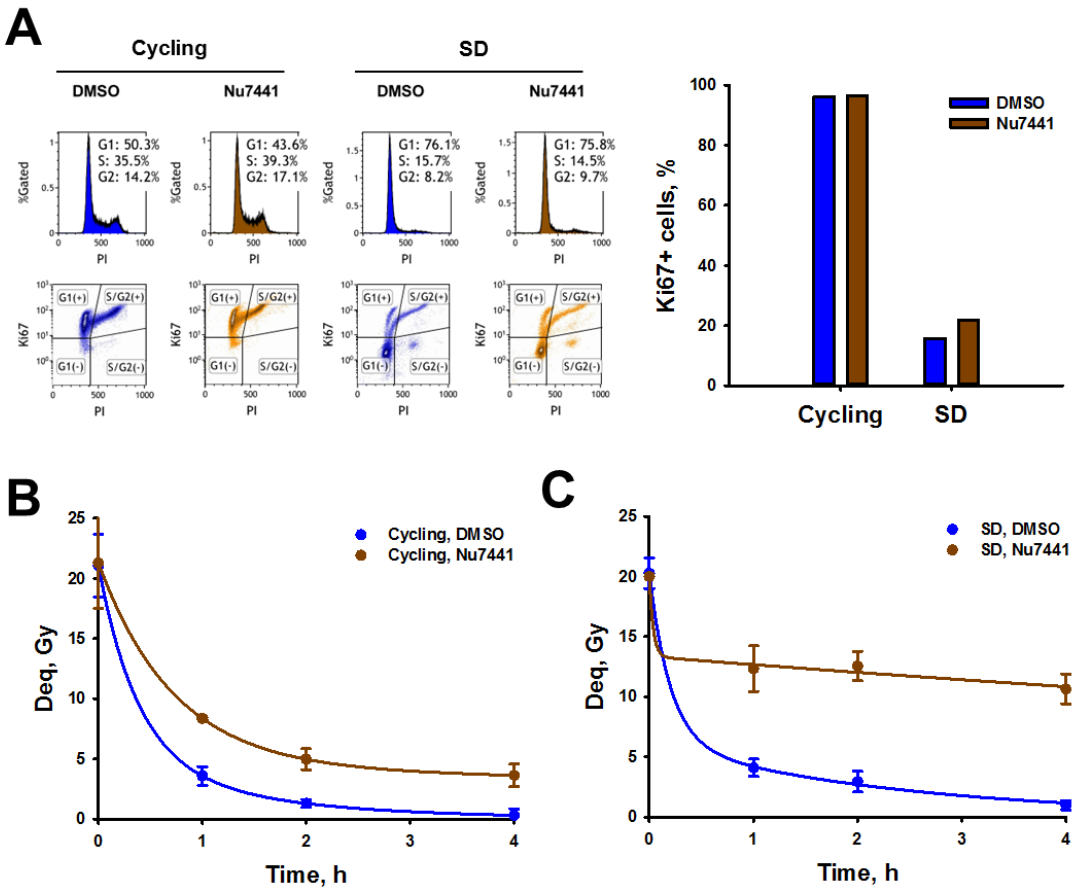

Figure 18: Alt-EJ is impaired in serum deprived cells of ectodermal origin.
A) Flow cytometric validation of cell cycle status in cycling and serum deprived (SD) RPE-1 cells. Result of one experiment is shown. B-C) PFGE analysis of DNA DSB repair in cycling (B) and serum deprived cells (C). Shown data points represent means and StDev from 8 determinations in two independent experiments.

Actively cycling and serum deprived cells were further subjected to PFGE analysis to assess alt-EJ efficiency (Figure 18B-C and Table 25). Repair kinetics followed four-parametric exponential decay functions. DMSO treated cycling and serum deprived cells efficiently resolved almost all generated DNA DSBs by NHEJ. To inhibit repair by c-NHEJ and to identify repair events of alt-EJ, cells were again treated with Dna-Pkcs inhibitor. Alt-EJ in cycling cells still resolved a big proportion of breaks. Similar to the DMSO treated control, Dna-Pkcs inhibited cycling cells resolved half of the damage in less than an hour. In contrast to that, DNA DSB repair by alt-EJ in serum deprived cells appeared to be clearly diminished. After 4 h of incubation, remaining DNA damage persisted at almost 11 Gy and it was extrapolated that it would take more than 5 h to resolve half of the damage.

Table 25: Alt-EJ is impaired in serum deprived cells of ectodermal origin: kinetics of DNA DSB decay.
A) Equations for DNA DSB repair kinetics. B) Half-life value (t_{10Gy}) and residual Deqs of repair kinetics. All data refer to DNA DSB repair kinetics shown in Figure 18B-C.

A

	DNA DSB repair kinetics
Cycling, DMSO	Four-parametric exponential decay function
Cycling, Nu7441	Four-parametric exponential decay function
SD, DMSO	Four-parametric exponential decay function
SD, Nu7441	Four-parametric exponential decay function

B

	t_{10Gy}	**Residual Deq**
Cycling, DMSO	22 min	0.3 Gy
Cycling, Nu7441	46 min	3.6 Gy
SD, DMSO	14 min	1.0 Gy
SD, Nu7441	5 h 33 min	10.6 Gy

Additionally, the question arose whether the decline of alt-EJ efficiency that was seen upon SD could be rescued. Fibroblastic 82-6 hTERT cells resumed to repair DNA DSBs by alt-EJ upon exiting G_0 phase and re-entry into the cell cycle and it was hypothesized that similar behavior could be detected in epithelial RPE-1 hTERT cells, as well. In order to investigate the potential rescue of alt-EJ, serum deprived RPE-1 hTERT cells were submitted to SR. They were transferred to fresh cell culture medium containing 10 % serum and were incubated for 12 or 24 h, respectively.

Cell cycle status of serum deprived and serum replenished cells was monitored by two-parametric flow cytometry for PI and Ki67 staining, which revealed gradual decrease of cells with DNA content of G_1 phase cells and gradual increase of proliferative activity with increasing duration of SR (Figure 19A).

While cells were re-entering the cell cycle, PFGE analysis was conducted (Figure 19B and Table 26). Repair kinetics followed four-parametric exponential decay functions. After 12 h of SR, cells repaired much better by alt-EJ than serum deprived cells. Half of the damage was repaired in less than an hour and residual Deq accounted for 5.8 Gy, thus dropped by almost 50 %. Additional 12 h of SR improved alt-EJ efficiency even further. Half of the damage was repaired in 18 min and the residual Deq almost equaled the data of Dna-Pkcs inhibited cycling cells.

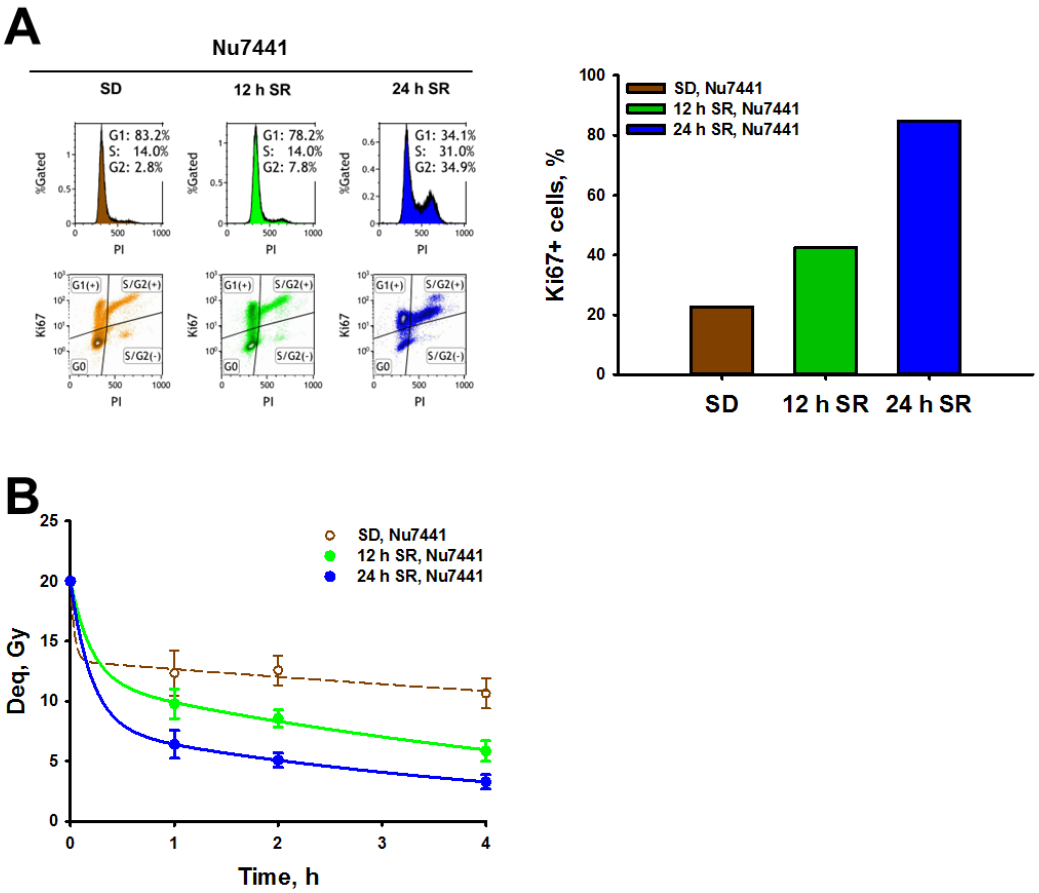

Figure 19: Impaired alt-EJ is rescued upon SR in cells of ectodermal origin.
A) Flow cytometric validation of cell cycle status in serum deprived (SD) and serum replenished (SR) RPE-1 hTERT cells. Result of one experiment is shown. B) PFGE analysis of alt-EJ in serum replenished cells. Shown data points represent means and StDev from 4-8 determinations in two independent experiments. Dashed line represents repair in serum deprived cells which was conducted for the previous figure.

Table 26: Impaired alt-EJ is rescued upon SR in cells of ectodermal origin: kinetics of DNA DSB decay.
A) Equations for DNA DSB repair kinetics. B) Half-life value (t_{10Gy}) and residual Deqs of repair kinetics. All data refer to DNA DSB repair kinetics shown in Figure 19B.

A

	DNA DSB repair kinetics
SD, Nu7441	Four-parametric exponential decay function
12 h SR, Nu7441	Four-parametric exponential decay function
24 h SR, Nu7441	Four-parametric exponential decay function

B

	t_{10Gy}	**Residual Deq**
SD, Nu7441	5 h 33 min	10.6 Gy
12 h SR, Nu7441	57 min	5.8 Gy
24 h SR, Nu7441	18 min	3.3 Gy

Collectively, in human epithelial cells similar trends in DNA DSB repair could be detected as in human fibroblasts (Figure 15 and Figure 16). DNA DSB repair by alt-EJ declined upon SD and was rescued upon SR. Yet, the almost complete

abrogation of alt-EJ, which was seen in human fibroblasts, could not be detected in human epithelial cells. This could be explained by incomplete cell cycle withdrawal of epithelial cells and a persisting subpopulation of actively cycling cells upon SD. Nevertheless, the last experiments conducted in RPE-1 hTERT cells demonstrated that cell cycle dependent dynamics of alt-EJ efficiency are not only specific for human fibroblasts, but can be detected in other human cell lines, too.

7.6 Rescue of abrogated alt-EJ coincides with the onset of proliferative activity

In Figure 16 it was shown that alt-EJ was rescued after re-entry into the cell cycle. At this point, it was desirable to determine the earliest time point in which alt-EJ would be initiated after cells exit G_0 phase. It was hypothesized that re-initiation of alt-EJ would be connected to the onset of proliferative activity and it was cogitated at which time point this would occur in 82-6 hTERT cells. 12 h of SR were not sufficient to initiate proliferative activity and SR for 24 h was too long as approximately one fifth of the cellular population already had transited until G_2 phase. A first exploratory approach attempted to determine temporal requirements for the onset of proliferative activity by two-parametric flow cytometry for PI and Ki67 staining (Figure 20).

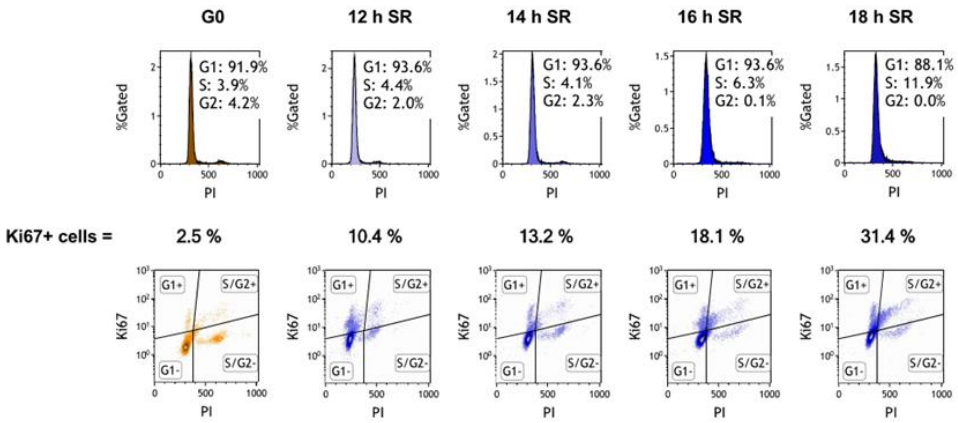

Figure 20: Temporal requirements for the onset of proliferative activity after G_0 phase.
G_0 phase cells were serum replenished (SR) for the indicated amounts of time. DNA content was evaluated by PI staining. Actively cycling cells were identified by Ki67 immunostaining.

G_0 phase 82-6 hTERT cells were serum replenished with 10 % of serum for different durations of time and analyzed for cell cycle distribution and proliferative activity. PI staining revealed a slight drop in G_1 phase and increase in S phase population earliest after 18 h of SR. However, proliferative activity increased earlier. Ki67 analysis displayed a shift from negative to positive signal in cells with DNA content of

G_0/G_1 phase cells after 16 h and revealed a further transition from G_1 phase to S/G_2 phase in cells with positive signal after 18 h of SR. Therefore, it was inferred that 16 h of SR is a good time point to analyze alt-EJ efficiency in early proliferating cells (refer also to Figure 21A).

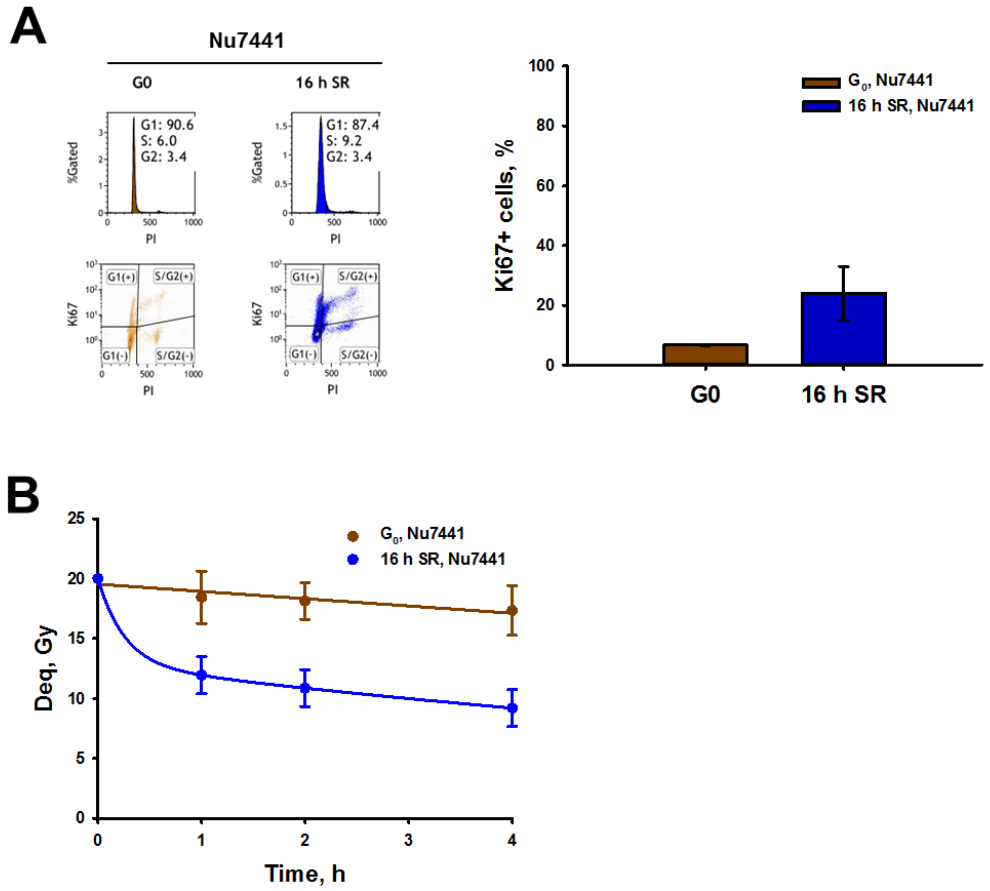

Figure 21: Rescue of abrogated alt-EJ coincides with the onset of proliferative activity.
A) Flow cytometric validation of cell cycle status of G_0 phase and serum replenished (SR) cells. Representative histograms of three independent experiments. Shown bars represent means, vertical lines represent StDev obtained from three independent experiments. B) PFGE analysis of alt-EJ in G_0 phase cells and serum replenished cells. Shown data points represent means and StDev from 11-12 determinations in three independent experiments.

DNA DSB repair efficiency of 16 h serum replenished and Dna-Pkcs inhibited cells is depicted in Figure 21B and Table 27. While DNA DSB repair by alt-EJ was found to be abrogated in G_0 phase cells, alt-EJ in 16 h serum replenished cells was certainly improved and kinetics switched back to four-parametric exponential decay function. Within the course of the experiment, remaining DNA damage decreased to a residual Deq of 9.2 Gy and t_{10Gy} was reached after 3 h. In comparison to cells being serum replenished with 10 % of serum for 12 h (Figure 16B), alt-EJ improved pronouncedly. Moreover, in comparison to alt-EJ efficiency in cycling cells (Figure 15B), it became apparent that alt-EJ upon 16 h of SR followed similar trends.

Table 27: Rescue of abrogated alt-EJ coincides with the onset of proliferative activity: kinetics of DNA DSB decay.
A) Equations for DNA DSB repair kinetics. B) Half-life value (t_{10Gy}) and residual Deqs of repair kinetics. All data refer to DNA DSB repair kinetics shown in Figure 21B.

A

	DNA DSB repair kinetics
G_0 phase, Nu7441	Linear decay function
16 h SR, Nu7441	Four-parametric exponential decay function

B

	t_{10Gy}	**Residual Deq**
G_0 phase, Nu7441	15 h 54 min	17.3 Gy
16 h SR, Nu7441	3 h	9.2 Gy

In summary, it was surprising that such short time of SR and modest increase of proliferative activity led to a similar repair as Dna-Pkcs inhibited cycling cells displayed, which were never serum deprived (Figure 15B). The coincidence between proliferative activity and improvement of alt-EJ paved the way for further questions: Ki67 positive serum replenished cells were predominantly found to be in G_1 phase, but partially transited until S and G_2 phase, too. To which extend did cells in the respective cell cycle phases contribute to the observed effect? Was the rescue of alt-EJ caused by G_2, S phase or G_1 phase cells? In addition, cell cycle re-entry and alt-EJ rescue were induced by addition of cell culture serum. It is the growth factors contained in cell culture serum that constitute cell cycle inducing stimulus in G_0 phase. Could abrogated alt-EJ in G_0 phase be rescued upon single growth factor treatment, as well? Finally, in which mechanistic way do serum or growth factors, potentially, regulate alt-EJ efficiency? These questions will be discussed in the following sections.

7.7 Rescue of abrogated alt-EJ cannot be explained by increased alt-EJ efficiency in G_2 phase cells

When G_0 phase cells got serum replenished for 16 h, alt-EJ efficiency improved pronouncedly and it coincided with the onset of proliferative activity and a re-entry into the cell cycle. Cells transited mostly from G_0 until G_1 phase, but partially even further to S and G_2 phase. In S and G_2 phase, DNA end resection machinery operates with high performance which eventually leads to an increase of alt-EJ efficiency reaching its peak in G_2 phase. So it could be speculated that S and G_2 phase subpopulations essentially contributed to the observed increase in alt-EJ in serum replenished cells.

In order to investigate the contribution of S and G_2 phase cells to the increase of alt-EJ efficiency, it first had to be verified that 16 h of SR indeed led to a further cell cycle transition beyond G_1 phase. In this thesis, S phase cells were so far identified by their DNA content only. But S phase cells can be identified even more reliably by their DNA synthesizing activity. Therefore, 82-6 hTERT cells were pulse-labelled with EdU. EdU is a thymidine analogue that is incorporated into synthesized DNA during S phase alongside to thymidine incorporation. Presence of EdU is assessed by coupling it to an azide dye which is imaged by flow cytometry. A positive EdU signal is revealing S phase cells synthesizing DNA. Inclusion of EdU staining in the heretofore existing flow cytometry protocol revealed a strong reduction of DNA synthesis activity from cycling to G_0 phase and only a very modest increase from G_0 phase to serum replenished cells (Figure 22A and B) while dynamics of proliferative activity that have been presented in paragraph 7.6 could be confirmed by Ki67 immunostaining (Figure 22A and C).

The sparse amount of S phase cells being detected upon 16 h of SR was indicative for those cells not contributing to the marked increase of alt-EJ efficiency. But more profound investigation of participation of S and G_2 phase cells in the seen effect was still necessary. Therefore, cells were treated with aphidicolin (APC). APC is an inhibitor of Pol α, δ and ε [118-120]. In the aforementioned publications, but also in others, it is stated that APC accumulates cells at G_1/S phase border [121, 122]. But due to its function of inhibiting polymerases and thereby preventing DNA synthesis at the level of DNA chain elongation, one would assume that APC is arresting cells within S phase. And indeed, other authors clearly state APC to blocking cells in S phase [123]. Additionally, Urbani showed that even if the DNA content of APC arrested cells resembles the DNA content of G_1 phase cells, cyclin A levels increase

[124]. As presented in the introduction in paragraph 4.4.2, cyclin A is an S phase cyclin binding to Cdk2 and controlling DNA replication. It gets degraded in late G_2 to early M phase. Urbani's experiments and also APC's nature of inhibiting DNA chain elongation were interpreted in favor of APC arresting cells in S phase rather than at the G_1/S phase border. Therefore, it was assumed that in the following experiment (Figure 23), APC treated cells would be able to transit into but not further than S phase. Any repair that might be observed could only be attributed to alt-EJ activity in G_1/S phase cells and repair executed by G_2 phase cells could be excluded.

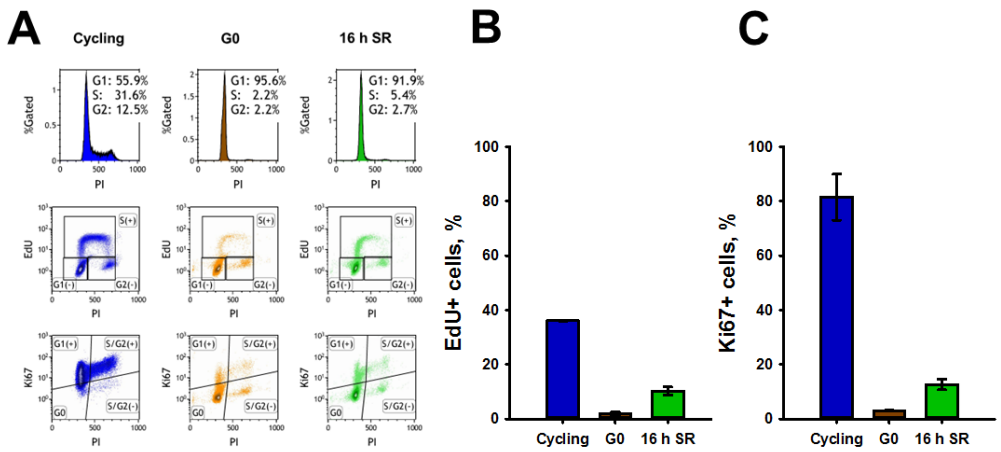

Figure 22: Establishment of a three-parametric flow cytometry protocol for identification of S phase cells. Flow cytometric investigation of the presence of S phase cells in cycling, G_0 phase and 16 h serum replenished (SR) cells. DNA synthesizing S phase cells were identified by a positive EdU signal. Representative histograms of two independent experiments. Shown bars represent means, vertical lines represent minimal and maximal values obtained from two independent experiments.

Three-parametric flow cytometry analysis for PI, EdU and Ki67 staining of G_0 phase and serum replenished cells revealed, that, according to DNA content, Pol α/δ/ε inhibition decreased already low amounts of G_2 phase cells even further (Figure 23A). In addition, EdU staining displayed a drop of DNA synthesizing cells, thus an abrogation of S phase upon Pol α/δ/ε inhibition. The inhibitor treatment did not affect proliferative activity as shown by Ki67 staining.

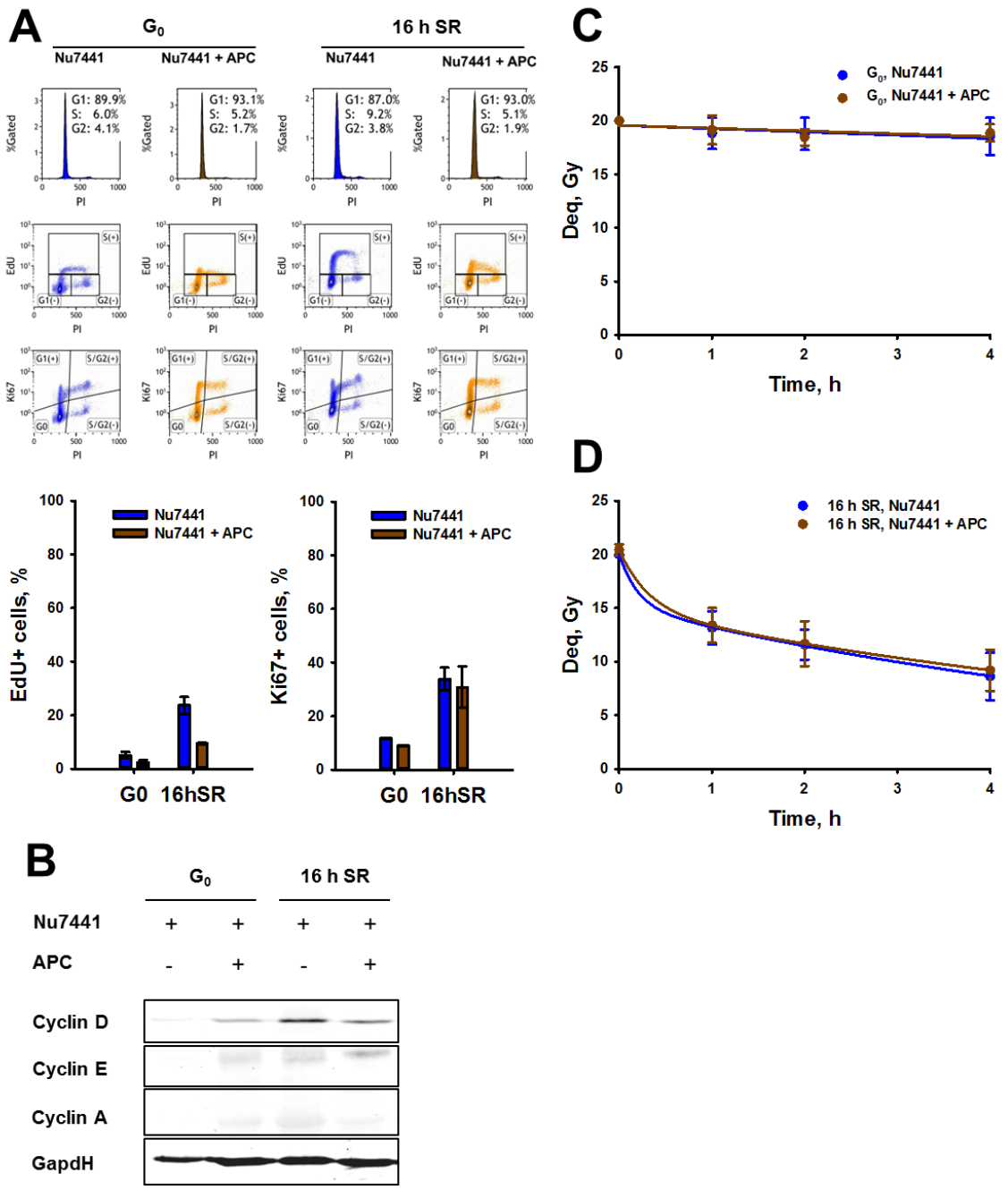

Figure 23: Rescue of abrogated alt-EJ cannot be explained by increased alt-EJ efficiency in G_2 phase cells.
A) Flow cytometric validation of G_0 phase and serum replenished (SR) cells. Representative histograms of two independent experiments. Shown bars represent means, vertical lines represent minimal and maximal values obtained from two independent experiments. B) Western blotting analysis of cyclins in G_0 phase and serum replenished cells. Representative blot of two independent experiments. C-D) PFGE analysis of alt-EJ in G_0 phase cells (C) and serum replenished cells (D). Shown data points represent means and StDev from 7-8 determinations in two independent experiments.

Cell cycle status in Pol α/δ/ε inhibited cells was further analyzed by Western blotting analysis (Figure 23B). Serum replenished cells strongly expressed G_1 phase cyclin D. Cyclin D is synthesized upon growth factor signaling after M phase and binds to Cdk4/6 during mid G_1 phase. It initiates G_1 phase transition by induction of cyclin E

and is degraded in late G_1/early S phase. Serum replenished cells did also show minor amounts of early S phase cyclin E, but did not express late S phase cyclin A. Similar to cyclin A, cyclin E binds to Cdk2. It controls chromosomal DNA replication. Once replication has started, cyclin E gets degraded (for more details see paragraph 4.4.2).

The findings here are not exactly in line with Urbani's results, but put additional evidence on the hypothesis that Pol α/δ/ε treatment allows the cells to enter S phase and arrests them there. As expected, G_0 phase control cells did not express S phase cyclins and only faint amounts of cyclin D.

G_0 phase cells and serum replenished cells were further subjected to PFGE analysis. Inhibition of Pol α/δ/ε did not have any effect on alt-EJ in G_0 phase cells (Figure 23C). There was almost no alt-EJ activity detected. But also in serum replenished cells, Pol α/δ/ε inhibition did not have an effect on alt-EJ (Figure 23D). In comparison to Dna-Pkcs inhibition alone, additional Pol α/δ/ε inhibition increased t_{10Gy} and residual Deq only very marginally (Table 28).

Table 28: Rescue of abrogated alt-EJ cannot be explained by increased alt-EJ efficiency in G_2 phase cells: kinetics of DNA DSB decay.
A) Equations for DNA DSB repair kinetics. B) Half-life value (t_{10Gy}) and residual Deqs of repair kinetics. All data refer to DNA DSB repair kinetics shown in Figure 23C-D.

A

	DNA DSB repair kinetics
G_0 phase, Nu7441	Linear decay function
G_0 phase, Nu7441 + APC	Linear decay function
16 h SR, Nu7441	Four-parametric exponential decay function
16 h SR, Nu7441 + APC	Four-parametric exponential decay function

B

	t_{10Gy}	**Residual Deq**
G_0 phase, Nu7441	> 24 h	18.5 Gy
G_0 phase, Nu7441 + APC	> 24 h	18.9 Gy
16 h SR, Nu7441	2 h 59 min	8.6 Gy
16 h SR, Nu7441 + APC	3 h 18 min	9.2 Gy

Taken together, it was first shown that staining procedure for identification of DNA synthesizing cells could be included in the existing flow cytometry protocol. The new three-parametric flow cytometry analysis confirmed a firm shift into G_0 phase upon SD (additionally to a lack of proliferative activity, almost no DNA synthesizing activity was seen) and suggested that SR for 16 h generated rather G_1 phase cells (very

moderate increase of DNA synthesizing activity). Second, flow cytometry and Western blotting analysis could demonstrate that Pol α/δ/ε inhibition by APC arrested cells within S phase. Third, exclusion of late S and G_2 phase cells from the serum replenished cell population did not cause an alteration of alt-EJ efficiency, thus showing that the observed rescue of alt-EJ could be narrowed down to G_1 and early S phase cells. This is an important finding, as, in general, G_2 phase cells are considered to show strong alt-EJ efficiency. Here, it is demonstrated that a strong performance of alt-EJ can also occur earlier and that late S and G_2 phase cells do not contribute to this effect.

7.8 Rescue of abrogated alt-EJ can be allocated to G_1 phase

In the last paragraph it was shown that late S and G_2 phase cells did not cause the rescue of abrogated alt-EJ that was seen upon SR. Thus, it was inquired whether improved repair could be related to early S phase cells. To investigate this, cells were treated with L-mimosine (MIM). The mode of action of MIM has been debated extensively over time. MIM has the potential to lower dNTP pools [125] and to inhibit thymidylate synthesis [126, 127] and was thereby assumed to arrest cells in S phase. Others showed a contribution of MIM in inhibition of DNA replication initiation [128] and, indirectly, cyclin E-associated kinase activity [129]. Those and others [123, 124] consider MIM to arrest cells in late G_1 phase. On close review of presented publications about MIM it became clear, that function of MIM is dependent on the chosen cell line and treatment. In higher doses, which were similar or identical to the dose used here, cells were arrested in late G_1 phase [123, 128] and it was hypothesized that MIM treated 82-6 hTERT cells would be arrested in G_1 phase, too. If MIM induced G_1 phase arrest turned out to be valid, S phase cells could be excluded from experimentation and effects of their absence could be studied.

Treatment with MIM lead to a thorough depletion of EdU signal and thus entirely prevented cells from entering S phase, as was revealed by three-parametric flow cytometry analysis. MIM treatment did not affect proliferative activity (Figure 24A). Western blotting analysis displayed only weak expression of cyclin D in G_0 phase control cells, which was increased upon SR (Figure 24B). In serum replenished cells, there was also a slight increase of S phase cyclin E expression detected upon MIM treatment. On first sight, this is contradicting flow cytometry findings. However, MIM was shown to arrest cells in G_1 phase by inhibition of cyclin E-associated kinase

activity without affecting cyclin E protein levels [129]. The second S phase cyclin, cyclin A, could not be detected upon SR. Thus, serum replenished and MIM treated cells were considered to be successfully blocked in G_1 phase.

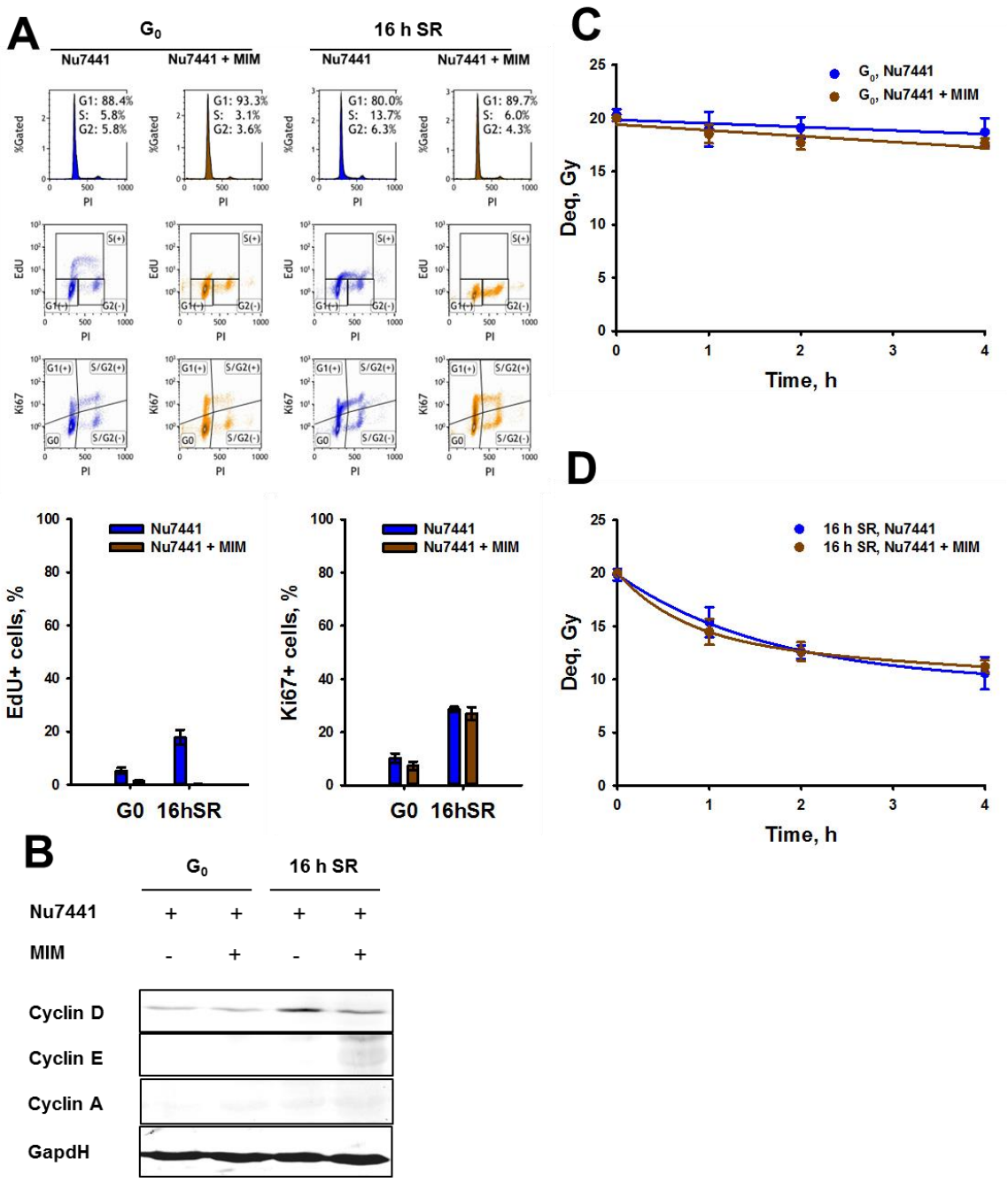

Figure 24: Rescue of abrogated alt-EJ can be allocated to G_1 phase.
A) Flow cytometric validation of G_0 phase and serum replenished (SR) cells. Representative histograms of two independent experiments. Shown bars represent means, vertical lines represent minimal and maximal values obtained from two independent experiments. B) Western blotting analysis of cyclins in G_0 phase and serum replenished cells. Representative blot of two independent experiments. C-D) PFGE analysis of alt-EJ in G_0 phase cells (C) and serum replenished cells (D). Shown data points represent means and StDev from 7-8 determinations in two independent experiments.

PFGE analysis is presented in Figure 24C-D and Table 29 and revealed MIM treatment to having only marginal effects on alt-EJ in G_0 phase cells. Repair by alt-EJ

could barely be detected. Alt-EJ in serum replenished and MIM treated cells was not altered, either. MIM induced G_1 phase arrest changed t_{10Gy} and residual Deq only minimally, if compared to Dna-Pkcs inhibition alone.

Table 29: Rescue of abrogated alt-EJ can be allocated to G_1 phase: kinetics of DNA DSB decay.
A) Equations for DNA DSB repair kinetics. B) Half-life value (t_{10Gy}) and residual Deqs of repair kinetics as shown in Figure 24C-D.

A

	DNA DSB repair kinetics
G_0 phase, Nu7441	Linear decay function
G_0 phase, Nu7441 + MIM	Linear decay function
16 h SR, Nu7441	Four-parametric exponential decay function
16 h SR, Nu7441 + MIM	Four-parametric exponential decay function

B

	t_{10Gy}	**Residual Deq**
G_0 phase, Nu7441	> 24 h	18.7 Gy
G_0 phase, Nu7441 + MIM	17 h 15 min	17.7 Gy
16 h SR, Nu7441	5 h 21 min	10.6 Gy
16 h SR, Nu7441 + MIM	6 h 30 min	11.2 Gy

Altogether, flow cytometry and Western blotting analysis confirmed that SR for 16 h generated mainly G_1 phase cells. The amounts of S and G_2 phase cells deriving upon this treatment were marginal and could be neglected. Exclusion of S and G_2 phase cells from the serum replenished cell population did not cause a clear alteration of alt-EJ efficiency, thus showing that the observed rescue of alt-EJ can be allocated only to G_1 phase cells. This is very interesting, as, in general, S/G_2 phase cells are considered to show strong alt-EJ efficiency. But here it is demonstrated, that a strong performance of alt-EJ can also occur very early in the cell cycle, namely in G_1 phase.

7.9 Rescue of abrogated alt-EJ can be further curtailed to early G_1 phase

Rescue of abrogated alt-EJ was shown to occur in G_1 phase. To further narrow down the exact onset of alt-EJ recurrence after G_0 phase, it was investigated whether alt-EJ would be even present in early G_1 phase. Therefore, 82-6 hTERT cells were treated with PD-0332991 (PD). PD arrests cells between early and late G_1 phase by inhibiting cyclin D-associated Cdk4 and 6 [130]. Any repair that might be observed could only be attributed to alt-EJ activity in early G_1 phase and repair executed in late G_1 phase could be excluded.

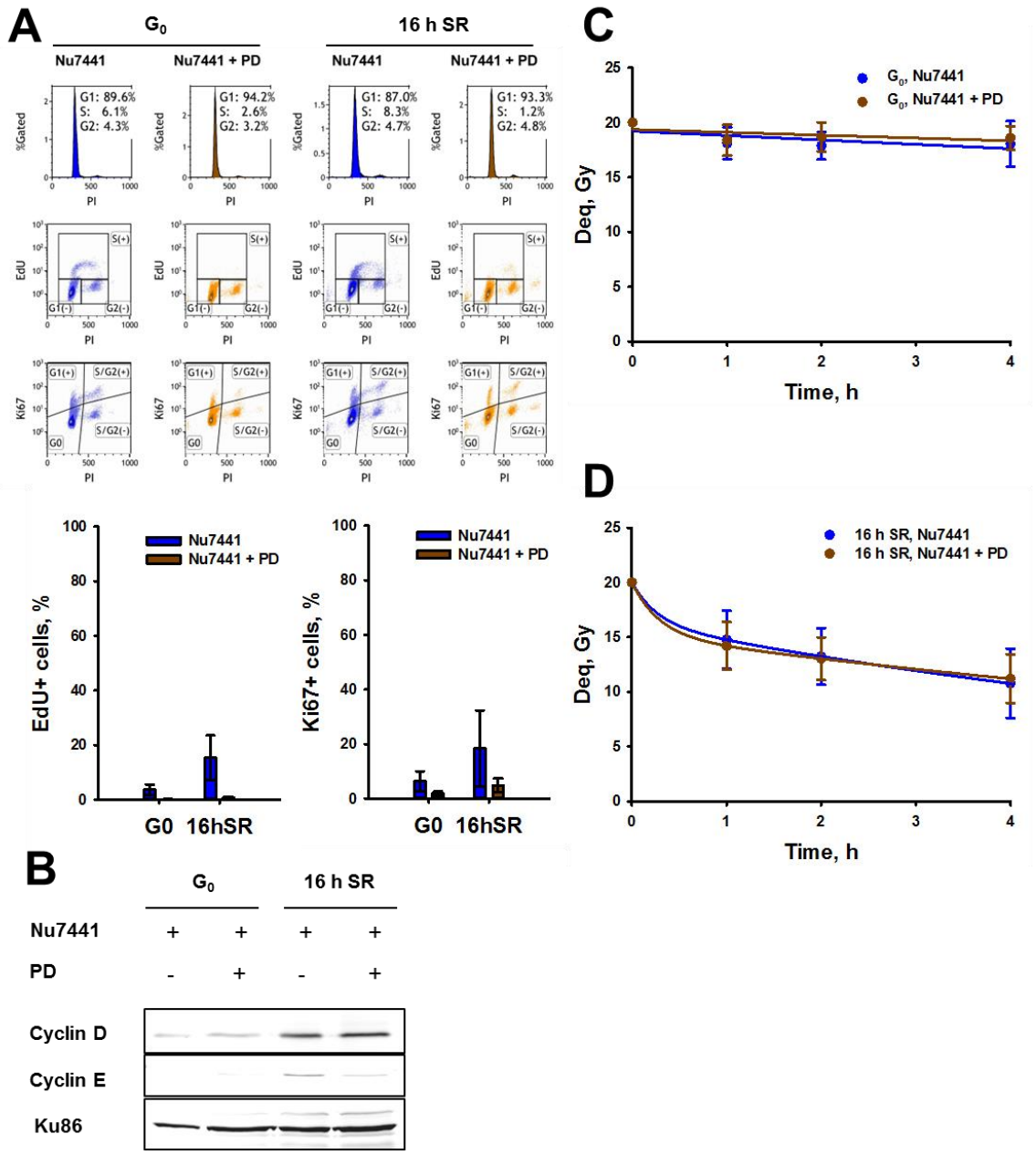

Figure 25: Rescue of abrogated alt-EJ can be further curtailed to early G_1 phase.
A) Flow cytometric validation of G_0 phase and serum replenished (SR) cells. Histograms are representative for two of three independent experiments. The third experiment showed same trends, but in higher numbers. Shown bars represent means, vertical lines represent StDev obtained from all three independent experiments. B) Western blotting analysis of cyclins in G_0 phase and serum replenished cells. Blots are representative for two of three independent experiments. The third experiment showed same trends, but in a higher dimension. C-D) PFGE analysis of alt-EJ in G_0 phase cells (C) and serum replenished cells (D). Shown data points represent means and StDev from 11-12 determinations in three independent experiments.

Three-parametric flow cytometry analysis of serum replenished cells showed, according to DNA content, that Cdk 4/6 inhibition sufficiently maintained high levels of G_1 phase cells (Figure 25A) and did not allow further transition through the cell cycle. This could be verified by EdU staining: Cdk 4/6 inhibition successfully prevented S phase entry. Besides, the treatment caused a noticeable decrease in Ki67 immunostaining. This is a peculiar effect that has been observed by others, too [130]

and is discussed in paragraph 8.2. But Western blotting analysis (Figure 25B) showed that decrease of Ki67 in Cdk 4/6 inhibited cells did not tamper establishment of G_1 phase upon SR: G_1 phase cyclin D was expressed similarly in Cdk 4/6 inhibited cells and control cells. Moreover, cyclin D expression was clearly higher in both serum replenished conditions than in G_0 phase cells. Western blotting analysis also supported the notion that Cdk4/6 inhibition prevented S phase entry, since early S phase cyclin E was barely detectable.

G_0 phase cells and serum replenished cells were further subjected to PFGE analysis (Figure 25C-D and Table 30). Inhibition of Cdk4/6 did not have an effect on alt-EJ in G_0 phase cells. There was almost no alt-EJ activity detected. But also in serum replenished cells, Cdk4/6 inhibition did not have an effect on alt-EJ. In comparison to Dna-Pkcs inhibition alone, additional Cdk4/6 inhibition increased t_{10Gy} and residual Deq only very marginally.

Table 30: Rescue of abrogated alt-EJ can be further curtailed to early G_1 phase: kinetics of DNA DSB decay.
A) Equations for DNA DSB repair kinetics. B) Half-life value (t_{10Gy}) and residual Deqs of repair kinetics as shown in Figure 25C-D.

A

	DNA DSB repair kinetics
G_0 phase, Nu7441	Linear decay function
G_0 phase, Nu7441 + PD	Linear decay function
16 h SR, Nu7441	Four-parametric exponential decay function
16 h SR, Nu7441 + PD	Four-parametric exponential decay function

B

	t_{10Gy}	**Residual Deq**
G_0 phase, Nu7441	23 h 2 min	18.1 Gy
G_0 phase, Nu7441 + PD	> 24 h	18.6 Gy
16 h SR, Nu7441	4 h 43 min	10.8 Gy
16 h SR, Nu7441 + PD	5 h 29 min	11.2 Gy

In summary, this experiment showed that even early G_1 phase cells could execute DNA DSB repair by alt-EJ. Thus, alt-EJ occurred much earlier than expected. It is also very interesting, that efficiency of alt-EJ seemed to be disconnected from the presence of proliferation marker Ki67. In this thesis, Ki67 immunostaining was only used to verify successful shift from cycling cells to G_0 phase and re-entry into the cell cycle. But as high efficiency of alt-EJ coincided with presence of Ki67, the impression might have been created that alt-EJ is dependent on Ki67. Here, first hints were

shown that Ki67 expression and presence of alt-EJ might be discrete from one another. Alt-EJ seemed to operate with similar efficiency in serum replenished cells, even if Ki67 expression was suppressed by Cdk 4/6 inhibition.

7.10 Rescue of abrogated alt-EJ can be induced by single growth factor administration, as well

One part of the questions that have been posed in the end of paragraph 7.6 could be answered already: exclusion of G_2, S and late G_1 phase cells from the experimental setup showed that improvement of alt-EJ upon SR could be performed by early G_1 phase cells. This alt-EJ rescue was induced by SR. It is the growth factors contained in cell culture serum that constitute cell cycle inducing stimulus in G_0 phase. Thus, it was inquired whether abrogated alt-EJ in G_0 phase could be rescued upon single growth factor treatment, as well.

As experiments were conducted in 82-6 hTERT fibroblast cells, it was decided to use basic fibroblast growth factor (bFGF) for the treatment. To study effects of bFGF on alt-EJ efficiency, G_0 phase cells were transferred to fresh cell culture medium containing only bFGF instead of serum. In Figure 21 it was shown that 16 h of SR were sufficient to rescue abrogated alt-EJ. In order to compare effects of bFGF to this result, bFGF treatment was set to be 16 h, too.

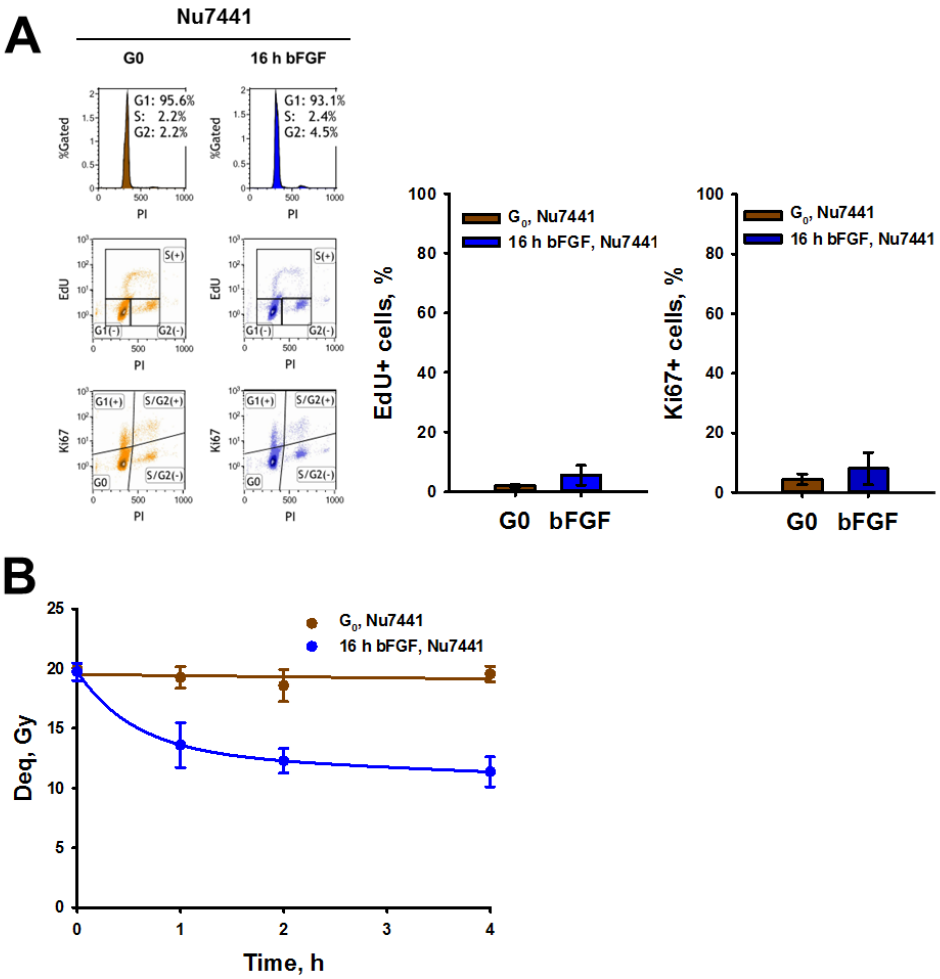

Figure 26: Rescue of abrogated alt-EJ can be induced by single growth factor administration, as well.
A) Flow cytometric validation of cell cycle status of G_0 phase and bFGF treated cells. Representative histograms of three independent experiments. Shown bars represent means, vertical lines represent StDev obtained from three independent experiments. B) PFGE analysis of alt-EJ in G_0 phase cells and bFGF treated cells. Shown data points represent means and StDev from 4-12 determinations in three independent experiments.

Cell cycle response of G_0 phase cells to bFGF treatment was monitored by three-parametric flow cytometry analysis for PI, EdU and Ki67 staining (Figure 26A) and it was discovered that bFGF had hardly any effect on cell cycle distribution. Changes in DNA synthesizing activity and proliferative activity were, if present, very marginal. But results of PFGE analysis were striking (Figure 26B and Table 31): while DNA DSB repair by alt-EJ was again found to be abrogated in G_0 phase control cells, alt-EJ in bFGF treated cells was clearly improved. Repair kinetics switched back to four-parametric exponential decay function and within the course of the experiment, remaining DNA damage decreased to a residual Deq of 11.4 Gy, which means that approximately 43 % of the breaks were resolved. T_{10Gy} was extrapolated to occur after approximately 8 h.

Table 31: Rescue of abrogated alt-EJ can be induced by single growth factor administration: kinetics of DNA DSB decay.
A) Equations for DNA DSB repair kinetics. B) Half-life value (t_{10Gy}) and residual Deqs of repair kinetics as shown in Figure 26B.

A

	DNA DSB repair kinetics
G_0 phase, Nu7441	Linear decay function
16 h bFGF, Nu7441	Four-parametric exponential decay function

B

	t_{10Gy}	**Residual Deq**
G_0 phase, Nu7441	> 24 h	19.5 Gy
16 h bFGF, Nu7441	8 h 2 min	11.4 Gy

In conclusion, abrogated alt-EJ could also be rescued by treatment with a single growth factor, here bFGF, instead of cell culture serum. This is indicating that alt-EJ efficiency is not necessarily dependent on cell culture serum, but that stimulation by single growth factors can be sufficient. Furthermore, although the effect was not as strong as it was seen in cells being serum replenished for 16 h (Figure 21), almost half of induced breaks were resolved in this condition. This is very interesting if one takes into consideration that improvement of alt-EJ efficiency was not accompanied by clear changes in cell cycle distribution. Alt-EJ rescue appeared independently of a re-gain in DNA synthesizing or proliferative activity. This is putting more weight on the hypothesis that was postulated in the end of paragraph 7.9: it was first shown that alt-EJ efficiency and presence of proliferation marker Ki67 might be discrete from one another. Here, similar effects were seen and it was wondered how they were caused. It was speculated that growth factor signaling could contribute to alt-EJ promotion in G_0 phase and subsequent G_1 phase and the next paragraphs of this thesis take an effort on gaining further understanding on the molecular background of this hypothesis.

7.11 Survey of growth factor downstream signaling pathways that might be involved in alt-EJ regulation

In the last paragraph it was shown that 43 % of DNA DSBs could be resolved within the course of the experiment when G_0 phase cells were treated with bFGF. This effect was similar to alt-EJ efficiency that was seen when G_0 phase cells were serum replenished. Growth factors constitute a major part of cell culture serum and it was assumed that rescue of alt-EJ upon SR and bFGF treatment might be a result of growth factor downstream signaling. So, in a next step, it was investigated how

growth factor downstream signaling in cycling 82-6 hTERT cells looks like and how it would change upon SD induced G_0 phase and subsequent SR or bFGF treatment. Growth factor signaling was monitored by Western blotting. In order to discover potential changes in the three major signaling pathways, Pi3k, MAPK and Plcγ pathway, it was decided to have a closer look on the respective protein in each pathway that constitutes a main hub for integrating downstream signaling. In case of Pi3k pathway, Akt/phosphorylated (p) Akt was chosen. For MAPK pathway, it was decided for Erk/pErk and for Plcγ pathway, Plcγ/pPlcγ itself was selected (Figure 27A). Analysis of non-phosphorylated proteins was conducted to achieve an overview of the general presence of Akt, Erk and Plcγ during the treatments. This was supposed to serve as control, as it was assumed that protein levels would stay stable during the experiment. Analysis of phosphorylated proteins was conducted to monitor active growth factor signaling (Figure 27B).

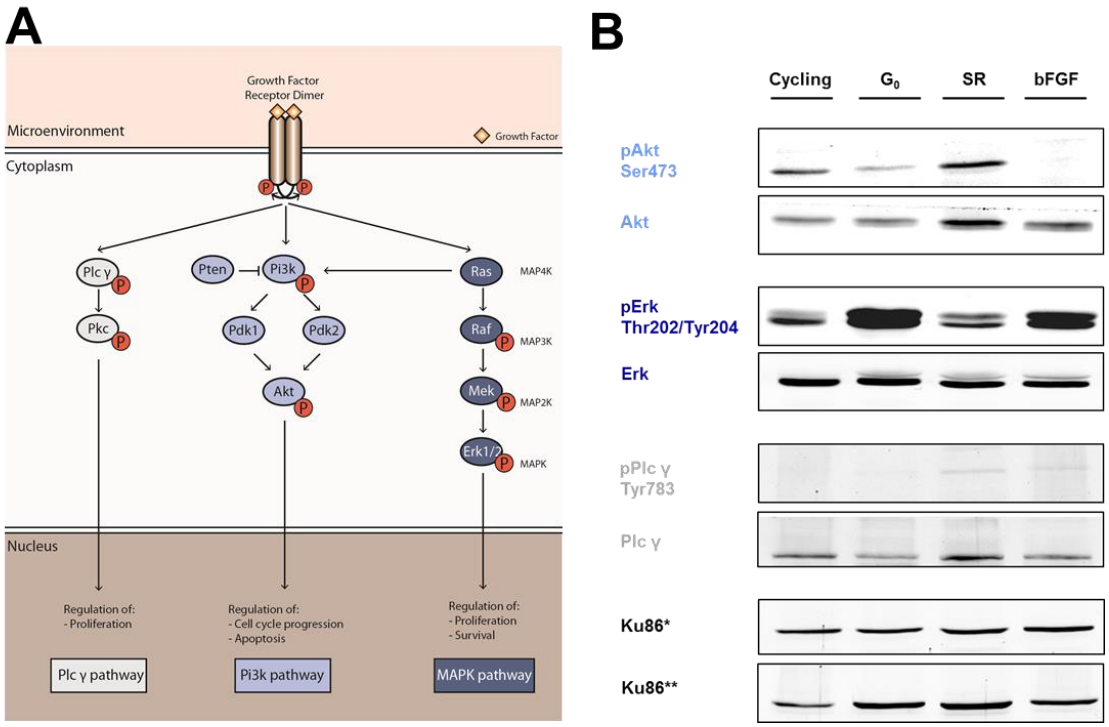

Figure 27: Investigation of growth factor downstream signaling pathways that might be involved in alt-EJ regulation.
A) A simplified overview of the major growth factor downstream signaling cascades is shown. For further details, see paragraph 4.5). B) Western blot analysis of growth factor downstream signaling in cycling, G_0 phase, serum replenished (SR) and bFGF treated cells. Blots are representative for three independent experiments. *Loading control for membrane incubated with antibodies directed against non-phosphorylated proteins. **Loading control for membrane incubated with antibodies directed against phosphorylated proteins.

The experiment revealed differential patterns for expression of non-phosphorylated proteins in general and also, in particular, for phosphorylation mediated growth factor

downstream signaling in cells that were cycling, in G_0 phase, serum replenished or bFGF treated.

Results of Akt/pAkt analysis are presented first. Expression of non-phosphorylated Akt could be detected in all conditions. It did not change from cycling cells to G_0 phase and further to bFGF treated cells. Only during SR an increase of Akt expression could be detected. A closer look on the phosphorylation status of Akt at serine 473 (pAkt Ser473) showed that Pi3k pathway was active in cycling cells. Signal for pAkt Ser473 decreased clearly when cells ceased cycling and entered G_0 phase and rose again when cells resumed cycling. When G_0 phase cells were treated with bFGF, pAkt Ser473 could not be detected at all. Thus, phosphorylation pattern of Akt followed the dynamics of proliferative activity that was presented in this thesis so far. As Akt is known to generally induce proliferation, it is of no surprise that pAkt Ser473 signal was high in proliferatively active cycling and serum replenished cells. The result is in accordance with textbook knowledge. Along these lines, the fact that bFGF treatment did not induce a gain in pAkt Ser473 signal at all is noteworthy for two reasons. First, it is supporting the observation that bFGF treatment alone did not cause G_0 phase cells to re-enter the cell cycle (Figure 26A). Second, it might indicate that pAkt Ser473 was not causative for the improvement of alt-EJ seen upon bFGF treatment (Figure 26B). Nonetheless, a more forward experiment investigating the potential role of pAkt Ser473 in alt-EJ regulation seemed to be necessary to verify these indications and will be described in the following paragraph.

Results of Erk analysis were quite different. Expression of non-phosphorylated Erk remained stable during the course of the experiment. And in comparison to pAkt Ser473, signal for phosphorylated Erk at threonine 202 and tyrosine 204 (pErk Thr202/Tyr204) displayed an inversed pattern. Signal was detected in all conditions, but was strongly increased in G_0 phase cells and upon bFGF treatment. Before the experiment was conducted, it was hypothesized that Erk phosphorylation would be similar to the one seen for Akt. But here it was recognized that the Erk phosphorylation pattern was quite opposite to Akt signaling, being strongly upregulated when cells were starved or were starved and received single growth factor treatment thereupon. MAPK pathway is predominantly known to induce proliferation, on the other hand it also responds to stress stimuli in order to promote survival [131] and it is within the bounds of possibility that upregulation of pErk Thr202/Tyr204 signaling in the present study was a starvation caused stress signal. By any means, the weaker phosphorylation signal of Erk at Thr202/Tyr204 in cycling

and serum replenished cells might be connected to their high alt-EJ efficiency. A more detailed inspection of this issue is presented in paragraph 7.13.

Finally, results of Plcγ/pPlcγ analysis are described. In general, signal of non-phosphorylated Plcγ was weaker than Akt or Erk signal. Its expression was higher in cycling and serum replenished cells than in G_0 phase and upon bFGF treatment and seemed to be dependent on the used treatment conditions. A signal for phosphorylated Plcγ at tyrosine 783 (pPlcγ Tyr783) could not be detected.

Therefore, it was concluded that signaling through Plcγ pathway was inferior in 82-6 hTERT cells and that Akt and MAPK pathways seemed to be more promising candidates for investigating growth factor signaling induced regulation of alt-EJ efficiency.

7.12 Regulation of alt-EJ efficiency is independent of pAkt Ser473 signaling

Growth factor downstream signaling via pAkt Ser473 was highly active in cycling cells with high alt-EJ efficiency and very weak in G_0 phase when alt-EJ was absent (Figure 27B). So, it was recognized as a potential promoter of alt-EJ efficiency. To investigate this hypothesis, cycling 82-6 hTERT cells were treated with MK-2206 (MK), which allosterically inhibits Akt phosphorylation [132] and DNA DSB repair by alt-EJ was measured by PFGE analysis. If pAkt Ser473 signaling influenced alt-EJ regulation, lack of active pAkt Ser473 signaling in cycling cells would decrease alt-EJ efficiency similarly to what was seen in G_0 phase cells.

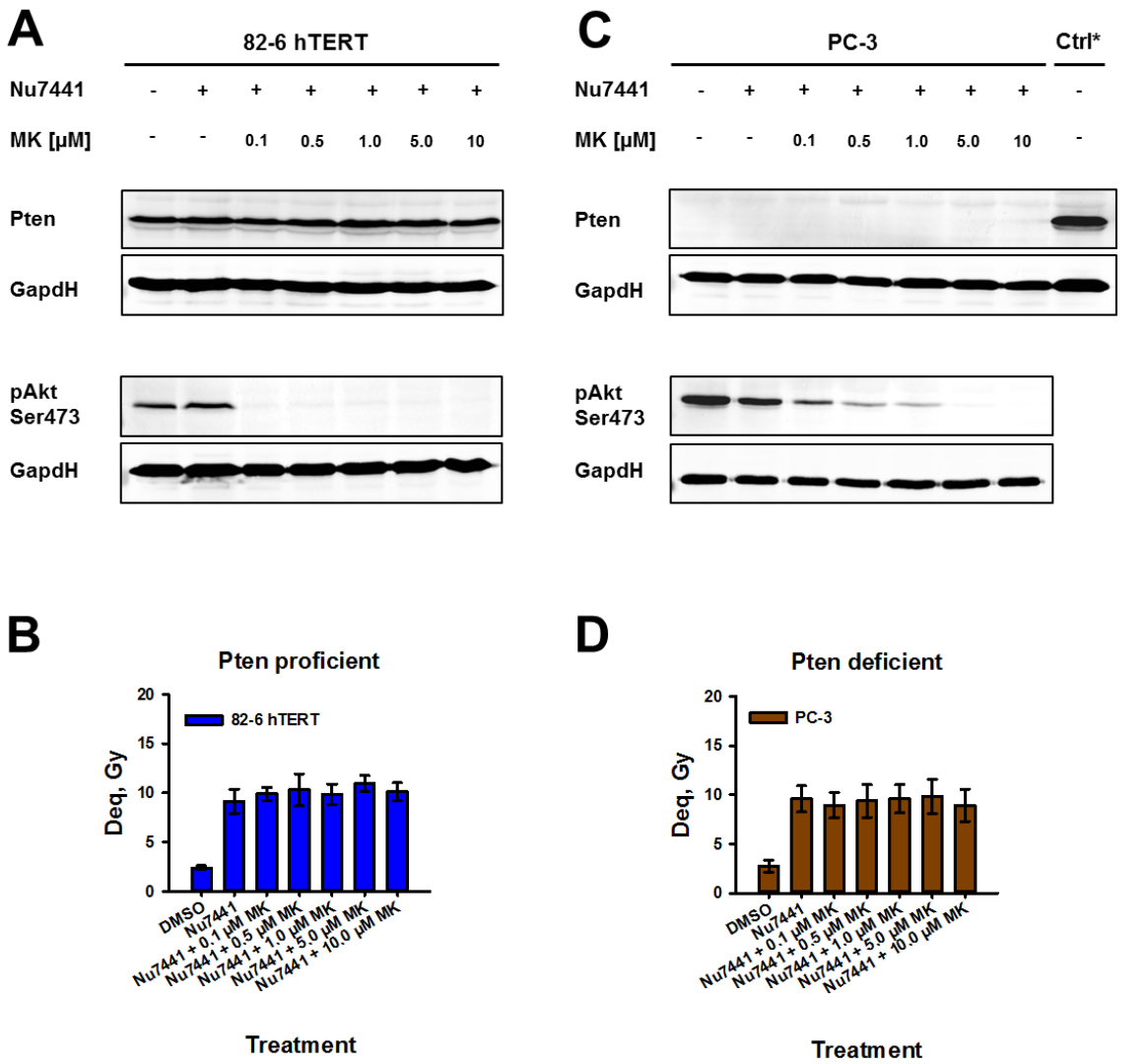

Figure 28: Regulation of alt-EJ efficiency is independent of pAkt Ser473 signaling.

A) Western blotting analysis of Pten expression and phosphorylation of Akt at Ser473 in cycling 82-6 hTERT cells. Result of one experiment is shown. B) PFGE analysis of DNA DSB repair in cycling 82-6 hTERT cells 2 h after irradiation. Shown bars represent means and StDev from 8 determinations in two independent experiments. C) Western blotting analysis of Pten expression and phosphorylation of Akt at Ser473 in cycling PC-3 cells. Result of one experiment is shown. Ctrl* shows Pten proficient 82-6 hTERT cells. D) PFGE analysis of DNA DSB repair in cycling PC-3 cells 2 h after irradiation. Shown bars represent means and StDev from 8 determinations in two independent experiments.

Successful inhibition of pAkt Ser473 was monitored by Western blotting analysis (Figure 28A). It was discovered that small amounts of Akt inhibitor (0.1 µM) were already sufficient to efficiently block phosphorylation of Akt at Ser473. Cells were irradiated and remaining DNA DSB damage was measured 2 h after irradiation (Figure 28B). DMSO treated control cells demonstrated adequate repair capacity by NHEJ, resolving 88 % of the breaks within the given time. As seen in many experiments before, Dna-Pkcs inhibited cells repaired less effectively, having 46 % of

DNA DSBs unresolved. Additional Akt inhibition did not decrease alt-EJ efficiency any further. Even an increase of inhibitor dose by a factor of 100 did not show an effect.
However, in literature it is described that Akt signaling activity is increased when cells are deficient for the gene PTEN. Generally, Pten protein inhibits Pi3k pathway (Figure 27A), but loss-of-function mutations of PTEN lead to a Pi3k pathway deregulation, rendering it to be hyperactive. This is altering the cellular response to Pi3k pathway inhibition: PTEN deficient cells show more sensitivity towards Pi3k/Akt inhibition [133-135]. It was wondered whether 82-6 hTERT cells are PTEN proficient or deficient. Literature search yielded no results and so a Western blotting experiment was conducted to answer this question (Figure 28A). It turned out that 82-6 hTERT cells must be PTEN proficient as strong expression of Pten protein could be detected (in turn, Akt inhibition did not affect Pten expression) and it was decided to repeat experimentation with a PTEN deficient cell line. Human prostate cancer cell line 3 (PC-3) was shown to be PTEN deficient [136, 137], which was verified here, as well (Figure 28C). PC-3 cells were inhibited for Akt signaling and although higher doses of inhibitor were necessary than in 82-6 hTERT cells, it could be demonstrated that successful Akt inhibition was possible with doses ≥ 5.0 µM. PC-3 cells were further subjected to PFGE analysis (Figure 28D). Similarly to 82-6 hTERT cells, cycling PC-3 cells treated only with DMSO repaired proficiently 2 h after irradiation. Dna-Pkcs inhibited cells resolved DNA DSBs by alt-EJ, but did so in a far less efficient way, having 48 % of DNA DSBs unrepaired after the given time. Additional Akt inhibition did not decrease alt-EJ efficiency, either.
Taken together, it was shown that inhibition of pAkt Ser473 signaling did not have an impact on alt-EJ efficiency in cycling cells, neither in PTEN proficient 82-6 hTERT cells nor in PTEN deficient PC-3 cells. Therefore, growth factor signaling via pAkt Ser473 was ruled out as a potential promoter of alt-EJ efficiency.

7.13 Regulation of alt-EJ efficiency is independent of pErk Thr202/Tyr204 signaling

Signaling via pErk Thr202/Tyr204 was highly active in G_0 phase cells when alt-EJ was absent and weaker in cycling cells with high alt-EJ efficiency (Figure 27B). Thus, pErk Thr202/Tyr204 signaling was considered to be a possible negative regulator of alt-EJ efficiency. In order to explore effects of pErk Thr202/Tyr204 on alt-EJ efficiency, 82-6 hTERT cells in G_0 phase were treated with trametinib (TRA). TRA inhibits Mek [138], which is one kinase upstream of Erk (Figure 27A). In this setup, it

was hypothesized that the lack of active pErk Thr202/Tyr204 signaling in G_0 phase cells would increase alt-EJ efficiency similarly to what was detected in serum replenished cells.

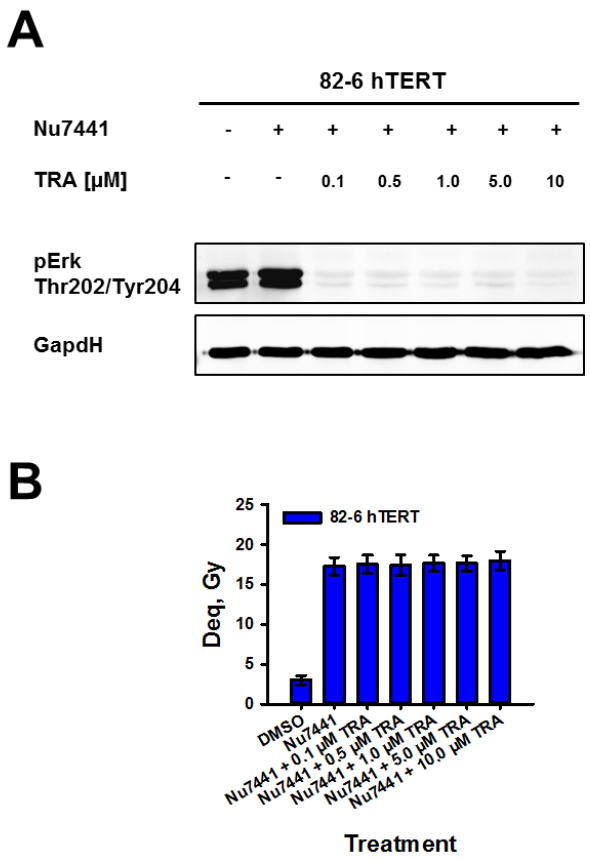

Figure 29: Regulation of alt-EJ efficiency is independent of pErk Thr202/Tyr204 signaling.
A) Western blotting analysis of phosphorylation of Erk at Thr202/Tyr204 in 82-6 hTERT cells in G_0 phase. Blots are representative for two independent experiments. B) PFGE analysis of DNA DSB repair in G_0 phase 82-6 hTERT cells 2 h after irradiation. Shown bars represent means and StDev from 8 determinations in two independent experiments.

Effective inhibition of pErk Thr202/Tyr204 was monitored by Western blotting analysis (Figure 29A). It was detected that already small amounts of Mek inhibitor (0.1 µM) were sufficient to adequately block phosphorylation of Erk at Thr202/Tyr204.

Cells were irradiated and remaining DNA DSB damage was evaluated 2 h after irradiation by PFGE (Figure 29B). DMSO treated control cells displayed sufficient repair capacity by NHEJ, resolving 85 % of the breaks within the given time. Dna-Pkcs inhibited cells repaired considerably worse, having 87 % of DNA DSBs unresolved after 2 h. Additional pErk Thr202/Tyr204 inhibition did not rescue alt-EJ efficiency. Even an increase of inhibitor dose by a factor of 100 did not show an effect.

Therefore, also pErk Thr202/Tyr204 signaling had to be excluded from the list of potential regulators of alt-EJ efficiency, and, in general, the hypothesis that growth factor downstream signaling would be involved in regulation of alt-EJ appeared unlikely and was rejected. Nevertheless, there was one last candidate in mind which was suspected to participate in control of alt-EJ activity and investigation in this regard will be presented below.

7.14 Investigation of CtIP expression in different growth states

Except from growth factor signaling, downregulation of alt-EJ in G_0 phase could be also caused by changes in expression of alt-EJ repair factors. Expression of repair factor CtIP is a prerequisite for alt-EJ initiation. Thus, it was investigated how expression of CtIP would change during cell cycle exit towards G_0 phase and subsequent cell cycle re-entry.

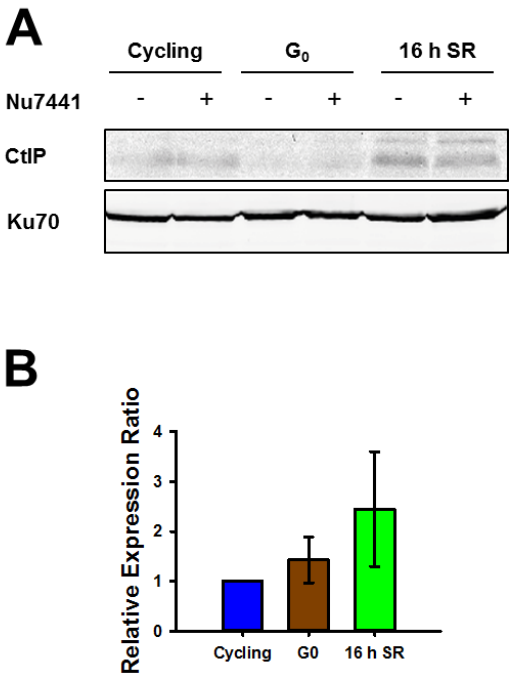

Figure 30: Investigation of CtIP expression in different growth states.

A) Western blotting analysis of CtIP protein expression in cycling cells, G_0 phase cells and serum replenished (SR) cells. Blots are representative for two independent experiments. B) RT-qPCR analysis of CTIP mRNA expression in the respective growth states. Relative expression ratio was compared to expression of housekeeping gene GAPDH. Shown bars represent means and StDev from three independent experiments.

Actively cycling 82-6 hTERT cells were serum deprived to yield G_0 phase cells and subsequently serum replenished for 16 h. Cells were subjected to protein expression analysis by Western blotting (Figure 30A). This revealed detectable expression of

CtIP in actively cycling cells, a downregulation of the protein in G_0 phase and a recovery and even an increase of CtIP expression during SR.

Cells were further subjected to mRNA expression analysis by RT-qPCR (Figure 30B). CTIP mRNA was detected in all growth states and it even increased upon G_0 phase induction and during SR. For actively cycling cells, this finding is divergent from newest results from the Institute of Medical Radiation Biology, where the current thesis was conducted. In those experiments (data not shown), CTIP expression in actively cycling cells was higher than in G_0 phase cells. But despite the question, whether CTIP mRNA expression is elevated or reduced in G_0 phase, it was detectable. Therefore, it was concluded that downregulation of CtIP protein in this growth state occurred rather on a (post-) translational than a transcriptional level. Additionally, it was speculated that this downregulation of CtIP protein might be involved in alt-EJ abrogation in G_0 phase and that its presence in cycling and serum replenished cells would cause increased efficiency of this pathway.

7.15 Abrogation of alt-EJ is coincident with a decrease of CtIP expression

In the previous experiment it was detected that CtIP protein was expressed very differently in cycling and in G_0 phase cells. It was present in cycling cells being capable of repairing DNA DSBs by alt-EJ. In G_0 phase cells, when alt-EJ was abrogated, CtIP was absent. In order to tackle the question whether CtIP might be involved in regulation of alt-EJ efficiency in different growth states, it was decided to manipulate its expression and to measure DNA DSB repair thereupon.

An experiment was conducted in which CtIP expression in serum replenished cells should be decreased under the assumption that this would also decrease alt-EJ efficiency. For this purpose, the antibiotic cycloheximide (CHX) was used. CHX derives from bacterium *Streptomyces griseus* and inhibits eukaryotic protein synthesis by blocking elongation of the developing amino acid chain during translation [139, 140].

Three-parametric flow cytometry analysis for PI, EdU and Ki67 staining showed the impact of translation inhibition on cell cycle distribution in G_0 phase and serum replenished 82-6 hTERT cells (Figure 31A). DNA synthesis activity and proliferative activity of G_0 phase cells were low and not much affected by the treatment. In cells being serum replenished for 16 h, the effects were bigger. Inhibition of translation was suppressing DNA synthesis and was decreasing proliferation.

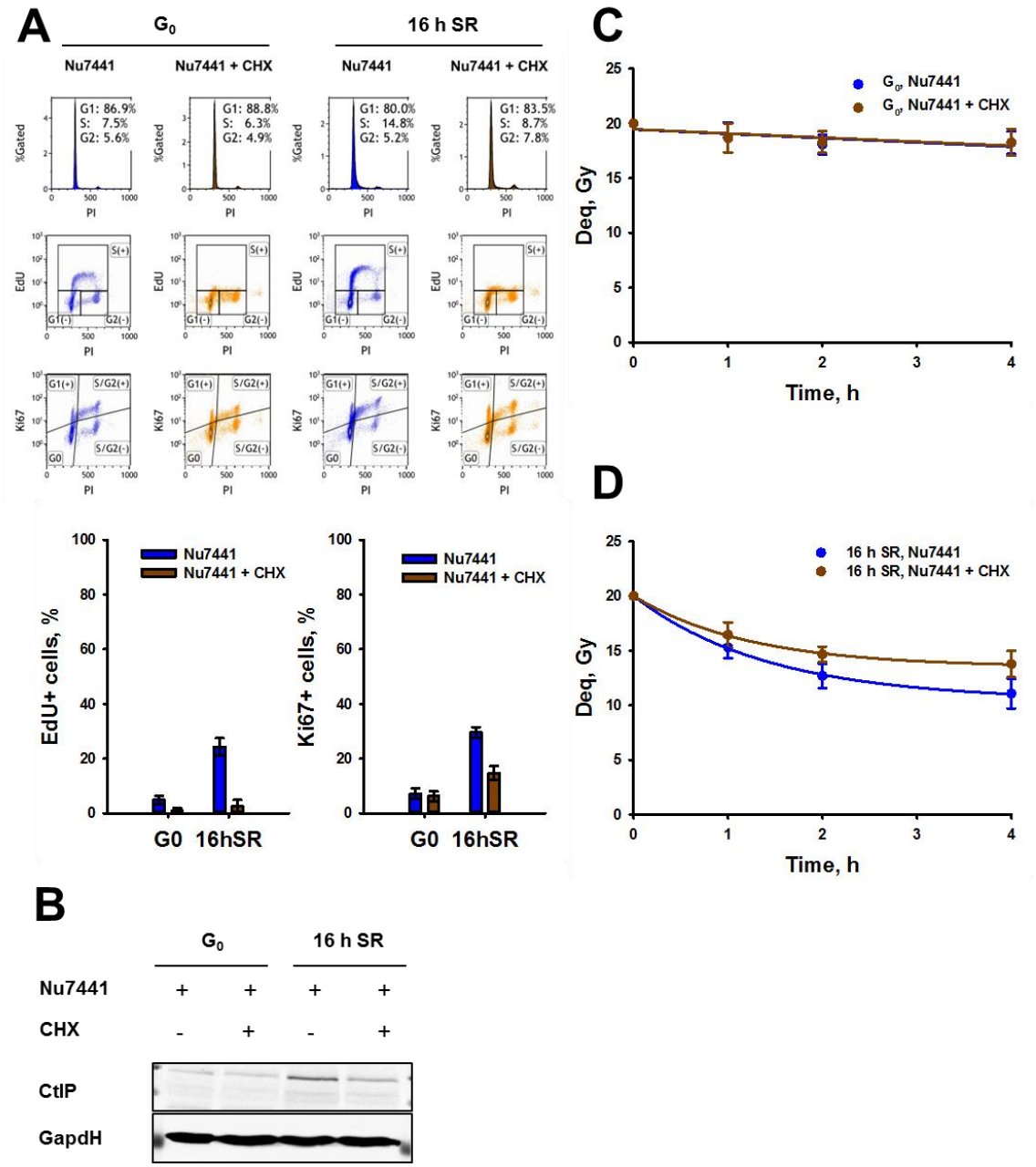

Figure 31: Abrogation of alt-EJ is coincident with a decrease of CtIP expression.

A) Flow cytometric validation of G_0 phase and serum replenished (SR) cells. Histograms are representative for two independent experiments. Shown bars represent means, vertical lines represent minimal and maximal values obtained from two independent experiments. B) Western blot analysis of CtIP in G_0 phase and serum replenished cells. Blots are representative for two independent experiments. C-D) PFGE analysis of alt-EJ in G_0 phase cells (C) and serum replenished cells (D). Shown data points represent means and StDev from 6-8 determinations in two independent experiments.

Changes of CtIP expression under the given treatment were monitored by Western blotting analysis (Figure 31B). In G_0 phase control cells, CtIP expression was very low and, not surprisingly, inhibition of protein synthesis had no further impact on its expression. During SR, CtIP expression increased again, but here the treatment had

a clear impact. CtIP expression was successfully suppressed and remained at a low level when translation was inhibited.

Cells were further subjected to PFGE analysis (Figure 31C-D and Table 32). Inhibition of translation had no effect on alt-EJ in G_0 phase control cells. There was almost no alt-EJ activity detected. But, very importantly, the recovery of alt-EJ that was normally seen in serum replenished cells, was impaired when cells were treated with the translation inhibitor. While DNA DSB repair by alt-EJ led to a residual Deq of 11.1 Gy in serum replenished cells, this was decreased in CHX treated cells and here residual Deq was measured to be 13.8 Gy. Both conditions did not enable cells to reach the reference time t_{10Gy}. In serum replenished cells, final residual damage was approximated to be converging towards 10.5 Gy. Additional inhibition of translation was approximated to a final residual damage that converged towards 13.5 Gy.

Table 32: Abrogation of alt-EJ is coincident with a decrease of CtIP expression: kinetics of DNA DSB decay.
A) Equations for DNA DSB repair kinetics. B Half-life value (t_{10Gy}) and residual Deqs of repair kinetics as shown in Figure 31C-D.

A

	DNA DSB repair kinetics
G_0 phase, Nu7441	Linear decay function
G_0 phase, Nu7441 + CHX	Linear decay function
16 h SR, Nu7441	Four-parametric exponential decay function
16 h SR, Nu7441 + CHX	Four-parametric exponential decay function

B

	t_{10Gy}	**Residual Deq**
G_0 phase, Nu7441	> 24 h	18.3 Gy
G_0 phase, Nu7441 + CHX	> 24 h	18.3 Gy
16 h SR, Nu7441	$\lim_{Deq} \rightarrow$ 10.5 Gy	11.1 Gy
16 h SR, Nu7441 + CHX	$\lim_{Deq} \rightarrow$ 13.5 Gy	13.8 Gy

In conclusion, treating cells with translation inhibitor CHX had two effects. It effectively prevented increase of CtIP expression which occurred when G_0 phase cells re-entered the cell cycle again and it impaired recovery of alt-EJ efficiency at the same time. This is a very important finding as it shows that absence of CtIP is coincident with impairment of alt-EJ efficiency and is a first hint that CtIP might be involved in the regulation of this repair pathway.

7.16 Rescue of alt-EJ is coincident with an increase of CtIP expression

In G_0 phase cells, when alt-EJ was abrogated, CtIP was absent. And the preceding analysis demonstrated that decrease of CtIP expression in serum replenished cells was accompanied by abrogation of alt-EJ efficiency, too. Vice versa, cells were able to repair DNA DSBs by alt-EJ when CtIP was present. Therefore, in the final experiment of this thesis, CtIP expression was supposed to be modified so that it would be present in G_0 phase cells and it was hypothesized that this would also increase alt-EJ efficiency thereupon. CtIP is known to be expressed but degraded via the ubiquitin-proteasome pathway during G_0 phase (see paragraph 4.8.3) so that net expression of the protein is very low. In order to raise CtIP expression in 82-6 hTERT cells in G_0 phase, bortezomib (BOR) was used. BOR is a proteasome inhibitor targeting the 20S core particle and thereby preventing degradation of ubiquitylated proteins [141-143] and, presumably, of CtIP, as well.

The effect of proteasomal inhibition on cell cycle distribution of G_0 phase and serum replenished cells was monitored by three-parametric flow cytometry analysis for PI, EdU and Ki67 staining (Figure 32A). DNA synthesis activity and proliferative activity of G_0 phase cells were low and not clearly affected by the treatment. The effect was bigger in cells being serum replenished for 16 h: here, proteasomal inhibition was suppressing DNA synthesis and was decreasing proliferation.

Western blotting analysis displayed the changes of CtIP expression during the experiment (Figure 32B). In serum replenished control cells, CtIP expression was present. In G_0 phase cells, CtIP expression was very low due to its proteasomal degradation in this phase. However, when proteasomal degradation was inhibited, CtIP expression was clearly higher in G_0 phase and even exceeded the signal that was detected in serum replenished cells.

Efficiency of alt-EJ was evaluated by PFGE analysis (Figure 32C-D and Table 33).

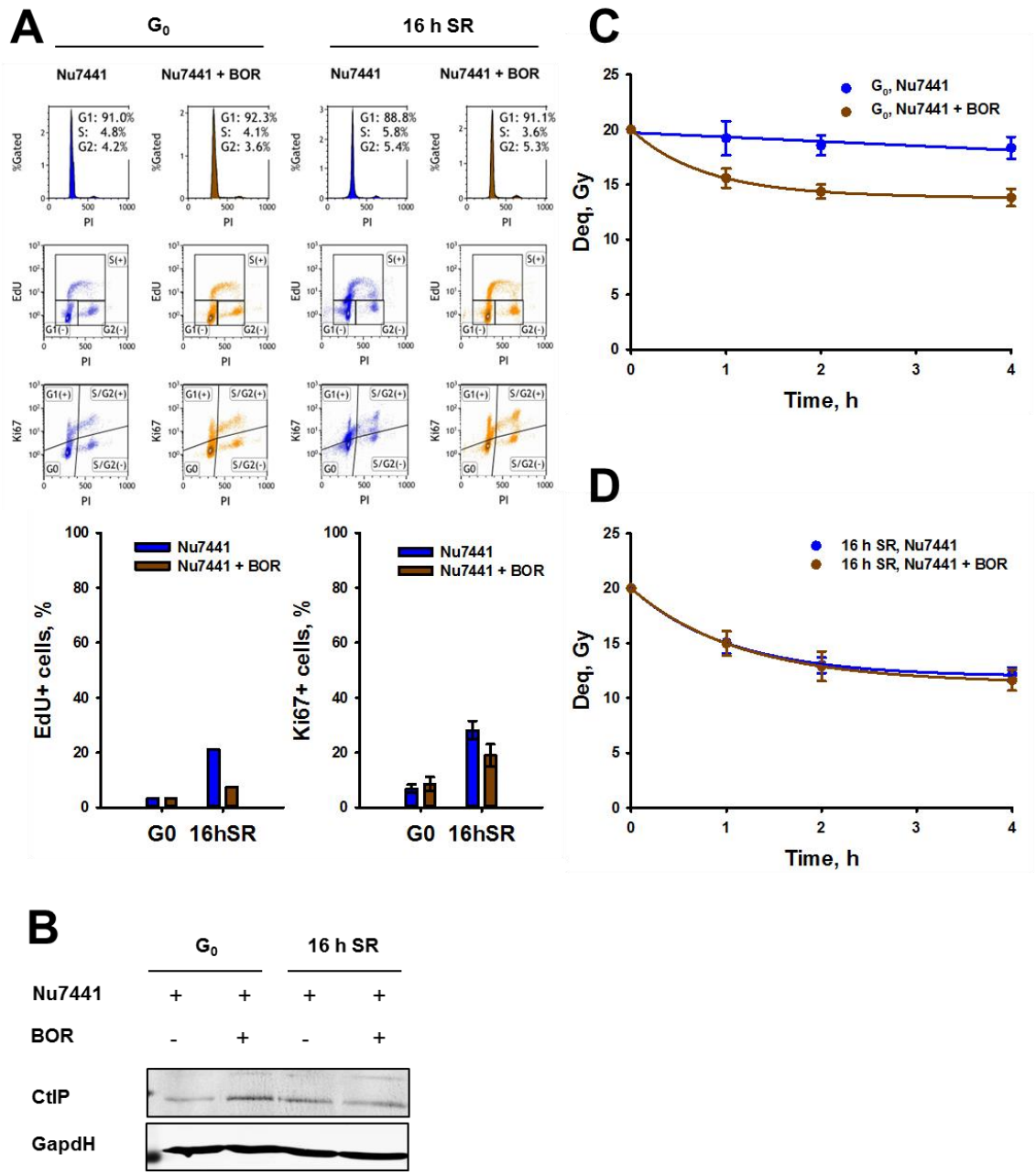

Figure 32: Rescue of alt-EJ is coincident with an increase of CtIP expression.

A) Flow cytometric validation of G_0 phase and serum replenished (SR) cells. Histograms for PI and Ki67 staining are representative for two independent experiments, EdU staining was conducted twice but failed once. Shown bars for Ki67 positive cells represent means, vertical lines represent minimal and maximal values obtained from two independent experiments. B) Western blotting analysis of CtIP in G_0 phase and serum replenished cells. Blots are representative for two independent experiments. C-D) PFGE analysis of alt-EJ in G_0 phase cells (C) and serum replenished cells (D). Shown data points represent means and StDev from 4-8 determinations in two independent experiments.

Serum replenished control cells displayed no further beneficial effect of proteasomal inhibition on the already decent repair in this condition. But, most importantly, the abrogation of alt-EJ that was normally seen in G_0 phase cells was certainly improved when cells were inhibited for proteasomal degradation. DNA DSB damage decay

changed from linear to four-parametric exponential decay function. And while DNA DSB repair by alt-EJ led to a residual Deq of 18.3 Gy in G_0 phase cells, the residual Deq decreased to be 13.8 Gy if proteasome inhibitor treatment was applied.

Table 33: Rescue of alt-EJ is coincident with an increase of CtIP expression: kinetics of DNA DSB decay.
A) Equations for DNA DSB repair kinetics. B) Half-life value (t_{10Gy}) and residual Deqs of repair kinetics as shown in Figure 32C-D.

A

	DNA DSB repair kinetics
G_0 phase, Nu7441	Linear decay function
G_0 phase, Nu7441 + BOR	Four-parametric exponential decay function
16 h SR, Nu7441	Four-parametric exponential decay function
16 h SR, Nu7441 + BOR	Four-parametric exponential decay function

B

	t_{10Gy}	**Residual Deq**
G_0 phase, Nu7441	> 24 h	18.3 Gy
G_0 phase, Nu7441 + BOR	> 24 h	13.8 Gy
16 h SR, Nu7441	$\lim_{Deq} \rightarrow$ 11.9 Gy	12.2 Gy
16 h SR, Nu7441 + BOR	> 24 h	11.6 Gy

In summary, proteasomal inhibition sufficiently blocked degradation of CtIP in G_0 phase. Concomitantly, it resolved abrogation of alt-EJ and clearly improved its efficiency in non-cycling cells. This is of paramount importance for the presented thesis as, so far, rescue of alt-EJ was only detected when cells re-entered the cell cycle upon SR or growth factor treatment. But here it is demonstrated that alt-EJ can also be employed in G_0 phase. Rescue of alt-EJ in G_0 phase is coincident with presence of CtIP and is putting further weight on the hypothesis that CtIP might be involved in regulation of alt-EJ efficiency during the cell cycle.

8. Discussion

8.1 On the necessity of radiobiological basic research for clinical improvements in radiotherapy

Radiotherapy is the most widely applied technique to treating solid cancers in the Western world. In the USA, approximately 60 % of cancer patients receive radiotherapy [144]. Irradiation regimens have been developed to improve the outcome of therapy, for example by refining fractionated dose treatment plans, applying different radiation modalities, but also by implementing sophisticated 3D treatment plans or organ motion tracking during irradiation. Nevertheless, sparing healthy (non-proliferative) tissue from harmful irradiation and excluding it from treatment plans remains a challenge in the daily routine of oncology. Aside from improving radiation treatment plans, radiotherapy is also combined with other techniques to improve the outcome, for example chemotherapeutic agents, immunotherapy and surgery.

Despite the advances of modern radiotherapy, cancer recurrence and radiorestance remain significant obstacles. Implementation of recent findings in radiation biology could be of benefit for development of better radiotherapeutic treatment strategies. Differences between tissue types that should be considered are diverging chromatin architecture, differential radiosensitivity in different cell cycle phases or the ability to employ DNA damage repair mechanisms. For example, in terms of chromatin architecture, it is known that lymphocytes are more radiosensitive than many other cell types. In T cells, one lymphocyte subset, it was demonstrated that this can be attributed to their highly condensed chromatin state [145]. Differences in radiosensitivity can be also found among different cell cycle phases. S and G_2 phase cells are more radiosensitive than G_1 phase cells [7]. Finally, the outcome of DNA damage that is administered during radiotherapy depends strongly on the DNA DSB repair pathways the irradiated cells are able to utilize [146]. There are several repair pathways to eliminate DNA DSBs from the genome. And they do so with varying fidelity. One of these pathways is alt-EJ and its presence and efficiency fluctuates dramatically throughout the cell cycle. It operates with pronounced efficiency in G_2 phase, is weaker in G_1 phase and is not present in G_0 phase. In part, the human body is composed of differentiated G_0 phase cells and their inability to employ alt-EJ constitutes a major difference to proliferating tumor cells.

Molecular mechanisms governing the differences in radiosensitivity between healthy and tumorigenic tissues, or different cellular subsets in general, can be of clinical interest as they can be used to develop novel therapeutic approaches which might protect healthy tissue and further sensitize tumors to IR.

8.2 Establishment of protocols for cell cycle manipulation, G_0 phase induction and cell cycle re-entry

In this thesis, investigation of alt-EJ efficiency in non-cycling cells was first conducted in plateau phase cells (Figure 13). Plateau phase of growth can be induced by different conditions, for example by exhaustive cellular consumption of nutrients or by lack of space occurring at high cell densities [22]. In the literature [76, 85] and also in the current project it was initially decided to conduct experiments in plateau phase for a special reason: permitting cells to run into their natural plateau phase of growth appeared to resemble *in vivo* conditions more closely than G_0 phase induction by SD. In a living organism, it is more likely that cells encounter high cell densities within a tissue, and react accordingly, than experience absolute exclusion of growth factors from the microenvironment, as it is generated upon SD. However, conducting experiments in plateau phase of growth has certain disadvantages. First, it is questionable what actually causes the stop of proliferation, lack of nutrients, lack of space or both. The proximate cause of seen effects cannot be irrevocably determined. Second, final amount of nutrients and space after 8 days of incubation (Figure 13A-B) could not be assessed. Third, it is not possible to set a clear cut between the two comparative conditions “proliferating” and “non-proliferating” as depletion of nutrients and/or space occur not at once but gradually, thus on a sliding scale. It was therefore decided to switch to a cleaner experimental setup and to induce cell cycle exit by SD (Figure 14). In this approach only one experimental parameter, presence of growth factors, is manipulated and observed effects can be directly attributed to it. Moreover, deprivation of growth factors does not appear over time but instantly at a defined time point and constitutes a decrease from an amount that is sufficient to maintain a cell culture to 0 %. As evident by the results shown in Figure 13 and Figure 15, SD also provides a greater dynamic range of the observed endpoints. During plateau phase, alt-EJ was hampered and measured residual Deq accounted for 10.7 Gy. In serum deprived G_0 phase cells, alt-EJ was severely abrogated and the residual Deq was measured to be 17.8 Gy. Thus, the observed effect on alt-EJ was more pronounced upon SD. It is speculated that the marked

disparity of repaired DNA DSBs in plateau phase and G_0 phase in the end of the experiment, a difference of 7.1 Gy, results from the rather heterogeneous cell population that is generated during plateau phase induction. It is speculated that a certain subset of cells is still cycling and thus employs alt-EJ with higher efficiency than G_0 phase cells. This effect could be attributed to their potential ability to express autocrine growth factors upon starvation. A similar phenomenon might have also occurred upon SD of epithelial RPE-1 hTERT cells (Figure 17). In this experiment, it was seen that proliferative activity, identified by proliferation marker Ki67, dropped from 98 % to 17 % after 48 h of SD in cells that were initially kept in serum containing medium. It was expected that further starvation would decrease proliferative activity even more and it would approach levels that were seen in fibroblasts. Yet, additional 24 h of SD had the opposite effect and proliferative activity almost doubled. Here, it appeared that protracted SD permitted cells to express growth factors on their own, leading to a subpopulation which was persistently cycling.

However, in the predominantly used cell line in this thesis, 82-6 hTERT fibroblasts, SD induced cell cycle exit to G_0 phase and its readout Ki67 was functional and reliable. For example, this can be seen in Figure 15A, where proliferative activity decreased by over 90 % during 48 h of SD. The reliability of Ki67 as a proliferation marker can be backed up by findings of others, too. In histopathology, it is used for detection of highly proliferative cells, identification of potential cancer entities and can even be referred to as a prognostic marker to some extent. Some examples of where Ki67 labelling index can be applied in clinics are pancreatic cancer [147], breast cancer [148] and non-small cell lung cancer [149]. There are also recent findings in basic research confirming that Ki67 is a reliable proliferative marker as it is present in actively cycling cells, low when cells exit the cell cycle and absent in fully quiescent cells [150]. Sobecki and colleagues claimed that, although Ki67 expression oscillates throughout the cell cycle, it can be used as a marker for cell cycle inhibition. Furthermore, they had a deeper look in Ki67 regulation which explains observations from the current thesis: in Figure 25A it was shown that inhibition of Cdk 4/6 clearly decreased expression of Ki67. In the aforementioned study, Sobecki and colleagues explained why: the promotor of Ki67 is bound by E2F proteins that, in general, cause the gene's transcription. In early G_1 phase, however, E2F is bound and inhibited by non-phosphorylated Rb protein. Cyclin D-Cdk4/6-complex phosphorylates and thereby inactivates Rb protein and E2F mediated transcription of Ki67 can be

executed. Inhibition of Cdk 4/6 thereby impedes Ki67 expression in an indirect way and it is concluded that Ki67 is a late marker for cell cycle entry.

One might speculate that low levels of Ki67 upon Cdk 4/6 inhibition in Figure 25A could be also attributed to a blocked re-entry into the cell cycle after G_0 phase induction. However, successful entry into G_1 phase could be demonstrated by the clearly increased levels of cyclin D in this condition (Figure 25B). In summary, Ki67 is a useful tool for the discrimination of actively cycling and G_0 phase cells.

This thesis was also aiming at investigating alt-EJ efficiency upon re-entry into the cell cycle after induction of quiescence. This objective was the third and most important reason why, except for the first data set, all experiments were conducted with serum deprived G_0 phase cells instead of plateau phase cells. When cell cultures reach their natural plateau phase of growth, high cell densities are generated. Those spatial conditions do not allow any further proliferation. In contrast to this, SD was conducted when cell cultures reached approximately 50 % confluence, thereby leaving enough space for further proliferation if serum replenished in G_0 phase. Successful re-entry into the cell cycle could be shown several times in the current thesis. In Figure 14 it is seen that proliferative activity rose about 50 % within 24 h of SR after G_0 phase. Also in RPE-1 hTERT cells, which are of different germinal layer origin, SR had an effect on proliferation (Figure 19A). In further experiments, temporal requirements of cell cycle re-entry were more precisely defined. First, it was demonstrated that 12 h of SR were not sufficient (Figure 16A). Second, Figure 20 showed that the earliest onset of cell cycle re-entry in 82-6 hTERT cells could occur after 16 h of SR. Finally, an additional set of experiments was conducted to identify the exact cell cycle phase formerly G_0 phase cells would have had reached after 16 h of SR. In Figure 22 to Figure 25 an array of cell cycle inhibitors was used to sequentially exclude first G_2, then S and eventually late G_1 phase cells from the experiment setup and it was found that after 16 h of SR the cell population mainly consisted of early G_1 phase cells. This conclusion was not only based on flow cytometry analyses of proliferative activity and DNA synthesis activity, but also with the aid of Western blotting analyses of cyclin expression and, moreover, by a critical literature research about the functions of the used cell cycle phase inhibitors.

8.3 Methods for DNA DSB repair assessment by PFGE

In order to assess the amount of DNA DSB repair following IR, PFGE analyses were conducted. The technique measures intensity of fluorescently labeled DNA fragments released in an agarose gel, which is indicative of unrepaired DNA DSBs. By measuring damage at given time points after IR, amount of repair that has taken place can be estimated. In contrast to the Comet assay, PFGE was the method of choice as it allows to assess the overall damage induced in a large population of cells. Although the investigated cell populations in many experiments were rather homogenous, for example G_0 phase or G_1 phase cells, small cell subsets of other cell cycle phases could not be entirely excluded (as seen in flow cytometry histograms). The inherited statistical robustness in terms of signal acquisition (approximately 1×10^6 cells per data point) that PFGE possesses permits a reliable estimation of the overall damage induced in a population and is less sensitive to small cell subsets. However, it must be kept in mind that the high dose (20 Gy), that was applied in order to achieve reliable results is not in accordance with clinical irradiation regimens as it is above lethal doses for whole body irradiations.

Kinetic data obtained in PFGE experiments were fitted with a second order four-parametric exponential decay model. This model is in line with the existing hypothesis [78] that decrease of DNA DSBs over time is due to the function of two repair pathways alt-EJ and c-NHEJ, both removing this kind of damage from the genome at an exponential rate. In case one of these pathways is inhibited, the rate of decay in the function becomes slower but still follows the exponential model. In case both pathways are compromised, the function will ideally be linear with a slope of zero. This switch in decay models was observed in most experiments. Upon compromising first c-NHEJ and then alt-EJ, DNA DSB repair followed a linear function with a very small slope. For example, this is seen in Figure 15C, where the regression curve switches from exponential decay to linear decay, or in Figure 21B, where it switches back from being linear to being exponential. The low value of the slope of linear decay functions is within limits of measurement uncertainty and cannot be statistically distinguished from zero.

In order to present PFGE results in a more comprehensive way and to making it accessible to comparison it was decided to use half-life values of the exponential decay functions (t_{10Gy}). As in some experimental setups calculated t_{10Gy} values were falling outside of the measured time intervals, residual damage at the last measured time point is presented, too.

8.4 Alt-EJ abrogation in G_0 phase and its rescue in G_1 phase

One important finding of this thesis is the complete abrogation of DNA DSB repair by alt-EJ upon G_0 phase induction. In Figure 15C it is seen that repair kinetics underwent a dramatic shift from four-parametric exponential decay to linear decay and that DNA DSB repair conducted by Dna-Pkcs inhibited G_0 phase cells accounted for only 2.2 Deq. This observation is in line with other results from the current working group, finding a strong cell cycle dependency of alt-EJ [76, 86]. But it can be further substantiated by findings of others. Bindra and colleagues developed an I-SceI-based reporter assay to studying mutagenic NHEJ in living cells [151]. In this case, mutagenic NHEJ meets the definition of alt-EJ as it was presented in paragraph 4.7.3. In this report, cell starvation was executed by plateau phase induction and by a combination of plateau phase induction and SD to 0.1 %. G_1/G_0 phase cell subsets were identified via flow cytometry analysis for PI staining. The authors found a strong inhibition of mutagenic NHEJ in these conditions, despite the different approaches for cell starvation and G_0 phase identification. This is very interesting, as Bindra and colleagues used a completely different system to study alt-EJ in G_0 phase cells, but came to similar conclusions.

An even more important finding of this thesis is the recovery of alt-EJ when G_0 phase cells were serum replenished. In Figure 16B-C it is shown that 24 h of SR strongly improved alt-EJ efficiency and that assessed residual Deqs were similar to those seen in Dna-Pkcs inhibited cells that had never been serum deprived (Figure 15B). This strong rescue was accompanied by a clear increase in proliferative activity, which rose up to more than 50 %. Furthermore, PI staining revealed high amounts of S and G_2 phase cells. Thus, it was concluded that 24 h of SR had given enough time to the cells to fully transit through the cell cycle. As S and G_2 phase cells are known to engage alt-EJ very efficiently, the strong recovery of alt-EJ upon 24 h of SR was, therefore, no surprise. Same trends were seen upon SR of formerly serum deprived RPE-1 hTERT cells (Figure 19B). This is of note as it demonstrates that the observed effect of alt-EJ recovery is not limited to fibroblasts, but can be detected in cells of a different germinal layer origin, as well.

Moreover, it was astonishing that alt-EJ could be rescued almost fully upon much lower durations of SR (16 h, Figure 21). Prior to experimentation, it was expected that alt-EJ efficiency would only recover upon a high increase of proliferative activity, but this experiment showed that rescue coincided with the very beginning of proliferative activity and was a first hint that alt-EJ might be functional even if former G_0 phase

cells had just entered early G_1 phase. To further investigate this assumption, G_2 phase cells were excluded from experimentation, as they usually show strong alt-EJ efficiency and it might have been speculated that this cell subset would account for the strong recovery upon SR (Figure 23). Nevertheless, exclusion of G_2 phase cells by Pol α/δ/ε inhibition did not lead to reduced alt-EJ efficiency in serum replenished cells. Similar effects were seen when S phase cells were excluded from the experimental setup, too (Figure 24), thus concluding that a clear rescue of alt-EJ can be performed without alt-EJ proficient S and G_2 phase cells and in the sole presence of G_1 phase cells which are normally considered to have a lower efficiency for alt-EJ. Further weight was put on this hypothesis by Figure 25. In this very important experiment, late G_1 phase cells were excluded from experimentation by Cdk 4/6 inhibition and the seen repair could be only attributed to early G_1 phase cells. This experiment is of great interest as it also contains further information: it shows that alt-EJ upregulation is not associated with Ki67 expression, two entities that, so far, coincided in this thesis.

Finally, it was demonstrated that rescue of alt-EJ was sufficient even upon administration of one growth factor instead of SR, here bFGF (Figure 26). The improvement in alt-EJ took place in the absence of an increase in proliferative activity. This substantiated the hypothesis that alt-EJ efficiency is independent of Ki67 expression. It was further assumed that alt-EJ reconstitution might occur even upstream of growth factor mediated cyclin expression. This paved the way for the detailed investigation of the involvement of growth factor signaling in regulation of alt-EJ, which will be discussed in the next paragraph.

8.5 Growth factor signaling seems not to be involved in alt-EJ regulation

The assumption that growth factor downstream signaling could be involved in alt-EJ regulation was further investigated. Therefore, presence and activity of three major signaling pathways Pi3k, MAPK and Plcγ were monitored by Western blotting analyses for proteins that function as main hubs for integrating signaling in their respective pathways (Figure 27).

For Plcγ pathway, Plcγ/pPlcγ itself was chosen. Yet, active pPlcγ was barely detectable in all conditions, so that it was concluded that Plcγ signaling plays an inferior role in 82-6 hTERT cells and could be neglected.

For Pi3k pathway, Akt/pAkt was selected (Figure 27). Expression of non-phosphorylated Akt was rather unaffected from treatment conditions, but a slight increase could be detected after SR. One explanation could be, that Akt expression is mildly oscillating throughout the cell cycle, which averages to an intermediate expression signal in a heterogeneous cell population. Upon 16 h of SR however, the cell population was synchronized, which might have accounted for the detected signal increase. Phosphorylation pattern of Akt at Ser473 followed the dynamics of proliferative activity, it was high in cycling and serum replenished cells and low in G_0 phase and upon bFGF treatment. In order to investigate whether this was only coincidental or whether Akt signaling was involved in alt-EJ regulation, phosphorylation of Akt was inhibited and alt-EJ efficiency in cycling cells was measured thereupon. Very interestingly though, this treatment did not affect DNA DSB repair by alt-EJ (Figure 28), even in the absence of Pi3k regulator Pten which is known to render cells hypersensitive to Pi3k and Akt manipulation [133-135]. Hence, it was concluded that alt-EJ regulation is independent from pAkt Ser473 signaling and that, in broader terms, Akt signaling in general might not have an impact on alt-EJ. This is of interest, as regulation of c-NHEJ by Akt has been demonstrated by others. Recently, it was demonstrated that certain phosphorylation patterns of Akt, namely pAkt Thr308 and pAkt Ser473 are decisive for its regulative functions in DNA DSB repair [152]. Akt can interact with several (partially newly discovered) repair factors, for example c-NHEJ proteins Xlf and Ube2S (ubiquitin-conjugating enzyme E2 S). Ube2S gets recruited to sites of DNA DSBs and complexes with Dna-Pkcs and Ku. Its knockdown leads to decreased c-NHEJ efficiency. Ube2S is protected from proteasomal degradation by Akt [152-154]. Xlf on the other hand is negatively regulated by Akt [152, 153, 155]. Moreover, Akt also regulates HRR factors like Merit40, which interacts with Brca1 and is important for DNA DSB recognition. Its activity is increased upon Akt-mediated phosphorylation [152, 153, 156, 157].

For the investigation of MAPK pathway, Erk/pErk was chosen (Figure 27). Expression of non-phosphorylated Erk remained stable during the treatment. In the meantime, phosphorylated Erk at Thr202/Tyr204 was strongly upregulated upon SD and after treatment with bFGF. As MAPK pathway is associated with survival promotion [131], it was assumed that this upregulation might be a stress response to starvation. In a next experiment, it was assessed whether upregulation of pErk Thr202/Tyr204 was involved in the abrogated alt-EJ efficiency in G_0 phase (Figure 29). Although pErk Thr202/Tyr204 signaling was inhibited very effectively, an impact on alt-EJ could not

be detected. This is of interest, too, as MAPK signaling is capable of altering radiation responses. The expression of Xrcc1 is regulated by MAPK pathway [158]: Ras was shown to cause radioresistance in cells and it was assumed that this is probably caused by activation of a paracrine positive feedback loop increasing EGFR ligand production [28, 159]. In line with these findings it was shown that targeting both, Akt and MAPK pathway proteins can improve radiation response [160].

8.6 Regulation of alt-EJ coincides with CtIP expression

In a last set of experiments, the potential role of CtIP in the regulation of alt-EJ was investigated. First, it was seen that CtIP protein expression was absent in G_0 phase (Figure 30A). As CTIP mRNA was still detected (Figure 30B), it was concluded that expression was rather regulated on a (post-) translational than a transcriptional level. Absence of CtIP in G_0 phase is in line with the findings of others, too [108]. In order to investigate whether CtIP is involved in alt-EJ regulation, its expression was first inhibited by the antibiotic CHX in serum replenished cells (Figure 31). Very interestingly, downregulation of CtIP was accompanied by an attenuation of alt-EJ efficiency. In G_0 phase cells, no further effect was detected, as repair and CtIP expression were minimal, already. CtIP is a known mediator of alt-EJ and its absence is very likely to affect this repair pathway. Nevertheless, it must be kept in mind that CHX inhibits eukaryotic proteins synthesis in general [139, 140]. Therefore, synthesis of other proteins was inhibited, too, and these alterations might have caused the observed effect, as well.

In a last experiment, it was attempted to prevent the downregulation of CtIP in G_0 phase cells and to thereby rescuing alt-EJ in this condition (Figure 32). Abrogation of CtIP degradation was executed by application of proteasome inhibitor BOR. Here, it was astonishing to see that, indeed, a clear improvement of alt-EJ in G_0 phase was possible! While alt-EJ in general resulted in a residual Deq of 18.3 Gy in G_0 phase, further treatment with BOR increased repair and led to a residual Deq of 13.8 Gy. Also here it must be stated, that BOR did not simply prevent proteasomal degradation of CtIP alone. Also other proteins that might be normally downregulated in G_0 phase could have been protected by this treatment and could have caused the observed effect. Nevertheless, this finding is of paramount importance as it is adding further substance to the idea that CtIP is involved in the regulation of alt-EJ at the transition

from G_0 to G_1 phase and, moreover, it shows that a positive modulation of alt-EJ in G_0 phase cells is achievable.

In general, presence and function of CtIP throughout the cell cycle is discussed controversially. It is often reported that CtIP expression is low in G_1 phase and that the protein executes its function in DNA DSB repair mainly in S and G_2 phase [94, 161]. It was also stated that CtIP is downregulated after mitotic exit [108] or degraded in G_1 phase [97], respectively. At least the last statement is in contradiction with the observation that the protein is absolutely essential in G_1 phase. Its presence is required for G_1 to S phase transition as it is involved in the dissociation of Rb from its promoter and its absence in this cell cycle phase is lethal [93, 95]. Also it was shown that it is involved in alt-EJ in G_1 phase [9, 99, 110].

The last mentioned papers suggesting a role for CtIP in alt-EJ in G_1 phase are aiming at its role as a transcription factor. However, CtIP could also indirectly impact DNA DSB repair in this cell cycle phase. In 2015, it was shown that Rb family proteins are directly involved in c-NHEJ as they associate with Xrcc5 and Xrcc6. In the absence of Rb, c-NHEJ was reduced and chromosomal aberrations increased [162, 163]. This is very interesting and new insight into DNA DSB repair in G_1 phase and might offer the possibility of therapeutic exploitation via synthetic lethality [164]. In the background of the current thesis this is interpreted as follows: as CtIP seems to be a major factor of alt-EJ as well as of HRR, its inhibition in an Rb deficient context would leave cells with no viable DNA DSB repair mechanism.

9. Summary

The presented study aimed to bringing further insight into regulation of DNA DSB repair pathway alt-EJ. Determinants influencing efficiency of this pathway are cell cycle dynamics, growth factor signaling and CtIP function. Partially, these determinants influence each other mutually, so that it was decided to examine alt-EJ regulation at their interface.

For this purpose, experimentation was conducted mainly at transition of G_0 phase, when alt-EJ is absent, to G_1 phase, when it is present. Used cell lines were human and predominantly non-tumorigenic, exemplifying DNA DSB repair in healthy tissue. Fibroblasts and epithelial cells were chosen to demonstrate that seen effects were independent from germinal layer origin. Resolution of DNA DSBs by repair pathway c-NHEJ was excluded by DNA-Pkcs inhibitor treatment.

In a first methodological experiment set, temporal requirements for cell cycle exit to G_0 phase and subsequent cell cycle re-entry were investigated by conducting SD and replenishment. Flow cytometric analysis for PI and Ki67 intensity allowed discrimination between different cell cycle phases. Generation of non-cycling G_0 phase cells by SD and the possibility to identify them by Ki67 immunostaining enabled the investigation of DNA DSB repair by alt-EJ in these cells. DNA DSB repair was analyzed by PFGE and revealed a severe abrogation of alt-EJ in G_0 phase. Re-entry into the cell cycle was induced by SR and caused complete recovery of alt-EJ.

It was desirable to determine the earliest time point in which alt-EJ would be initiated after cells exit G_0 phase. Therefore, flow cytometric analysis was expanded to more reliably distinguish single cell cycle phases within the subset of cycling cells by EdU staining. Verification was conducted by analysis of cyclins by Western blotting. Additionally, an assortment of cell cycle inhibitors was used to stepwise excluding G_2, S and late G_1 phase cells from the experimental setup and alt-EJ efficiency was measured thereupon. Surprisingly, rescue of alt-EJ could be curtailed to early G_1 phase. One would assume that G_2 phase cells, being highly efficient in alt-EJ, would have contributed to the pathway recovery. So it was astonishing to see that G_1 phase cells were sufficiently capable of rescuing alt-EJ.

Rescue of abrogated alt-EJ could be induced by single growth factor administration, here bFGF, as well. Growth factors constitute a major part of cell culture serum and it was assumed that rescue of alt-EJ upon SR and bFGF treatment might be a result of growth factor downstream signaling. Major signaling pathways were monitored by

Western blotting and Akt/pAkt and Erk/pErk were considered to be potential of alt-EJ. However, a modulating function for these two proteins could not be detected and the hypothesis that growth factor downstream signaling would be involved in alt-EJ regulation appeared unlikely and was rejected for the time being.

The conducted investigation of growth factor signaling contribution to alt-EJ regulation was quite punctiform as the manual examination of more signaling factors would have been beyond the scope of the current project. Nevertheless, growth factor signaling was shown to be involved in the modulation of other DNA DSB repair pathways, so it remains interesting in the context of alt-EJ. In future projects, it might be interesting to apply screening techniques to find further promising candidate proteins, for example by enzyme-linked immunosorbent assays (ELISA).

Aside from growth factor signaling, downregulation of alt-EJ in G_0 phase could be also caused by the detected downregulation of CtIP protein expression. Therefore, it was decided to manipulate its expression and to measure DNA DSB repair thereupon. Decrease of CtIP expression in G_1 phase cells was conducted by application of the antibiotic cycloheximide which inhibits overall protein synthesis. This treatment was coincidental with an abrogation of alt-EJ. Importantly, this was a first hint of CtIP being involved in alt-EJ recovery at the transition from G_0 to G_1 phase. In a final experiment, degradation of CtIP in G_0 phase was prevented by proteasome inhibitor bortezomib. Bortezomib treatment resolved alt-EJ abrogation partially and clearly improved its efficiency in G_0 phase. This is of paramount importance for this thesis as, elsewise, rescue of alt-EJ was only detected when cells re-entered G_1 phase. But here it could be shown that alt-EJ can be employed in G_0 phase if CtIP is present.

Contribution of CtIP to alt-EJ regulation should be further investigated in future studies, as here used cycloheximide and bortezomib affected overall protein expression. Exclusive inhibition of the protein as well as CtIP knock-downs or knock-ins would sharpen the knowledge about the molecular regulation of alt-EJ. Additionally, utilization of already existing cellular clones of CtIP [109], affecting its downregulation, could establish a quantitative connection between expression of the repair factor and cellular radiosensitization and could boost the development of individualized radiotherapy rationales.

10. Zusammenfassung

Ziel der vorliegenden Studie war es, weitere Einblicke in die Regulation des DNS-DSB-Reparaturwegs alt-EJ zu gewinnen. Determinanten, die die Effizienz dieses Reparaturwegs beeinflussen, sind die Zellzyklusdynamik, die Signalwege von Wachstumsfaktoren sowie die Funktion von CtIP. Diese Determinanten beeinflussen sich teilweise gegenseitig, sodass beschlossen wurde, die alt-EJ-Regulation an ihrer Schnittstelle zu untersuchen.

Zu diesem Zweck wurden Experimente hauptsächlich am Übergang der G_0-Phase, wenn alt-EJ nicht präsent ist, zur G_1-Phase, wenn alt-EJ vorhanden ist, durchgeführt. Verwendete Zelllinien waren humanen Ursprungs und überwiegend nicht-tumorigen, was beispielhaft die DNS-DSB-Reparatur in gesundem Gewebe zeigt. Fibroblasten und Epithelzellen wurden ausgewählt, um zu zeigen, dass die beobachteten Effekte unabhängig vom Ursprung der Keimschicht waren. Die Auflösung von DNS-DSB durch den Reparaturweg c-NHEJ wurde durch die Behandlung mit einem DNA-PKcs-Inhibitor ausgeschlossen.

In ersten methodischen Experimenten wurden die zeitlichen Anforderungen für den Austritt aus dem Zellzyklus in die G_0-Phase und den anschließenden Wiedereintritt in den Zellzyklus untersucht, indem Serumentzug und –auffrischung durchgeführt wurden. Die durchflusszytometrische Analyse von PI- und Ki67-Intensität ermöglichte die Unterscheidung zwischen verschiedenen Zellzyklusphasen. Die Erzeugung von nicht-zyklierenden G_0-Phase-Zellen durch Serumentzug und die Möglichkeit, sie durch Ki67-Immunfärbung zu identifizieren, ermöglichten die Untersuchung der DNS-DSB-Reparatur durch alt-EJ in diesen Zellen. DNS-DSB-Reparatur wurde mittels PFGE analysiert und ergab eine schwerwiegende Beeinträchtigung von alt-EJ in der G_0-Phase. Der Wiedereintritt in den Zellzyklus wurde durch Serumauffrischung induziert und bewirkte eine vollständige Erholung von alt-EJ. Es war zudem wünschenswert, den frühesten Zeitpunkt zu bestimmen, zu dem alt-EJ nach Verlassen der G_0-Phase initiiert werden würde. Daher wurde die durchflusszytometrische Analyse erweitert, um einzelne Zellzyklusphasen innerhalb der Menge der zyklierenden Zellen durch EdU-Färbung zuverlässiger zu unterscheiden. Die Überprüfung erfolgte durch Western-Blot-Analyse von Cyclinen. Zusätzlich wurde eine Auswahl von Zellzyklusinhibitoren verwendet, um G_2-, S- und späte G_1-Phase-Zellen schrittweise aus dem Versuchsaufbau auszuschließen. Überraschenderweise konnte die Erholung von alt-EJ auf die frühe G_1-Phase

eingegrenzt werden. Grundsätzlich würde man annehmen, dass G_2-Phase-Zellen, die hocheffizient für alt-EJ sind, zur Wiederherstellung des Reparaturwegs beigetragen hätten. Dementsprechend war es erstaunlich zu sehen, dass G_1-Phase-Zellen in der Lage waren, alt-EJ hinreichend anzuwenden. Die Wiederherstellung von stark beeinträchtigtem alt-EJ konnte auch durch die Verabreichung eines einzelnen Wachstumsfaktors, hier bFGF, induziert werden. Wachstumsfaktoren machen einen Großteils von Zellkulturseren aus, und es wurde angenommen, dass die Wiederherstellung von alt-EJ nach Serumauffrischung oder Behandlung mit bFGF eine Folge der Signalübertragung durch Wachstumsfaktoren ist. Die wichtigsten Wachstumsfaktor-Signalwege wurden durch Western blotting überprüft und Akt/pAkt und Erk/pErk als potentiell interessant für die Regulierung von alt-EJ eingestuft. Eine Modulationsfunktion für diese beiden Proteine konnte jedoch nicht nachgewiesen werden, und die Hypothese, dass Wachstumsfaktor-Signale an der alt-EJ-Regulation beteiligt sein könnten, erschien unwahrscheinlich und wurde vorerst zurückgewiesen.
Die durchgeführte Untersuchung des Beitrags von Wachstumsfaktor-Signalen zur Regulierung von alt-EJ war recht punktuell, da die manuelle Untersuchung weiterer Signalfaktoren den Rahmen des aktuellen Projekts gesprengt hätte. Es wurde jedoch bereits gezeigt, dass Signale von Wachstumsfaktoren an der Modulation anderer DNS-DSB-Reparaturwege beteiligt sind, sodass sie im Kontext von alt-EJ weiterhin interessant erscheinen. In zukünftigen Projekten könnte es aufschlussreich sein, Screening-Techniken anzuwenden, um weitere vielversprechende Kandidaten zu ermitteln, beispielsweise durch enzymgebundene Immunosorbens-Assays.
Abgesehen von der Wachstumsfaktorsignalisierung könnte eine Herunterregulierung von alt-EJ in der G_0-Phase auch durch die nachgewiesene Herunterregulierung der CtIP-Proteinexpression in dieser Zellzyklus-Phase verursacht werden. Daher wurde beschlossen, die CtIP-Expression zu manipulieren und daraufhin die DNS-DSB-Reparatur zu messen. Die Verringerung der CtIP-Expression in G_1-Phase-Zellen wurde durch das Antibiotikum Cycloheximid herbeigeführt. Dieses hemmt die gesamte Proteinsynthese. Die Behandlung koinzidierte mit einer Aufhebung von alt-EJ. Wichtig ist, dass dies ein erster Hinweis darauf ist, dass CtIP am Übergang von der G_0- zur G_1-Phase an der Erholung von alt-EJ beteiligt ist. In einem letzten Experiment wurde der Abbau von CtIP in der G_0-Phase durch den Proteasom-Inhibitor Bortezomib verhindert. Die Behandlung mit Bortezomib löste die Beeinträchtigung von alt-EJ in dieser Zellzyklus-Phase teilweise auf und steigerte dessen Effizienz deutlich. Das ist für dieses Projekt von größter Bedeutung, da

ansonsten die Erholung von alt-EJ nur dann festgestellt wurde, wenn G_0-Phase-Zellen wieder in die G_1-Phase eintraten. Hier konnte jedoch gezeigt werden, dass alt-EJ in der G_0-Phase verwendet werden kann, wenn CtIP vorhanden ist.

Der Beitrag von CtIP zur alt-EJ-Regulation könnte in zukünfitgen Studien weiter untersucht werden. Dies ist vor allem wichtig, da die hier verwendeten Reagenzien Cycloheximid und Bortezomib die gesamt Proteinexpression beeinflussten. Die ausschließliche Hemmung von CtIP sowie Knock-Downs oder Knock-Ins dieses Proteins würden das Wissen über die molekulare Regulation von alt-EJ schärfen. Darüber hinaus könnte die Verwendung von bereits vorhanden CtIP-Klonen [109], die die Herunterregulierung des Proteins beeinflussen, einen quantitativen Zusammenhang zwischen der Expression des Reparaturfaktors und der zellulären Radiosensibilisierung herstellen und die Entwicklung individualisierter strahlentherapeutischer Konzepte fördern.

11. Bibliography

1. Siegel, R.L., K.D. Miller, and A. Jemal, *Cancer Statistics, 2017.* CA Cancer J Clin, 2017. 67(1): p. 7-30.
2. *Bericht zum Krebsgeschehen in Deutschland 2016*, 2016, Zentrum für Krebsregisterdaten im Robert Koch-Institut.
3. Hanahan, D. and R.A. Weinberg, *The Hallmarks of Cancer.* Cell, 2000. 100: p. 57-70.
4. Hanahan, D. and R.A. Weinberg, *Hallmarks of Cancer: The Next Generation.* Cell, 2011. 144: p. 646-674.
5. Alberts, B., et al., *Molecular Biology of The Cell*. Fifth Edition ed2008, New York: Garland Science, Taylor & Francis Group.
6. Mladenov, E., et al., *DNA double-strand-break repair in higher eukaryotes and its role in genomic instability and cancer: Cell cycle and proliferation-dependent regulation.* Seminars in Cancer Biology, 2016. 37-38: p. 51-64.
7. Hall, E.J. and A.J. Giaccia, *Radiobiology for the Radiologist*. Sixth Edition ed2006, Philadelphia, Baltimore, New York, London, Buenos Aires, Hong Kong, Sydney, Tokyo: Lippincott Williams & Wilkins.
8. Ciccia, A. and S.J. Elledge, *The DNA Damage Response: Making It Safe to Play with Knives.* Molecular Cell, 2010. 40(2): p. 179-204.
9. Polo, S.E. and S.P. Jackson, *Dynamics of DNA damage response proteins at DNA breaks: a focus on protein modifications.* Genes & Development, 2011. 25(5): p. 409-433.
10. Jeggo, P.A., L.H. Pearl, and A.M. Carr, *DNA repair, genome stability and cancer: a historical perspective.* Nature Reviews. Cancer, 2016. 16(1): p. 35-42.
11. Jackson, S.P. and J. Bartek, *The DNA-damage response in human biology and disease.* Nature, 2009. 461(7267): p. 1071-1078.
12. Sulli, G., R. Di Micco, and F.d.A. di Fagagna, *Crosstalk between chromatin state and DNA damage response in cellular senescence and cancer.* Nature Reviews. Cancer, 2012. 12(10): p. 709-720.
13. Mirza-Aghazadeh-Attari, M., et al., *53BP1: A key player of DNA damage response with critical functions in cancer.* DNA Repair (Amst), 2019. 73: p. 110-119.
14. Moore, J.D., *In the wrong place at the wrong time: does cyclin mislocalization drive oncogenic transformation?* Nature Reviews. Cancer, 2013. 13(3): p. 201-208.
15. Aguilar, V. and L. Fajas, *Cycling through metabolism.* EMBO Mol Med, 2010. 2(9): p. 338-48.
16. Wilson, A.C., *Setting the stage for S phase.* Mol Cell, 2007. 27(2): p. 176-7.
17. Löbrich, M. and P.A. Jeggo, *The impact of a negligent G2/M checkpoint on genomic instability and cancer induction.* Nature Reviews. Cancer, 2007. 7(11): p. 861-869.
18. Kastan, M.B. and J. Bartek, *Cell-cycle checkpoints and cancer.* Nature, 2004. 432: p. 316-323.
19. Oakes, V., et al., *Cyclin A/Cdk2 regulates Cdh1 and claspin during late S/G2 phase of the cell cycle.* Cell Cycle, 2014. 13(20): p. 3302-11.
20. Massague, J., *G1 cell-cycle control and cancer.* Nature, 2004. 432(7015): p. 298-306.
21. Zetterberg, A. and O. Larsson, *Kinetic analysis of regulatory events in G1 leading to proliferation or quiescence of Swiss 3T3 cells.* Proc Natl Acad Sci U S A, 1985. 82(16): p. 5365-9.

22. Cheung, T.H. and T.A. Rando, *Molecular regulation of stem cell quiescence.* Nature Reviews. Molecular Cell Biology, 2013. 14(6): p. 329-340.
23. Ito, M., et al., *Stem cells in the hair follicle bulge contribute to wound repair but not to homeostasis of the epidermis.* Nature Medicine, 2005. 11: p. 1351.
24. Zou, P., et al., *p57(Kip2) and p27(Kip1) cooperate to maintain hematopoietic stem cell quiescence through interactions with Hsc70.* Cell Stem Cell, 2011. 9(3): p. 247-61.
25. Yarden, Y. and M.X. Sliwkowski, *Untangling the ErbB signalling network.* Nat Rev Mol Cell Biol, 2001. 2(2): p. 127-37.
26. Lemmon, M.A. and J. Schlessinger, *Cell signaling by receptor-tyrosine kinases.* Cell, 2010. 141(7): p. 1117-1134.
27. Downward, J., *PI 3-kinase, Akt and cell survival.* Semin Cell Dev Biol, 2004. 15(2): p. 177-82.
28. Rodemann, H.P., K. Dittmann, and M. Toulany, *Radiation-induced EGFR-signaling and control of DNA-damage repair.* International Journal of Radiation Biology, 2007. 83(11-12): p. 781-791.
29. Xu, N., et al., *Akt: A Double-Edged Sword in Cell Proliferation and Genome Stability.* Journal of Oncology, 2012. 2012: p. ID951724.
30. Qi, M. and E.A. Elion, *MAP kinase pathways.* J Cell Sci, 2005. 118(Pt 16): p. 3569-72.
31. Freeley, M., D. Kelleher, and A. Long, *Regulation of Protein Kinase C function by phosphorylation on conserved and non-conserved sites.* Cell Signal, 2011. 23(5): p. 753-62.
32. Griner, E.M. and M.G. Kazanietz, *Protein kinase C and other diacylglycerol effectors in cancer.* Nat Rev Cancer, 2007. 7(4): p. 281-94.
33. Gerdes, J., et al., *Production of a mouse monoclonal antibody reactive with a human nuclear antigen associated with cell proliferation.* Int J Cancer, 1983. 31(1): p. 13-20.
34. Gerdes, J., et al., *Cell cycle analysis of a cell proliferation-associated human nuclear antigen defined by the monoclonal antibody Ki-67.* J Immunol, 1984. 133(4): p. 1710-5.
35. Scholzen, T. and J. Gerdes, *The Ki-67 protein: from the known and the unknown.* J Cell Physiol, 2000. 182(3): p. 311-22.
36. Schonk, D.M., et al., *Assignment of the gene(s) involved in the expression of the proliferation-related Ki-67 antigen to human chromosome 10.* Hum Genet, 1989. 83(3): p. 297-9.
37. Schluter, C., et al., *The cell proliferation-associated antigen of antibody Ki-67: a very large, ubiquitous nuclear protein with numerous repeated elements, representing a new kind of cell cycle-maintaining proteins.* J Cell Biol, 1993. 123(3): p. 513-22.
38. Endl, E. and J. Gerdes, *The Ki-67 protein: fascinating forms and an unknown function.* Exp Cell Res, 2000. 257(2): p. 231-7.
39. MacCallum, D.E. and P.A. Hall, *Biochemical characterization of pKi67 with the identification of a mitotic-specific form associated with hyperphosphorylation and altered DNA binding.* Exp Cell Res, 1999. 252(1): p. 186-98.
40. Hofmann, K. and P. Bucher, *The FHA domain: a putative nuclear signalling domain found in protein kinases and transcription factors.* Trends Biochem Sci, 1995. 20(9): p. 347-9.
41. Brown, D.C. and K.C. Gatter, *Ki67 protein: the immaculate deception?* Histopathology, 2002. 40(1): p. 2-11.
42. Sun, Z., et al., *Rad53 FHA Domain Associated with Phosphorylated Rad9 in the DNA Damage Checkpoint.* Science, 1998. 281(5374): p. 272-274.

43. Bullwinkel, J., et al., *Ki-67 protein is associated with ribosomal RNA transcription in quiescent and proliferating cells.* J Cell Physiol, 2006. 206(3): p. 624-35.
44. Rahmanzadeh, R., et al., *Chromophore-assisted light inactivation of pKi-67 leads to inhibition of ribosomal RNA synthesis.* Cell Prolif, 2007. 40(3): p. 422-30.
45. Cuylen, S., et al., *Ki-67 acts as a biological surfactant to disperse mitotic chromosomes.* Nature, 2016. 535(7611): p. 308-12.
46. Burma, S., B.P.C. Chen, and D.J. Chen, *Role of non-homologous end joining (NHEJ) in maintaining genomic integrity.* DNA Repair, 2006. 5(9-10): p. 1042-1048.
47. San Filippo, J., P. Sung, and H. Klein, *Mechanism of Eukaryotic Homologous Recombination.* Annual Review of Biochemistry, 2008. 77: p. 229-257.
48. Symington, L.S. and J. Gautier, *Double-Strand Break End Resection and Repair Pathway Choice.* Annual Review of Genetics, 2011. 45: p. 247-271.
49. Dueva, R. and G. Iliakis, *Alternative pathways of non-homologous end joining (NHEJ) in genomic instability and cancer.* Translational Cancer Research, 2013. 2(3): p. 163-177.
50. Buisson, R., et al., *Coupling of Homologous Recombination and the Checkpoint by ATR.* Mol Cell, 2017. 65(2): p. 336-346.
51. Ghezraoui, H., et al., *Chromosomal translocations in human cells are generated by canonical nonhomologous end-joining.* Mol Cell, 2014. 55(6): p. 829-842.
52. Iliakis, G., et al., *Mechanisms of DNA double strand break repair and chromosome aberration formation.* Cytogenetic and Genome Research, 2004. 104: p. 14-20.
53. Fell, V.L. and C. Schild-Poulter, *The Ku heterodimer: Function in DNA repair and beyond.* Mutation Research/Reviews in Mutation Research, 2015. 763(0): p. 15-29.
54. Chiruvella, K.K., Z. Liang, and T.E. Wilson, *Repair of Double-Strand Breaks by End Joining.* Cold Spring Harbor Perspectives in Biology, 2013. 5(5): p. a012757.
55. Radhakrishnan, S.K., N. Jette, and S.P. Lees-Miller, *Non-homologous end joining: Emerging themes and unanswered questions.* DNA Repair, 2014. 17: p. 2-8.
56. Uematsu, N., et al., *Autophosphorylation of DNA-PKCS regulates its dynamics at DNA double-strand breaks.* Journal of Cell Biology, 2007. 177(2): p. 219-229.
57. Ma, Y., et al., *Hairpin Opening and Overhang Processing by an Artemis/DNA-Dependent Protein Kinase Complex in Nonhomologous End Joining and V(D)J Recombination.* Cell, 2002. 108: p. 781-794.
58. Paull, T.T., *Saving the Ends for Last: The Role of Pol μ in DNA End Joining.* Molecular Cell, 2005. 19: p. 294-296.
59. Daley, J.M., et al., *DNA Joint Dependence of Pol X Family Polymerase Action in Nonhomologous End Joining.* Journal of Biological Chemistry, 2005. 280(32): p. 29030-29037.
60. Andres, S.N., et al., *A human XRCC4–XLF complex bridges DNA.* Nucleic Acids Research, 2012. 40(4): p. 1868-1878.
61. Roy, S., et al., *XRCC4/XLF Interaction Is Variably Required for DNA Repair and Is Not Required for Ligase IV Stimulation.* Molecular and Cellular Biology, 2015. 35(17): p. 3017-3028.

62. Oh, S., et al., *DNA ligase III and DNA ligase IV carry out genetically distinct forms of end joining in human somatic cells.* DNA Repair, 2014. 21(0): p. 97-110.
63. Lieber, M.R., *The Mechanism of Double-Strand DNA Break Repair by the Nonhomologous DNA End-Joining Pathway.* Annual Review of Biochemistry, 2010. 79: p. 1.1-1.31.
64. Cheong, N., et al., *DNA-PK-independent rejoining of DNA double-strand breaks in human cell extracts in vitro.* International Journal of Radiation Biology, 1999. 75: p. 67-81.
65. Beck, C., et al., *Poly(ADP-ribose) polymerases in double-strand break repair: Focus on PARP1, PARP2 and PARP3.* Experimental Cell Research, 2014. 329(1): p. 18-25.
66. Wang, M., et al., *PARP-1 and Ku compete for repair of DNA double strand breaks by distinct NHEJ pathways.* Nucleic Acids Research, 2006. 34(21): p. 6170-6182.
67. Soni, A., et al., *Inhibition of Parp1 by BMN673 Effectively Sensitizes Cells to Radiotherapy by Upsetting the Balance of Repair Pathways Processing DNA Double-Strand Breaks.* Mol Cancer Ther, 2018. 17(10): p. 2206-2216.
68. Rosidi, B., et al., *Histone H1 functions as a stimulatory factor in backup pathways of NHEJ.* Nucleic Acids Research, 2008. 36(5): p. 1610-1623.
69. Haince, J.-F., et al., *PARP1-dependent Kinetics of Recruitment of MRE11 and NBS1 Proteins to Multiple DNA Damage Sites.* Journal of Biological Chemistry, 2008. 283(2): p. 1197-1208.
70. Ceccaldi, R., B. Rondinelli, and A.D. D'Andrea, *Repair Pathway Choices and Consequences at the Double-Strand Break.* Trends in Cell Biology, 2015. 26(1): p. 52-64.
71. Ceccaldi, R., et al., *Homologous-recombination-deficient tumours are dependent on Pol[thgr]-mediated repair.* Nature, 2015. 518(7538): p. 258-262.
72. Paul, K., et al., *DNA ligases I and III cooperate in alternative non-homologous end-joining in vertebrates.* PLoS ONE, 2013. 8(3): p. e59505.
73. Arakawa, H., et al., *Functional redundancy between DNA ligases I and III in DNA replication in vertebrate cells.* Nucleic Acids Research, 2012. 40(6): p. 2599-2610.
74. Wang, X., et al., *Caffeine-induced radiosensitization is independent of non-homologous end joining of DNA double strand breaks.* Radiation Research, 2003. 159: p. 426-432.
75. Wang, H., et al., *ATR Affecting Cell Radiosensitivity Is Dependent on Homologous Recombination Repair but Independent of Nonhomologous End Joining.* Cancer Research, 2004. 64: p. 7139-7143.
76. Windhofer, F., et al., *Marked dependence on growth state of backup pathways of NHEJ.* International Journal of Radiation Oncology Biology Physics, 2007. 68(5): p. 1462-1470.
77. Mladenov, E. and G. Iliakis, *Induction and repair of DNA double strand breaks: the increasing spectrum of non-homologous end joining pathways.* Mutat Res, 2011. 711(1-2): p. 61-72.
78. Metzger, L. and G. Iliakis, *Kinetics of DNA double strand breaks throughout the cell cycle as assayed by pulsed field gel electrophoresis in CHO cells.* International Journal of Radiation Biology, 1991. 59: p. 1325-1339.
79. Rothkamm, K., et al., *Pathways of DNA Double-Strand Break Repair during the Mammalian Cell Cycle.* Molecular and Cellular Biology, 2003. 23: p. 5706-5715.

80. Takata, M., et al., *Homologous recombination and non-homologous end-joining pathways of DNA double-strand break.* EMBO Journal, 1998. 17: p. 5497-5508.
81. Wang, H., et al., *Caffeine could not efficiently sensitize homologous recombination repair deficient cells to ionizing radiation-induced killing.* Radiation Research, 2003. 159: p. 420-425.
82. Iliakis, G., *Backup pathways of NHEJ in cells of higher eukaryotes: Cell cycle dependence.* Radiotherapy and Oncology, 2009. 92: p. 310-315.
83. Wu, W., et al., *Repair of radiation induced DNA double strand breaks by backup NHEJ is enhanced in G2.* DNA Repair, 2008. 7(2): p. 329-338.
84. Wu, W., et al., *Enhanced Use of Backup Pathways of NHEJ in G_2 in Chinese Hamster Mutant Cells with Defects in the Classical Pathway of NHEJ.* Radiation Research, 2008. 170: p. 512-520.
85. Singh, S.K., et al., *Widespread Dependence of Backup NHEJ on Growth State: Ramifications for the Use of DNA-PK Inhibitors.* International Journal of Radiation Oncology Biology Physics, 2011. 79(2): p. 540-548.
86. Singh, S.K., et al., *Inhibition of B-NHEJ in Plateau-Phase Cells Is Not a Direct Consequence of Suppressed Growth Factor Signaling.* International Journal of Radiation Oncology Biology Physics, 2012. 84(2): p. e237-e243.
87. Dittmann, K., C. Mayer, and H.-P. Rodemann, *Inhibition of radiation-induced EGFR nuclear import by C225 (Cetuximab) suppresses DNA-PK activity.* Radiotherapy and Oncology, 2005. 76(2): p. 157-161.
88. Szumiel, I., *Epidermal growth factor receptor and DNA double strand break repair: The cell's self-defence.* Cellular Signalling, 2006. 18(10): p. 1537-1548.
89. Kandel, E.S., et al., *Activation of Akt/Protein Kinase B Overcomes a G_2/M Cell Cycle Checkpoint Induced by DNA Damage.* Molecular and Cellular Biology, 2002. 22: p. 7831-7841.
90. Rodemann, H.P. and B.G. Wouters, *Molecular and translational radiation biology/oncology: what's up?* Radiother Oncol, 2011. 99(3): p. 257-61.
91. Toulany, M., et al., *Akt Promotes Post-Irradiation Survival of Human Tumor Cells through Initiation, Progression, and Termination of DNA-PKcs–Dependent DNA Double-Strand Break Repair.* Molecular Cancer Research, 2012. 10(7): p. 945-957.
92. Schaeper, U., et al., *Interaction between a cellular protein that binds to the C-terminal region of adenovirus E1A (CtBP) and a novel cellular protein is disrupted by E1A through a conserved PLDLS motif.* J Biol Chem, 1998. 273(15): p. 8549-52.
93. Liu, F. and W.H. Lee, *CtIP activates its own and cyclin D1 promoters via the E2F/RB pathway during G1/S progression.* Mol Cell Biol, 2006. 26(8): p. 3124-34.
94. Sartori, A.A., et al., *Human CtIP promotes DNA end resection.* Nature, 2007. 450: p. 509-514.
95. Chen, L., et al., *Cell cycle-dependent complex formation of BRCA1.CtIP.MRN is important for DNA double-strand break repair.* J Biol Chem, 2008. 283(12): p. 7713-20.
96. Huertas, P. and S.P. Jackson, *Human CtIP Mediates Cell Cycle Control of DNA End Resection and Double Strand Break Repair.* Journal of Biological Chemistry, 2009. 284(14): p. 9558-9565.
97. Buis, J., et al., *Mre11 regulates CtIP-dependent double-strand break repair by interaction with CDK2.* Nature Structural & Molecular Biology, 2012. 19(2): p. 246-252.

98. Mladenov, E., et al., *DNA double-strand break repair as determinant of cellular radiosensitivity to killing and target in radiation therapy.* Frontiers in Oncology, 2013. 3: p. Article 113.
99. Yun, M.H. and K. Hiom, *CtIP-BRCA1 modulates the choice of DNA double-strand-break repair pathway throughout the cell cycle.* Nature, 2009. 459(7245): p. 460-463.
100. Huertas, P., *DNA resection in eukaryotes: deciding how to fix the break.* Nature Structural & Molecular Biology, 2010. 17(1): p. 11-16.
101. Makharashvili, N. and T.T. Paull, *CtIP: A DNA damage response protein at the intersection of DNA metabolism.* DNA Repair, 2015. 32: p. 75-81.
102. Wang, H., et al., *The interaction of CtIP and Nbs1 connects CDK and ATM to regulate HR-mediated double-strand break repair.* PLoS Genet, 2013. 9(2): p. e1003277.
103. Makharashvili, N., et al., *Catalytic and noncatalytic roles of the CtIP endonuclease in double-strand break end resection.* Mol Cell, 2014. 54(6): p. 1022-33.
104. Kaidi, A., et al., *Human SIRT6 Promotes DNA End Resection Through CtIP Deacetylation.* Science, 2010. 329(5997): p. 1348-1353.
105. Soria-Bretones, I., et al., *DNA end resection requires constitutive sumoylation of CtIP by CBX4.* Nat Commun, 2017. 8(1): p. 113.
106. Germani, A., et al., *SIAH-1 interacts with CtIP and promotes its degradation by the proteasome pathway.* Oncogene, 2003. 22(55): p. 8845-51.
107. Steger, M., et al., *Prolyl Isomerase PIN1 Regulates DNA Double-Strand Break Repair by Counteracting DNA End Resection.* Molecular Cell, 2013. 50(3): p. 333-343.
108. Lafranchi, L., et al., *APC/CCdh1 controls CtIP stability during the cell cycle and in response to DNA damage.* EMBO Journal, 2014. 33(23): p. 2860-2879.
109. Ferretti, L.P., et al., *Cullin3-KLHL15 ubiquitin ligase mediates CtIP protein turnover to fine-tune DNA-end resection.* Nat Commun, 2016. 7: p. 12628.
110. You, Z. and J.M. Bailis, *DNA damage and decisions: CtIP coordinates DNA repair and cell cycle checkpoints.* Trends in Cell Biology, 2010. 20(7): p. 402-409.
111. Yu, X. and R. Baer, *Nuclear localization and cell cycle-specific expression of CtIP, a protein that associates with the BRCA1 tumor suppressor.* J Biol Chem, 2000. 275(24): p. 18541-9.
112. Ahn, J.-W., et al., *SERBP1 affects homologous recombination-mediated DNA repair by regulation of CtIP translation during S phase.* Nucleic Acids Research, 2015. 43(13): p. 6321-6333.
113. Pfaffl, M.W., *Relative quantification*, in *Real-time PCR*, T. Dorak, Editor 2006, Taylor & Francis Group: New York. p. 63-82.
114. Rubio, M.A., S.H. Kim, and J. Campisi, *Reversible manipulation of telomerase expression and telomere length. Implications for the ionizing radiation response and replicative senescence of human cells.* J Biol Chem, 2002. 277(32): p. 28609-17.
115. Huang, S., et al., *Accelerated telomere shortening and replicative senescence in human fibroblasts overexpressing mutant and wild-type lamin A.* Exp Cell Res, 2008. 314(1): p. 82-91.
116. Leahy, J.J.J., et al., *Identification of a highly potent and selective DNA-dependent protein kinase (DNA-PK) inhibitor (NU7441) by screening of chromenone libraries.* Bioorganic & Medicinal Chemistry Letters, 2004. 14(24): p. 6083-6087.

117. Bodnar, A.G., et al., *Extension of life-span by introduction of telomerase into normal human cells.* Science, 1998. 279: p. 349-352.
118. Pedrali-Noy, G., et al., *Synchronization of HeLa cell cultures by inhibition of DNA polymerase alpha with aphidicolin.* Nucleic Acids Res, 1980. 8(2): p. 377-87.
119. Goscin, L.P. and J.J. Byrnes, *DNA polymerase delta: one polypeptide, two activities.* Biochemistry, 1982. 21(10): p. 2513-8.
120. Wang, T.S., *Eukaryotic DNA polymerases.* Annu Rev Biochem, 1991. 60: p. 513-52.
121. Borner, M.M., et al., *Drug-induced apoptosis is not necessarily dependent on macromolecular synthesis or proliferation in the p53-negative human prostate cancer cell line PC-3.* Cancer Res, 1995. 55(10): p. 2122-8.
122. Baranovskiy, A.G., et al., *Structural basis for inhibition of DNA replication by aphidicolin.* Nucleic Acids Res, 2014. 42(22): p. 14013-21.
123. Krude, T., *Mimosine arrests proliferating human cells before onset of DNA replication in a dose-dependent manner.* Experimental Cell Research, 1999. 247: p. 148-159.
124. Urbani, L., S.W. Sherwood, and R.T. Schimke, *Dissociation of nuclear and cytoplasmic cell cycle progression by drugs employed in cell synchronization.* Exp Cell Res, 1995. 219(1): p. 159-68.
125. Gilbert, D.M., et al., *Mimosine arrests DNA synthesis at replication forks by inhibiting deoxyribonucleotide metabolism.* J Biol Chem, 1995. 270(16): p. 9597-606.
126. Mosca, P.J., H.B. Lin, and J.L. Hamlin, *Mimosine, a novel inhibitor of DNA replication, binds to a 50 kDa protein in Chinese hamster cells.* Nucleic Acids Research, 1995. 23: p. 261-268.
127. Lin, H.B., et al., *Mimosine targets serine hydroxymethyltransferase.* J Biol Chem, 1996. 271(5): p. 2548-56.
128. Hanauske-Abel, H.M., et al., *Inhibition of the G1-S transition of the cell cycle by inhibitors of deoxyhypusine hydroxylation.* Biochim Biophys Acta, 1994. 1221(2): p. 115-24.
129. Alpan, R.S. and A.B. Pardee, *$p21^{WAF1/CIP1/SDI1}$ is elevated through a p53-independent pathway by mimosine.* Cell Growth & Differentiation, 1996. 7: p. 893-901.
130. Fry, D.W., et al., *Specific inhibition of cyclin-dependent kinase 4/6 by PD 0332991 and associated antitumor activity in human tumor xenografts.* Mol Cancer Ther, 2004. 3(11): p. 1427-38.
131. Roux, P.P. and J. Blenis, *ERK and p38 MAPK-activated protein kinases: a family of protein kinases with diverse biological functions.* Microbiol Mol Biol Rev, 2004. 68(2): p. 320-44.
132. Hirai, H., et al., *MK-2206, an allosteric Akt inhibitor, enhances antitumor efficacy by standard chemotherapeutic agents or molecular targeted drugs in vitro and in vivo.* Mol Cancer Ther, 2010. 9(7): p. 1956-67.
133. DeGraffenried, L.A., et al., *Reduced PTEN expression in breast cancer cells confers susceptibility to inhibitors of the PI3 kinase/Akt pathway.* Ann Oncol, 2004. 15(10): p. 1510-6.
134. Andersen, J.N., et al., *Pathway-based identification of biomarkers for targeted therapeutics: personalized oncology with PI3K pathway inhibitors.* Sci Transl Med, 2010. 2(43): p. 43ra55.
135. De Velasco, M.A., et al., *Efficacy of targeted AKT inhibition in genetically engineered mouse models of PTEN-deficient prostate cancer.* Oncotarget, 2016. 7(13): p. 15959-76.

136. Fraser, M., et al., *PTEN Deletion in Prostate Cancer Cells Does Not Associate with Loss of RAD51 Function: Implications for Radiotherapy and Chemotherapy.* Clinical Cancer Research, 2012. 18(4): p. 1015-1027.
137. Byun, D.S., et al., *Frequent monoallelic deletion of PTEN and its reciprocal associatioin with PIK3CA amplification in gastric carcinoma.* Int J Cancer, 2003. 104(3): p. 318-27.
138. Abe, H., et al., *Discovery of a Highly Potent and Selective MEK Inhibitor: GSK1120212 (JTP-74057 DMSO Solvate).* ACS Med Chem Lett, 2011. 2(4): p. 320-4.
139. Schneider-Poetsch, T., et al., *Inhibition of eukaryotic translation elongation by cycloheximide and lactimidomycin.* Nat Chem Biol, 2010. 6(3): p. 209-217.
140. Garreau de Loubresse, N., et al., *Structural basis for the inhibition of the eukaryotic ribosome.* Nature, 2014. 513(7519): p. 517-22.
141. Jacquemont, C. and T. Taniguchi, *Proteasome Function Is Required for DNA Damage Response and Fanconi Anemia Pathway Activation.* Cancer Research, 2007. 67(15): p. 7395-7405.
142. Yang, Y., et al., *Inhibitors of ubiquitin-activating enzyme (E1), a new class of potential cancer therapeutics.* Cancer Res, 2007. 67(19): p. 9472-81.
143. Du, Z.-X., et al., *Role of oxidative stress and intracellular glutathione in the sensitivity to apoptosis induced by proteasome inhibitor in thyroid cancer cells.* BMC Cancer, 2009. 9(1): p. 56.
144. Thariat, J., et al., *Past, present, and future of radiotherapy for the benefit of patients.* Nat Rev Clin Oncol, 2013. 10(1): p. 52-60.
145. Pugh, J.L., et al., *Histone deacetylation critically determines T cell subset radiosensitivity.* J Immunol, 2014. 193(3): p. 1451-8.
146. Helleday, T., et al., *DNA repair pathways as targets for cancer therapy.* Nature Reviews. Cancer, 2008. 8(3): p. 193-204.
147. Khan, M.S., et al., *A comparison of Ki-67 and mitotic count as prognostic markers for metastatic pancreatic and midgut neuroendocrine neoplasms.* Br J Cancer, 2013. 108(9): p. 1838-45.
148. Petrelli, F., et al., *Prognostic value of different cut-off levels of Ki-67 in breast cancer: a systematic review and meta-analysis of 64,196 patients.* Breast Cancer Res Treat, 2015. 153(3): p. 477-91.
149. Wen, S., et al., *Ki-67 as a prognostic marker in early-stage non-small cell lung cancer in Asian patients: a meta-analysis of published studies involving 32 studies.* BMC Cancer, 2015. 15: p. 520.
150. Sobecki, M., et al., *Cell-Cycle Regulation Accounts for Variability in Ki-67 Expression Levels.* Cancer Res, 2017. 77(10): p. 2722-2734.
151. Bindra, R.S., et al., *Development of an assay to measure mutagenic non-homologous end-joining repair activity in mammalian cells.* Nucleic Acids Research, 2013. 41(11): p. e115.
152. Szymonowicz, K., et al., *Restraining Akt1 Phosphorylation Attenuates the Repair of Radiation-Induced DNA Double-Strand Breaks and Reduces the Survival of Irradiated Cancer Cells.* Int J Mol Sci, 2018. 19(8).
153. Szymonowicz, K., et al., *New Insights into Protein Kinase B/Akt Signaling: Role of Localized Akt Activation and Compartment-Specific Target Proteins for the Cellular Radiation Response.* Cancers (Basel), 2018. 10(3).
154. Hu, L., et al., *UBE2S, a novel substrate of Akt1, associates with Ku70 and regulates DNA repair and glioblastoma multiforme resistance to chemotherapy.* Oncogene, 2017. 36(8): p. 1145-1156.
155. Liu, P., et al., *Akt-Mediated Phosphorylation of XLF Impairs Non-Homologous End-Joining DNA Repair.* Molecular Cell, 2015. 57(4): p. 648-661.

156. Shao, G., et al., *MERIT40 controls BRCA1-Rap80 complex integrity and recruitment to DNA double-strand breaks.* Genes & Development, 2009. 23(6): p. 740-754.
157. Brown, Kristin K., et al., *MERIT40 Is an Akt Substrate that Promotes Resolution of DNA Damage Induced by Chemotherapy.* Cell Reports, 2015. 11(9): p. 1358-1366.
158. Toulany, M., et al., *PI3K-Akt signaling regulates basal, but MAP-kinase signaling regulates radiation-induced XRCC1 expression in human tumor cells in vitro.* DNA Repair, 2008. 7(10): p. 1746-1756.
159. Toulany, M., et al., *Blockage of Epidermal Growth Factor Receptor-Phosphatidylinositol 3-Kinase-AKT Signaling Increases Radiosensitivity of K-RAS Mutated Human Tumor Cells In vitro by Affecting DNA Repair.* Clinical Cancer Research, 2006. 12(13): p. 4119-4126.
160. Holler, M., et al., *Dual Targeting of Akt and mTORC1 Impairs Repair of DNA Double-Strand Breaks and Increases Radiation Sensitivity of Human Tumor Cells.* PLoS ONE, 2016. 11(5): p. e0154745.
161. Branzei, D. and M. Foiani, *Regulation of DNA repair throughout the cell cycle.* Nature Reviews. Molecular Cell Biology, 2008. 9(4): p. 297-308.
162. Cook, R., et al., *Direct Involvement of Retinoblastoma Family Proteins in DNA Repair by Non-homologous End-Joining.* Cell Reports, 2015. 10(12): p. 2006-2018.
163. Huang, P.H., R. Cook, and S. Mittnacht, *RB in DNA repair.* Oncotarget, 2015. 6(25): p. 20746-7.
164. Huang, P.H., et al., *Retinoblastoma family proteins: New players in DNA repair by non-homologous end-joining.* Mol Cell Oncol, 2016. 3(2): p. e1053596.

12. Acknowledgements

First, I have to express my deep gratitude to my supervisor, Prof. Dr. George Iliakis, for offering me a place in his institute and providing me with a research project, scientific advice and critical review. Importantly, I would also like to thank him for his strong contribution in the re-qualification of my training program.

This training program is the DFG-Graduiertenkolleg 1739 at Medical School Essen. It provided me with extensive scientific and non-scientific training, financial support and a mentor, Prof. Dr. Martin Schuler. He took the time looking at my data and offering resources from his lab. Thank you very much for this. Thanks go also to all my study mates from the grad school for team spirit and encouragement. Special thanks go to the smart Dr. Klaudia Szymonowicz for her kindness and for sharing her antibody treasure with me. Heartfelt thanks to Dr. Sophie Kalmbach and Dr. Alexandra Wolf for help in the lab and advice, but far more for our friendship.

Many thanks go to my colleagues in the Institute of Medical Radiation Biology. To Dr. Emil Mladenov for his amazing knowledge of biology and chemistry. To Dr. Fanghua Li for always knowing the right treatment conditions. To Dr. Veronika Mladenova and Dr. Aashish Soni for sharing workflows, encouragement and friendship. To Christian Möllers and Malihe Mesbah for always lending a helping hand. To Dr. Lisa Krieger for lovely lunch breaks and reminding me of the life outside of the lab. To Tamara Mußfeldt, for teaching me everything about cell lines and flow cytometers, for our conversations and for sharing her perfectly organized lab with me. I will miss you all.

And, of course, to the brilliant Dr. Simon Magin and Marcel Thissen, my office buddies and PFGE warriors, for help, advice, fun in the lab and terrible jokes. Live long and prosper!

With all my heart I thank my family, who always support and believe in me and make me feel at home. Especially I would like to thank my mother, my greatest inspiration in life.

And, finally, my deepest gratefulness goes to Vladimir Nikolov. For never ending help and patience, incredible support inside and outside of the lab, for uncompromised loyalty and reliability. He brightens up my life, stood by me in bad times and fixed me up with chicken soup when the darkest point was reached. Certainly, this thesis would not have been possible without you and I will never take your help for granted.

13. Curriculum vitae

Der Lebenslauf ist in der veröffentlichten Version aus Gründen des Datenschutzes nicht enthalten.

14. Declarations

Erklärung:

Hiermit erkläre ich, gem. § 7 Abs. (2) d) + f) der Promotionsordnung der Fakultät für Biologie zur Erlangung des Dr. rer. nat., dass ich die vorliegende Dissertation selbständig verfasst und mich keiner anderen als der angegebenen Hilfsmittel bedient, bei der Abfassung der Dissertation nur die angegeben Hilfsmittel benutzt und alle wörtlich oder inhaltlich übernommenen Stellen als solche gekennzeichnet habe.

Essen, den _____ _____

Unterschrift des Doktoranden

Erklärung:

Hiermit erkläre ich, gem. § 7 Abs. (2) e) + g) der Promotionsordnung der Fakultät für Biologie zur Erlangung des Dr. rer. nat., dass ich keine anderen Promotionen bzw. Promotionsversuche in der Vergangenheit durchgeführt habe und dass diese Arbeit von keiner anderen Fakultät/Fachbereich abgelehnt worden ist.

Essen, den _____ _____

Unterschrift des Doktoranden

Erklärung:

Hiermit erkläre ich, gem. § 6 Abs. (2) g) der Promotionsordnung der Fakultät für Biologie zur Erlangung der Dr. rer. nat., dass ich das Arbeitsgebiet, dem das Thema „Systematic analysis of alt-EJ regulation in irradiated cells at the interface of G_0/G_1 cell cycle phases: focus on growth factor signaling and CtIP“ zuzuordnen ist, in Forschung und Lehre vertrete und den Antrag von Anna Katharina Broich befürworte und die Betreuung auch im Falle eines Weggangs, wenn nicht wichtige Gründe dem entgegenstehen, weiterführen werde.

_____

Name des Mitglieds der Universität Duisburg-Essen in Druckbuchstaben

Essen, den _____ _____